CORA Cork Open Research Archive
Cartlann Taighde Oscailte Chorcaí

Title	Shortcuts to adiabaticity: Concepts, methods, and applications
Authors	Guéry-Odelin, D.;Ruschhaupt, Andreas;Kiely, Anthony;Torrontegui, E.;Martínez-Garaot, S.;Muga, Juan Gonzalo
Publication date	2019-10-24
Original Citation	Guéry-Odelin,D., Ruschhaupt, A., Kiely, A., Torrontegui, E. Martínez-Garaot, S. and Muga, J.G. (2019) 'Shortcuts to adiabaticity: Concepts, methods, and applications', Reviews Of Modern Physics, 91(4), 045001, (54 pp). doi: 10.1103/RevModPhys.91.045001
Type of publication	Article (peer-reviewed)
Link to publisher's version	https://journals.aps.org/rmp/abstract/10.1103/RevModPhys.91.045001 - 10.1103/RevModPhys.91.045001
Rights	© 2019 American Physical Society
Download date	2026-10-17 08:40:29
Item downloaded from	https://hdl.handle.net/10468/9796

Shortcuts to adiabaticity: Concepts, methods, and applications

D. Guéry-Odelin

Laboratoire de Collisions Agrégats Réactivité, CNRS UMR 5589, IRSAMC, Université de Toulouse (UPS), 118 Route de Narbonne, 31062 Toulouse CEDEX 4, France

A. Ruschhaupt and A. Kiely

Department of Physics, University College Cork, Cork, Ireland

E. Torrontegui

Instituto de Física Fundamental IFF-CSIC, Calle Serrano 113b, 28006 Madrid, Spain

S. Martínez-Garaot and J. G. Muga

Departamento de Química Física, UPV/EHU, Apdo. 644, 48080 Bilbao, Spain

(published 24 October 2019)

Shortcuts to adiabaticity (STA) are fast routes to the final results of slow, adiabatic changes of the controlling parameters of a system. The shortcuts are designed by a set of analytical and numerical methods suitable for different systems and conditions. A motivation to apply STA methods to quantum systems is to manipulate them on timescales shorter than decoherence times. Thus shortcuts to adiabaticity have become instrumental in preparing and driving internal and motional states in atomic, molecular, and solid-state physics. Applications range from information transfer and processing based on gates or analog paradigms to interferometry and metrology. The multiplicity of STA paths for the controlling parameters may be used to enhance robustness versus noise and perturbations or to optimize relevant variables. Since adiabaticity is a widespread phenomenon, STA methods also extended beyond the quantum world to optical devices, classical mechanical systems, and statistical physics. Shortcuts to adiabaticity combine well with other concepts and techniques, in particular, with optimal control theory, and pose fundamental scientific and engineering questions such as finding speed limits, quantifying the third law, or determining process energy costs and efficiencies. Concepts, methods, and applications of shortcuts to adiabaticity are reviewed and promising prospects are outlined, as well as open questions and challenges ahead.

DOI: 10.1103/RevModPhys.91.045001

CONTENTS

I. Introduction 2
A. Overview of shortcuts to adiabaticity 2
B. Motivation and scope of this review 3
II. Methods 4
A. Overview of inverse engineering approaches 4
1. Quantum transport 5
2. Spin manipulation 5
3. Beyond mean values 5
B. Counterdiabatic driving 6
1. Superadiabatic iterations 8
2. Beyond the basic formalism 9
a. "Physical" unitary transformations 9
b. Schemes that focus on one state 10
c. Effective counterdiabatic field 10
d. Dressed-states approach 10
e. Variational approach 11
f. Counterdiabatic Born-Oppenheimer dynamics 12
g. Constant CD-term approximation 12
C. Invariants and scaling laws 12
1. Lewis-Riesenfeld invariants 12
2. Examples of invariant-based inverse engineering 13
a. Two-level system 13
b. Lewis-Leach family 14
3. Scaling laws 15
4. Connection with Lax pairs 16
D. Variational methods 16
E. Fast forward 17
1. The original formalism 17
2. Streamlined fast-forward approach 18
3. Generalizations and terminology 19
F. FAQUAD and related approaches 19
G. Optimal control and shortcuts to adiabaticity 20
H. Robustness 21
1. Error sensitivity and its optimization using perturbation theory 21
a. Illustrative example: Control of a two-level system 21
b. Optimization using perturbation theory in other settings 22
2. Other approaches 23
I. Three-level systems 23

 © 2019 American Physical Society

1. Apply counterdiabatic shortcuts to the full three-level Λ system 23
2. Applying invariant-based inverse engineering shortcuts to the full three-level Λ system 24
3. Using STA techniques after mapping to a two-level system 24
J. Motional states mapped into a discrete system 24
III. Applications in Quantum Science and Technology 24
A. Trapped ions 25
1. Dynamical normal modes 25
2. Ion transport 27
3. Other operations 28
B. Double wells 29
C. Cavity quantum electrodynamics 29
D. Superconducting circuits 30
E. Spin-orbit coupling 31
F. Nitrogen-vacancy centers 31
G. Many-body and spin-chain models 32
H. Metrology 34
IV. The Energy Cost of STA, Engines, and the Third Law 34
A. Energy costs 34
B. Engines and refrigerators 37
C. Third law 38
V. Open Quantum Systems 38
A. Concept of adiabaticity for open systems 38
B. Engineering the environment 39
C. Mitigating the effect of environment 39
D. Non-Hermitian Hamiltonians 40
VI. Optical Devices 40
VII. Extension to Classical and Statistical Physics 42
A. Counterdiabatic methods in classical mechanics 42
B. Mechanical engineering 43
1. Cranes 43
2. Robustness issues 44
C. STA for isolated dilute gases 44
1. Boltzmann equation 44
2. Extension to Navier-Stokes equation 45
D. Shortcuts for systems in contact with a thermostat 45
1. The overdamped regime 45
2. Connection with free energy and irreversible work 46
3. Extensions 46
VIII. Outlook and Open Questions 46
List of Symbols and Abbreviations 47
Acknowledgments 47
Appendix A: Example of Lie Transform 47
Appendix B: Counterdiabatic Hamiltonian for a Two-level Hamiltonian with Complex Coupling 48
References 48

I. INTRODUCTION

A. Overview of shortcuts to adiabaticity

"Shortcuts to adiabaticity" (STA) are fast routes to the final results of slow, adiabatic changes of the controlling parameters of a system. Adiabatic processes are here broadly defined as those for which the slow changes of the controls leave some dynamical properties invariant, the "adiabatic invariants," such as the quantum number in quantum systems or phase-space areas in classical systems. Figure 1 informally portrays the central idea of shortcuts to adiabaticity. Figure 2 also illustrates the concept pictorially by comparing diabatic, adiabatic, and STA paths in a discrete system.

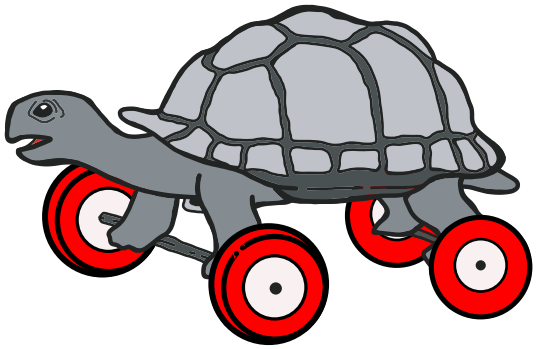

FIG. 1. A turtle on wheels is a good metaphor for shortcuts to adiabaticity. The image is inspired by the artist work of Andree Richmond.

The shortcuts rely on specific time dependences of the control parameters and/or on the addition of auxiliary time-dependent couplings or interactions with respect to some reference Hamiltonian or, more generally, a Liouvillian or transition-rate matrix. STA methods were first applied in simple quantum systems: two- and three-level systems or a particle in a time-dependent harmonic oscillator. They have since come to encompass a much broader domain since slow processes are quite common as a simple way to prepare the state of a system or to change conditions avoiding excitations in a wide spectrum of areas from atomic, molecular, and optical physics, solid state, or chemistry to classical mechanical systems and engineering. In parallel to such a large scope, different methods have been developed and applied.

This description of shortcuts needs some caveats and clarifications. In many quantum mechanical applications, the final state in an STA process reproduces the set of adiabatic probabilities to find the system in the eigenstates of the final Hamiltonian. The mapping of probabilities from

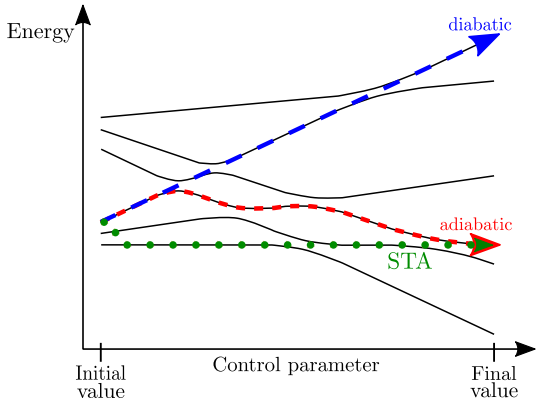

FIG. 2. Schematic example of adiabatic, diabatic, and STA processes. The system is initially in the third level. In the adiabatic path (short-dashed red) the system evolves always along the third level. In a diabatic evolution (long-dashed blue) the system gets excited by jumping across avoided crossings. Along an STA path (green dots) the system does not always travel along the third level but it arrives at the third level in a shorter time (the time dimension is not explicitly shown in the figure).

initial to final settings, without final excitation but allowing for excitations en route, holds for any possible initial state in some state-independent STA protocols and simple enough systems. These state-independent shortcuts are ideal for maximal robustness and to reduce dependence on temperature, so as to avoid costly and time-consuming cooling to the ground state. However, except for idealized models, state independence holds only approximately and for a domain of parameters, for example, within the harmonic approximation in a trapped ion. In other applications state independence is not really necessary or it may be difficult or impossible to achieve as in chaotic systems. Yet shortcuts may still be found for a chosen specific state, typically the ground state or for a state subspace.

A further caveat is that the scope of STA methods has in practice outstripped the original, pure aim in many applications. For example, these methods can be extended with minimal changes to drive general transitions, regardless of whether the initial and final states can be connected adiabatically, such as transitions where the initial state is an eigenstate of the initial Hamiltonian, whereas the final state is not an eigenstate of the final Hamiltonian. This broader perspective merges with inverse engineering methods of the Hamiltonian to achieve arbitrary transitions or unitary transformations.

Motivations.—There are different motivations for the speedup that depend on the setting. In optics, time is often substituted by length to quantify the rate of change so the shortcuts imply shorter, more compact optical devices. In mechanical engineering, we look for fast and safe protocols, say of robotic cranes, to enhance productivity. In microscopic quantum systems, slowness often implies decoherence, the accumulation of errors and perturbations, or even the escape of the system from its confinement. The shortcuts provide a useful toolbox to avoid or mitigate these problems and thus to develop quantum technologies. Moreover, with shorter process times experiments can be repeated more often to increase signal-to-noise ratios.

A generic and important feature of STA apart from the speed achieved is that there are typically many alternative routes for the control parameters, and this flexibility can be used to optimize physically relevant variables, for example, to minimize transient energy excitations and/or energy consumptions or to maximize robustness against perturbations.

Shortcuts to adiabaticity in quantum technologies.—Indeed, shortcuts have been mostly developed and applied for quantum systems, and much of the current interest in STA is rooted in the quest for quantum technologies. STA combine well with the two main paradigms of quantum information processing.

- In the gate-based paradigm, shortcuts to adiabaticity contribute to improve and speed up gates or state preparations and to perform elementary operations like moving atoms leaving them unexcited. Shortcuts to adiabaticity may be applied to all physical platforms, such as trapped ions, cold atoms, nitrogen-vacancy (N*V*) centers, superconducting circuits, quantum dots, or atoms in cavities.

Apart from fighting decoherence, implementing "scalable" architectures toward larger quantum systems is a second major challenge to develop quantum information processing. Scalability benefits from STA in two ways: directly, through the design of operations explicitly intended to achieve it (see an example in Sec. III.A), as well as indirectly, since a mitigated decoherence reduces the need for highly demanding, qubit-consuming error-correction codes.

- The second main paradigm of quantum information processing is adiabatic computing or quantum annealing, which may be accelerated or made possible by changing initial and/or final Hamiltonians, modifying the interpolation path between initial and final Hamiltonians, or adding auxiliary terms to the transient Hamiltonian. For adiabatic quantum computing and other applications with complex systems, progress is being made to find effective STA without using difficult-to-find information on spectra and eigenstates. The more recent paradigms of topological quantum information processing or measured based quantum computation may also benefit from STA.

Shortcuts to adiabaticity are also having an impact or are expected to be useful in quantum technologies other than quantum information processing such as interferometry and metrology, communications, and microengines or refrigerators in quantum thermodynamics.

Fundamental questions.—Finally, apart from being a practical aid to process design, STA also played a role and will continue to be instrumental in clarifying fundamental concepts such as quantum-classical relations, quantum speed limits and trade-off relations between timing, energy, robustness, entropy or information, the third law of thermodynamics, and the proper characterization of energy costs of processes.

B. Motivation and scope of this review

This review provides a broad overview of concepts, methods, and applications of shortcuts to adiabaticity. A strong motivation for writing it is the breadth of systems and areas where STA are used. The hope is that this work will assist in stimulating discussions and information transfer between different domains. There are already examples that demonstrate the benefits of such an interaction. Analogies found between systems as disparate as individual ions in Paul traps and mechanical cranes or optical waveguide devices and atomic internal states have proved fruitful. The link between Lewis-Riesenfeld invariants and Lax pairs is another unexpected example.

The development of STA methods and applications has been quite rapid since Chen, Ruschhaupt *et al.* (2010), where the expression shortcuts to adiabaticity was coined. Precedents before 2010 exist where STA concepts had been applied (Unanyan *et al.*, 1997; Emmanouilidou *et al.*, 2000; Couvert *et al.*, 2008; Motzoi *et al.*, 2009; Muga *et al.*, 2009; Rezek *et al.*, 2009; Salamon *et al.*, 2009; Schmiedl *et al.*, 2009; Masuda and Nakamura, 2010). In the post-2010 period, the early work of Demirplak and Rice (2003, 2005, 2008), and Berry (2009) on "counterdiabatic (CD) driving" has been particularly influential, as well as methodologies such as "inverse engineering," "invariants," "scaling laws," "fast-forward," (FF) or "local adiabatic" methods. To add further flexibility to this already rich scenario of approaches, some methods provide in general a multiplicity of control protocols. Moreover, STA methods relate synergistically to or overlap partially with other control methods. In particular STA blend

well with optimal control theory (OCT), decoherence-free subspaces (DFSs) (S. L. Wu *et al.*, 2017), linear response theory (Acconcia, Bonança, and Deffner, 2015), or perturbative and variational schemes (see Secs. II.H and II.D). There is in summary a dense network of different approaches and STA protocols available, frequently hybridized.

Some of the basic STA techniques rely on specific formalisms (invariants and scaling, CD driving, or fast-forward) that, within specific domains, can be related to each other and be made potentially equivalent because of underlying common structures. For example, a particular protocol to speed up the transport of a particle by defining a trap path may be found as the result of "invariant-based engineering," fast-forward, or "local-CD" approaches. This convergence for specific operations and methods might be misleading because it does not extend to all systems and circumstances. No single all-inclusive theory exists for all STA, and each of the major methodologies carries different limitations, different construction recipes, and different natural application domains. A widespread misconception is to identify "STA" with one particular approach, often CD driving, and even with one particular protocol within one approach. We shall indeed pay due attention to unifying concepts and connections among the STA formalisms, which are of course useful and worth stressing, but at the same time it is hard to overemphasize that the diversity of approaches is a powerful asset of the shortcuts to adiabaticity that explains their versatility.

New hybrid or approximate methods are being created as we write and more will be devised to adapt to diverse needs and systems. This review is also intended to map and characterize the options, help users to navigate among them, and encourage the invention of novel, more efficient or goal-adapted approaches. A number of techniques that fit naturally into the definition of STA but have not been usually tagged as STA will also be mentioned to promote transfer of ideas. Examples of this are the derivative removal of adiabatic gate (DRAG) and weak anharmonicity with average Hamiltonian (WAHWAH) approaches to implement fast pulses free from spurious transitions in superconducting qubits (Motzoi *et al.*, 2009; Schutjens *et al.*, 2013).

Terminology.—Not surprisingly, the various approaches to STA have been described and used with inconsistent terminologies by different groups and communities. Indeed the rapid growth of STA-related work and its extension across many disciplines has brought up different uses for the same words ("superadiabaticity" and "fast forward" are clear examples of polysemic terms), and different expressions for the same concept or method (for example, "transitionless quantum driving" and "counterdiabatic approach"). This review is also intended to clarify some commonly found uses or expressions, making explicit our preference when the polysemy may lead to confusion.

Scope and related reviews.—We intend the review to be didactical for the noninitiated but also comprehensive so that the experts in the different subfields can find a good starting point for exploring other STA-related areas. Several recent reviews on partial aspects or overlapping topics are useful companions: Torrontegui, Ibáñez *et al.* (2013) is the previous most comprehensive review on the subject, but the number of new applications in previously unexplored fields, experiments, and theoretical results since its publication clearly surpasses the work reviewed there. We mostly pay attention to the work done after Torrontegui, Ibáñez *et al.* (2013), but for presenting the key concepts some overlap is allowed. Work on the counterdiabatic method was reviewed recently by Kolodrubetz *et al.* (2017) with emphasis on geometric aspects and classical-quantum relations. For the approaches to speed up adiabatic computing, see Albash and Lidar (2018) and Takahashi (2019). For a review on STA to control quantum critical dynamics, see del Campo and Sengupta (2015). See also Menchon-Enrich *et al.* (2016) about the spatial adiabatic passage and Vitanov *et al.* (2017) about the stimulated Raman adiabatic passage (STIRAP), a technique that has often been sped up with STA. Finally, Masuda and Rice (2016) reviewed the counterdiabatic and fast-forward methods focusing on applications to polyatomic molecules and Bose-Einstein condensates (BEC). Also, a Focus issue of New Journal of Physics on Shortcuts to Adiabaticity provides a landscape of current tendencies (del Campo and Kim, 2019).

Structure.—The review is organized into "Methods" of STA in Sec. II and "Applications" from Sec. III to VII. We address applications of STA to quantum science and technology in Sec. III. This includes the main physical platforms and the quantum system is mainly considered as a closed quantum system. The connections between STA and quantum thermodynamic concepts, a topic between closed and open quantum systems, are reviewed in Sec. IV. STA and open quantum systems is the topic of Sec. V. Sections VI and VII deal with results and peculiarities of two fields that also offer a promising arena for practical applications: optics in Sec. VI and classical systems in Sec. VII.

We tried to keep acronyms to a minimum but some terms [among the most prominent: shortcuts to adiabaticity (STA) and counterdiabatic (CD)] appear so many times that the use of the acronym is well justified. Other acronyms are already of widespread use, such as OCT for optical control theory. To facilitate reading, a full list of acronyms is provided. As for notation, an effort toward consistency has been made, so the symbols often differ from the ones in the original papers. Beware of possible multiple uses of some symbols (constants, in particular). The context and text should help to avoid any confusion.

II. METHODS

A. Overview of inverse engineering approaches

We begin with an overview of inverse engineering. This expression refers to inferring the time variation of the control parameters from a chosen evolution of the physical system of interest. The notion is broadly applicable for quantum, classical, or stochastic dynamics and embraces many STA techniques. In this section we deal first with two simple examples for motional and internal degrees of freedom, where more sophisticated or auxiliary concepts and formalisms, e.g., related to invariants, counterdiabatic driving, or fast forward, are not explicitly used. Instead, the connection between dynamics and control is performed by solving for the control

function(s) in the effective equation of motion for a classical variable or a quantum mean value.

It is often necessary or useful to go beyond this simple inversion approach for several reasons. For example: the dynamical path of the system is not easy to design, the inversion is nontrivial, we are interested in finding state-independent protocols, the direct inversion leads to unrealizable control functions, or we look for stable controls, robust with respect to specific perturbations. To address these problems, in the following sections several auxiliary concepts and formal superstructures will be added to the simple inverse engineering idea in the different STA approaches. The first hint of a family of inversion methods dealing with detailed dynamics beyond mean values is given in Sec. II.A.3 after the two examples.

1. Quantum transport

Finding the motion of a harmonic trap to transport a quantum particle so that it starts in the ground state and ends up in the ground state of the displaced potential amounts to inversely solving a classical Newton equation (Schmiedl *et al.*, 2009; Torrontegui *et al.*, 2011). The equation of motion of the particle position x inside the potential reads

$$\ddot{x} + \omega_0^2 x = \omega_0^2 x_0(t), \tag{1}$$

where ω_0 is the angular frequency of the harmonic trap, $x_0(t)$ is the instantaneous position of its center, and the dots represent, here and in the following, time derivatives. Equation (1) describes a forced oscillator driven by the time-dependent force $F(t) = m\omega_0^2 x_0(t)$. We can interpolate the trajectory $x(t)$ between the initial position of the particle and the desired final position d. In addition, to ensure that the transport ends up at the lowest energy state, one needs to cancel out the first and second derivatives at the initial $t = 0$ and final time t_f (Torrontegui *et al.*, 2011). A simple polynomial interpolation of fifth degree can account for such boundary conditions (Torrontegui *et al.*, 2011),

$$x(t) = d\left[10\left(\frac{t}{t_f}\right)^3 - 15\left(\frac{t}{t_f}\right)^4 + 6\left(\frac{t}{t_f}\right)^5\right]. \tag{2}$$

Once $x(t)$ is defined, Eq. (1) can be easily inverted to give the corresponding expression for the driving term $x_0(t)$. Note that there are infinitely many interpolating functions consistent with the boundary conditions at initial and final times. This freedom is quite typical of different STA methods and can be exploited to satisfy other conditions, e.g., minimizing average energy of a particle during displacement. More parameters can be added in the interpolation functions to minimize the quantity of interest (Torrontegui *et al.*, 2011). For instance, the robustness against errors in the value of the angular frequency of the trap ω_0 can be enhanced using a Fourier reformulation of the transport problem (Guéry-Odelin and Muga, 2014); see an experimental application by An *et al.* (2016) and Sec. VII.B.2. The simple example provided here was generalized to take into account anharmonicities (Zhang, Chen, and Guéry-Odelin, 2015) and in 3D to manipulate Bose-Einstein condensates with an atom chip (Corgier *et al.*, 2018). Section II.H provides a deeper view on the techniques developed to enhance the robustness of a given protocol.

2. Spin manipulation

A similar approach can be used for designing the magnetic field components to induce a given trajectory of the mean value of a spin 1/2 $\mathbf{S}(t)$ on the Bloch sphere (Berry, 2009),

$$\mathbf{B}(t) = B_0(t)\mathbf{S}(t) + \frac{1}{\gamma}\mathbf{S}(t) \times \partial_t \mathbf{S}(t), \tag{3}$$

where γ is the gyromagnetic ratio and $B_0(t)$ is any time-dependent function. This solution is found by inverse engineering of the precession equation for the mean value of the spin,

$$\partial_t \mathbf{S}(t) = \gamma \mathbf{B}(t) \times \mathbf{S}(t). \tag{4}$$

In practice, we usually define the initial and target state and build up the solution by interpolation as before. Such an approach has been used for instance to manipulate a spin by defining the time evolution of the spherical angle of the spin on the Bloch sphere (Vitanov and Shore, 2015; Zhang, Chen, and Guéry-Odelin, 2017). The very same problem can be reformulated using other formalisms such as the Madelung representation (Zhang, Chen, and Guéry-Odelin, 2017) that yields an equation of motion that can be readily reversed. Other formulations of the inverse engineering approach can be made by a proper shaping of the evolution operator (Jing *et al.*, 2013; Kang *et al.*, 2016c) or by time rescaling (Bernardo, 2019). This method has been applied to two- (Zhang, Chen, and Guéry-Odelin, 2017), three- (Kang *et al.*, 2016c; Kang, Huang *et al.*, 2017), and four-level systems (Li, Martínez-Cercós *et al.*, 2018). Inverse engineering was also used for open quantum systems (Jing *et al.*, 2013; Impens and Guéry-Odelin, 2017).

3. Beyond mean values

Suppose now that a more detailed specification of the dynamics is needed and we focus on closed, linear quantum systems. We shall design the unitary evolution operator $U(t)$ by specifying a complete basis of dynamical states $|\psi_j(t)\rangle$ assumed to satisfy a time-dependent Schrödinger equation driven by a, to be determined, Hamiltonian,

$$U(t) = \sum_j |\psi_j(t)\rangle\langle\psi_j(0)| \tag{5}$$

[see other proposals for the form of U by Kang *et al.*, 2016c and Santos, 2018]. The corresponding Hamiltonian is given from the assumed dynamics by

$$H(t) = i\hbar \dot{U} U^\dagger. \tag{6}$$

As in the previous examples, a typical scenario is that the initial and final Hamiltonians are fixed by the experiment or the intended operation. With these boundary conditions the functions $|\psi_j(t)\rangle$ at initial and final times are usually chosen as

the eigenstates of the corresponding Hamiltonians, but there is freedom to interpolate them, and therefore $H(t)$, in between.

Several approaches depend on different ways to choose the orthogonal basis functions $|\psi_j(t)\rangle$: (a) in the counterdiabatic driving approach they are instantaneous eigenstates of a reference Hamiltonian $H_0(t)$; (b) in invariant-based engineering, they are eigenstates of the invariant of an assumed Hamiltonian form; and (c) more generally they can be just convenient functions. In particular, they can be parametrized so that $H(t)$ obeys certain constraints, such as making zero undesired terms or matrix elements. Note that (a), (b), and (c) are in a certain sense equivalent as they can be reformulated in each other's language, and they all rely on Eq. (6). For example, (b) or (c) do not explicitly need an $H_0(t)$, and (a) or (c) do not explicitly need the invariants, but $H_0(t)$ or the invariants could be found if needed. In particular, any linear combination $\sum c_j|\psi_j(t)\rangle\langle\psi_j(t)|$ with constant coefficients c_j is by construction an invariant of motion of $H(t)$. Inverse engineering may also be based on partial information, such as, e.g., using a single function of the set and imposing some additional condition on the Hamiltonian, for example, that the potential is local (i.e., diagonal) and real in coordinate space. These conditions are the essence of the streamlined version (Torrontegui, Martínez-Garaot *et al.*, 2012) of the fast-forward approach (Masuda and Nakamura, 2008, 2010). The following explores all these approaches in more detail.

B. Counterdiabatic driving

The basic idea of counterdiabatic driving is to add auxiliary interactions to some reference Hamiltonian $H_0(t)$ so that the dynamics follows exactly the approximate adiabatic evolution driven by $H_0(t)$. An illustrative analogy is a flat, horizontal road turn (the reference) that is modified by inclining the roadway surface about its longitudinal axis with a bank angle so that the vehicles can go faster without sliding off the road. After some precedents (Unanyan *et al.*, 1997; Emmanouilidou *et al.*, 2000), the CD driving paradigm was worked out and developed systematically by Demirplak and Rice (2003, 2005, 2008) for internal state transfer using control fields, then rediscovered in a different but equivalent way as "transitionless tracking" by Berry (2009), and used to design many control schemes after Chen, Lizuain *et al.* (2010), unaware of the work of Demirplak and Rice, employed Berry's method to control two- and three-level systems.

Berry's formulation.—We start with Berry's formulation because it is somewhat simpler. In Berry (2009), the starting point is a reference Hamiltonian

$$H_0(t) = \sum_n |n(t)\rangle E_n(t)\langle n(t)|. \tag{7}$$

We adopt for simplicity a notation appropriate for a discrete (real) spectrum and no degeneracies.[1] A state $|n(0)\rangle$ that is initially an eigenstate of $H_0(0)$ will continue to be so under slow enough driving with the form

$$|\psi_n(t)\rangle = e^{i\xi_n(t)}|n(t)\rangle, \tag{8}$$

where the adiabatic phases $\xi_n(t)$ are found by substituting Eq. (8) as an *Ansatz* into the time-dependent Schrödinger equation driven by $H_0(t)$,

$$\xi_n(t) = -\frac{1}{\hbar}\int_0^t dt' E_n(t') + i\int_0^t dt'\langle n(t')|\partial_{t'} n(t')\rangle. \tag{9}$$

We now seek a Hamiltonian $H(t)$ for which the approximate states $|\psi_n(t)\rangle$ become the exact evolving states,

$$i\hbar\partial_t|\psi_n(t)\rangle = H(t)|\psi_n(t)\rangle. \tag{10}$$

$H(t)$ is constructed using Eq. (6) from the unitary evolution operator

$$U(t) = \sum_n e^{i\xi_n(t)}|n(t)\rangle\langle n(0)|, \tag{11}$$

which obeys $i\hbar\partial_t U(t) = H(t)U(t)$, so that an arbitrary state evolves as

$$|\psi(t)\rangle = \sum_n |n(t)\rangle e^{i\xi_n(t)}\langle n(0)|\psi(0)\rangle. \tag{12}$$

After substituting Eq. (11) into Eq. (6), or alternatively differentiating Eq. (12), the Hamiltonian becomes

$$H(t) = H_0(t) + H_{CD}(t), \tag{13}$$

$$H_{CD}(t) = i\hbar\sum_n [|\partial_t n(t)\rangle\langle n(t)| - \langle n(t)|\partial_t n(t)\rangle|n(t)\rangle\langle n(t)|], \tag{14}$$

where H_{CD} is Hermitian and nondiagonal in the $|n(t)\rangle$ basis.

As a simple example of H_0 and H_{CD}, consider a two-level system with reference Hamiltonian

$$H_0(t) = \frac{\hbar}{2}\begin{pmatrix} -\Delta(t) & \Omega_R(t) \\ \Omega_R(t) & \Delta(t) \end{pmatrix}, \tag{15}$$

where $\Delta(t)$ is the detuning and $\Omega_R(t)$ is the real Rabi frequency. The counterdiabatic Hamiltonian has the form

$$H_{CD}(t) = \frac{\hbar}{2}\begin{pmatrix} 0 & -i\Omega_a(t) \\ i\Omega_a(t) & 0 \end{pmatrix}, \tag{16}$$

with $\Omega_a(t) = [\Omega_R(t)\dot{\Delta}(t) - \dot{\Omega}_R(t)\Delta(t)]/\Omega^2(t)$ and $\Omega(t) = \sqrt{\Delta^2(t)+\Omega_R^2(t)}$. See further simple examples in Appendix B.

Returning to the general expression (13), we note that H_{CD} is orthogonal to H_0 considering the scalar product $\mathrm{tr}(A^\dagger B)$ of two operators. Using $d\langle n(t)|m(t)\rangle/dt = 0$ it can be seen that H_{CD} is also orthogonal to $\dot{H}_0$ (Petiziol *et al.*, 2018). An alternative form for H_{CD} is found by differentiating $H_0(t)|n(t)\rangle = E_n(t)|n(t)\rangle$,

[1] Generalizations for degenerate levels, relevant, for example, to speed up holonomic quantum gates, may be found by Takahashi (2013b) and Zhang *et al.* (2015) or Karzig *et al.* (2015). Generalizations for non-Hermitian Hamiltonians $H_0(t)$ are discussed in Sec. V.D.

$$H_{CD} = i\hbar \sum_{m\neq n} \sum_{n} \frac{|m(t)\rangle\langle m(t)|\dot{H}_0|n(t)\rangle\langle n(t)|}{E_n - E_m}, \quad (17)$$

which, using the scaled time $s = t/t_f$, gives the scaling $H_{CD} \sim 1/t_f$. In general $H_{CD}(t)$ vanishes for $t < 0$ and $t > t_f$, either suddenly or continuously at the extreme times, so that the $|n(t)\rangle$ become eigenstates of the full Hamiltonian at the boundary times $t = 0^-$ and t_f^+.

In terms of the phases the total Hamiltonian (13) can be written as (Chen, Torrontegui, and Muga, 2011)

$$H(t) = J(t) + i\hbar \sum_{n} |\partial_t n(t)\rangle\langle n(t)|, \quad (18)$$

with

$$J(t) = -\hbar \sum_{n} |n(t)\rangle \dot{\xi}_n(t) \langle n(t)|. \quad (19)$$

Subtracting $H - H_{CD}$ we get an alternative form of H_0 consistent with Eqs. (7) and (9),

$$H_0 = \hbar \sum_{n} |n(t)\rangle[-\dot{\xi}_n + i\langle n(t)|\dot{n}(t)\rangle]\langle n(t)|. \quad (20)$$

If we write the same $H_0(t)$ [Eq. (7)] as before in an alternative basis with different phases $H_0(t) = \sum_n |n'(t)\rangle E_n(t)\langle n'(t)|$, where $|n'(t)\rangle = e^{i\phi_n}|n(t)\rangle$, the formalism goes through using primed functions ξ'_n and corresponding primed operators. [One example is $|n'(t)\rangle = e^{\xi_n(t)}|n(t)\rangle$ so that $\xi'_n(t) = 0$.] It is easy to check though that the terms compensate so that $H'_{CD}(t) = H_{CD}(t)$, i.e., a change of representation for $H_0(t)$ does not change $H(t)$, nor the CD-driving term, nor the physics.

Quite a different issue is to change the physics when imposing a set of basis functions $\{|n(t)\rangle\}$ and a set of phases $\{\xi_n(t)\}$ which are not *a priori* regarded as adiabatic (Chen, Torrontegui, and Muga, 2011). This procedure is essentially invariant-based inverse engineering since one is imposing some specific dynamics (thus some invariants) without presupposing a given $H_0(t)$. $U(t)$ in Eq. (11) becomes the primary object and the driving Hamiltonian is given by Eq. (18) with diagonal part (20), which defines $H_0(t)$, and a coupling, nondiagonal part (14). Now, changing the phases $\xi_n(t)$ modifies $H_0(t)$ and has an impact on the physical evolution of a general wave function $|\psi(t)\rangle$. Of course the populations $\mathcal{P}_n(t) \equiv |\langle n(t)|\psi(t)\rangle|^2 = \mathcal{P}_n(0)$ driven by Eq. (18) are not affected by phase shifts. The $\dot{\xi}_n(t)$ can be optimized to minimize energy costs (Hu *et al.*, 2018), robustness against decoherence (Santos and Sarandy, 2018), or intensity of the extra CD controls (Santos *et al.*, 2019).

A related procedure is to set the $|n(t)\rangle$ but consider $H_0(t)$ and the eigenvalues $E_n(t)$ controllable elements rather than given (Berry, 2009). For example, setting all $E_n(t) = 0$ cancels the dynamical phase. That means that for a given set of states $|n(t)\rangle$, $H_{CD}(t)$ alone (without an H_0) drives the same populations than $H(t) = H_0(t) + H_{CD}(t)$ for any choice of $E_n(t)$ (Chen, Lizuain *et al.*, 2010).

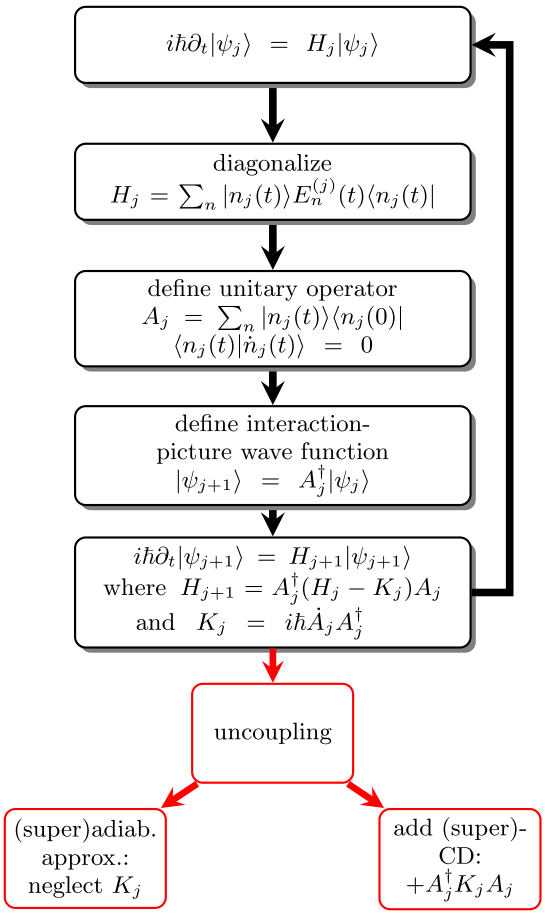

FIG. 3. Scheme for superadiabatic iterative interaction pictures. At the end of each iteration it is possible, apart from starting a new one, to either neglect the nondiagonal coupling in H_{j+1} (adiabatic approximation if $j = 0$ or superadiabatic approximation for $j \geq 1$) or add a term (CD for $j = 0$ or super-CD otherwise) to the Hamiltonian H_{j+1} to exactly cancel the coupling.

The formulation of Demirplak and Rice.—To follow some past and recent developments and generalizations it is worth finding the auxiliary Hamiltonian H_{CD} by the equivalent formulation of Demirplak and Rice (2003, 2005, 2008), which is the zeroth iteration $j = 0$ in Fig. 3.

In the following discussion we concentrate on $j = 0$. Among the possible phase choices for the eigenstates of $H_0(t)$, we now use the one that satisfies the "parallel transport" condition $\langle n_0(t)|\dot{n}_0(0)\rangle = 0$. Regardless of the "working" basis of eigenvectors $|n(t)\rangle$ one starts with, the parallel transported basis is found as

$$|n_0(t)\rangle = e^{-\int_0^t \langle n(t')|\dot{n}\rangle dt'}|n(t)\rangle. \quad (21)$$

Later on we shall see the consequences of applying or not applying parallel transport. A dynamical solution driven by $H_0(t)$ is written as $|\psi_0(t)\rangle$ and the instantaneous eigenvalues as $E_n^{(0)}(t)$. The extra notational burden of the index $j = 0$ may be ignored in many applications, in particular, for ordinary CD

driving, but it will be useful to cope with higher order suparadiabatic iterations later on.

The way to find the auxiliary driving term is to first express the dynamics in an adiabatic frame. For that we apply the transformation $|\psi_1(t)\rangle = A_0^\dagger(t)|\psi_0(t)\rangle$ to the dynamical states driven by $H_0(t)$, with $A_0(t) = \sum_n |n_0(t)\rangle\langle n_0(0)|$. In the resulting adiabatic frame the coupling, diabatic terms are made obvious, $-A_0^\dagger K_0 A_0$, where $K_0 = i\hbar\dot{A}_0 A_0^\dagger = \sum_n |\dot{n}_0(t)\rangle\langle n_0(t)|$. In this adiabatic frame we may (a) neglect the coupling (adiabatic approximation), or (b) cancel the coupling by adding $A_0^\dagger K_0 A$ to the Hamiltonian; see again Fig. 3. In the original, Schrödinger picture, also referred to as the laboratory frame hereafter, this addition amounts to using $H = H_0 + K_0$.

An alternative useful form for $K_0(t)$ is (Messiah, 1962)

$$K_0(t) = i\hbar \sum_n \frac{dP_n(t)}{dt} P_n(t), \tag{22}$$

where $P_n(t) = |n_0(t)\rangle\langle n_0(t)| = |n(t)\rangle\langle n(t)|$. K_0 may as well be written in an arbitrary basis of eigenvectors $|n(t)\rangle$, i.e., not necessarily parallel transported, $K_0(t) = i\hbar\sum_n |\dot{n}(t)\rangle\langle n(t)| - |n(t)\rangle\langle n(t)|\dot{n}\rangle\langle n(t)| = H_{CD}(t)$. This result proves that K_0 is identical to H_{CD} in Eq. (14). Since the projectors $P_n(t) = |n_0(t)\rangle\langle n_0(t)| = |n(t)\rangle\langle n(t)|$ are invariant with respect to phase choices of the eigenvectors, the form in which H_{CD} is usually written in Eq. (14) is invariant under different choices of phases for the eigenstates. In particular, this implies that K_0 is purely nondiagonal [Kato's condition (Kato, 1950; Demirplak and Rice, 2008)] in the arbitrarily chosen basis of eigenvectors of $H_0(t)$, $|n(t)\rangle$.

If we now return to the parallel transported basis in the interaction (adiabatic) picture, the addition of $A_0^\dagger K_0 A_0$ cancels the couplings so the dynamics is trivially solved with dynamical phase factors. In the Schrödinger picture,

$$|\psi_0(t)\rangle = e^{-(i/\hbar)\int_0^t E_n(t')dt'} |n_0(t)\rangle\langle n_0(0)|\psi_0(0)\rangle, \tag{23}$$

which is exactly Eq. (12) as can be seen by using Eq. (21).

If, instead of A_0, a more general transformation $\tilde{A} = \sum_n |n(t)\rangle\langle n(0)|$ is used, the coupling term in the interaction picture becomes $-\tilde{A}_0^\dagger \tilde{K}_0 \tilde{A}_0$, where

$$\begin{aligned}\tilde{K}_0 &= i\hbar\dot{\tilde{A}}_0\tilde{A}_0^\dagger \\ &= \sum_n |\dot{n}(t)\rangle\langle n(t)| = K_0 + i\hbar|n(t)\rangle\langle n(t)|\dot{n}(t)\rangle\langle n(t)|\end{aligned}$$

and its cancellation would lead in the laboratory picture to a different state,

$$\sum_n e^{-(i/\hbar)\int_0^t E_n(t')dt'} |n(t)\rangle\langle n(0)|\psi_0(0)\rangle, \tag{24}$$

although the probabilities are not affected.

Demirplak and Rice (2008) also pointed out that the operator

$$H_{CD}^{[n]} = i\hbar[dP_n/dt, P_n]_-, \tag{25}$$

which fulfils $P_m H_{CD} P_n = P_m H_{CD}^{[n]} P_n$ and $P_n H_{CD} P_m = P_n H_{CD}^{[n]} P_m$ for all m, as well as $P_m H_{CD}^{[n]} P'_m = 0$ for m, $m' \neq n$, uncouples the dynamics of level n. For $H_0 + H_{CD}^{[n]}$, $e^{i\xi_n(t)}|n(t)\rangle$ is an exact solution of the dynamics. This is an interesting simplification as we are often interested in only one state, typically the ground state. The last condition imposed by Demirplak and Rice (2008), $P_m H_{CD}^{[n]} P'_m = 0$ for m, $m' \neq n$, is not really necessary for the uncoupling of the nth level. Without it, a broad set of "state-dependent" CD operators $H_{CD}^{[n]} + Q_n B Q_n$, where $Q_n = 1 - P_n$ and B is any Hermitian operator, can be generated. This multiplicity may be useful and explains why different auxiliary state-dependent CD terms have been proposed (Patra and Jarzynski, 2017b; Setiawan *et al.*, 2017).

1. Superadiabatic iterations

Let us recap before moving ahead. The adiabatic interaction picture (IP) corresponds to expressing the quantum dynamics in the adiabatic basis of instantaneous eigenstates of $H_0(t)$. The dynamical equation in the adiabatic IP includes an effective Hamiltonian $H_1(t)$ with a diagonal (adiabatic) term and a coupling term; see Fig. 3.

We can repeat the sequence iteratively. In the first "superadiabatic" iteration, H_1 is diagonalized to find its instantaneous (parallel-transported) eigenstates $|n_1(t)\rangle$. With the new "superadiabatic basis" a new IP is generated driven by an effective Hamiltonian H_2 with a diagonal part in the superadiabatic basis and a coupling term. This new coupling term $-A_1^\dagger K_1 A_1$ may be (a) neglected (superadiabatic approximation) or (b) canceled by adding its negative, and so on. The canceling term to be added to H_0 in the Schrödinger picture is $H_{cd}^{(j)} = B_j K_j B_j^\dagger$, with $B_0 = 1$ and $B_j = \prod_{k=0}^{j-1} A_k$ for $j \geq 1$. Note that in general only the one generated in the zeroth iteration agrees with the standard CD term $H_{cd}^0 = H_{CD}$.

The recursive iterations were worked out by Garrido (1964), without considering the cancellations, to find out generalizations of the adiabatic approximation. Berry (1987) also used them to calculate a sequence of corrections to Berry's phase and introduced the name "superadiabatic transformations." Demirplak and Rice (2008) proposed to apply the superadiabatic iterative frame to generate alternative (to the simple CD approach) higher order coupling-canceling terms. Later Ibáñez, Chen, and Muga (2013) made explicit the conditions that the derivatives of $H_0(t)$ must satisfy at the time boundaries in order to really generate a shortcut to adiabaticity (rather than just a shortcut to superadiabaticity), i.e., a protocol that takes instantaneous eigenstates of $H_0(t = 0)$ to corresponding eigenstates of $H_0(t_f)$.

The naive expectation that each iteration will produce smaller and smaller couplings does not hold in general. They decrease up to an optimal iteration and then grow (Berry, 1987). Working with the optimal frame may or may not be worthwhile depending on whether the boundary conditions for derivatives of $H_0(t)$ are fulfilled (Ibáñez, Chen, and Muga, 2013).

An interesting feature of the superadiabatic sequence of coupling terms is that their operator structure changes with the iteration. For example, for a two-level system with Hamiltonian $X\sigma_x + Z(t)\sigma_z$, X is constant, where the $\sigma_{x,y,z}$ are Pauli matrices, the first (adiabatic) CD term K_0 is of the form $Y(t)\sigma_y$, see Eq. (16), whereas the second (first-order superadiabatic) coupling term in the Schrödinger frame reproduces the structure of H_0 with x and z components but not a y component. [For three-level systems see Huang *et al.* (2016), Kang *et al.* (2016b), Song, Ai *et al.* (2016), and Wu, Su, Ji, and Zhang (2017).] Unitarily transforming K_0 (see Sec. II.B.2) also provides a Hamiltonian without a y component, which is different from the term $H_{cd}^{(1)} = A_0 K_1 A_0^\dagger$ generated from the first superadiabatic iteration, see an explicit comparison by Ibáñez *et al.* (2012), where $H_{cd}^{(1)}$ was shown to have smaller intensity than H_{CD}.

To avoid confusion we discourage the use of the expression superadiabatic to refer to the regular CD approach (in fact a zeroth order in the superadiabatic iterative frame) or its unitarily transformed versions discussed in Sec. II.B.2. This use of the word superadiabatic, as being equivalent to CD driving or even generically to all shortcuts is, however, somewhat extended.

DRAG controls.—The DRAG framework was developed to avoid diabatic transitions to undesired levels in the context of superconducting quantum devices. It was recently reviewed by Theis *et al.* (2018) but we sketch the main ideas here since it is related to the superadiabatic scheme as formulated, e.g., by Ibáñez, Chen, and Muga (2013). A typical scenario is that the (super)-CD term $H_{cd}^{(j)} = B_j K_j B_j^\dagger$ is not physically feasible and does not match the controls in the lab. The DRAG approach addresses this problem by decomposing the controllable Hamiltonian that "corrects" the dynamics as $H^{\rm ctrl} = \sum_k u_k(t) h_k + \text{H.c.}$ with control fields $u_k(t)$ and coupling terms h_k. In a given superadiabatic frame partial contributions to $u_k(t)$ are found by projecting $H_{cd}^{(j)}$ into the assumed Hamiltonian structure. This generates an approximation to the exact uncoupling term so the diabatic coupling, even if not canceled exactly, is reduced. An important point is that further iterations, in contrast with the bare superadiabatic iterations, typically converge, so that the coupling eventually vanishes. A variant of this approach applies when the error terms are not independently controlled, because they all depend on some common control, e.g., a single laser field. Different perturbative approximations using a power series in the inverse gap energies were worked out systematically (Theis *et al.*, 2018).

2. Beyond the basic formalism

The CD Hamiltonian H_{CD} often implies different operators from those in H_0 that typically may be hard or even impossible to generate in the laboratory. Moreover, a lot of spectral information is in principle used to build H_{CD}, specifically the eigenvectors of H_0, so a number of strategies, reviewed hereafter, are put forward to avoid some terms in the auxiliary Hamiltonian, and/or the spectral information needed. Changing the phases $\xi_n(t)$ without modifying the $|n(t)\rangle$ changes H_0 but not H_{CD}, so it is not enough for these purposes (Ibáñez, Martínez-Garaot *et al.*, 2011).

a. "Physical" unitary transformations

A useful method to generate alternative, physically feasible shortcuts from an existing shortcut generated by counterdiabatic driving or otherwise, is to perform physical, rather than formal, unitary transformations (Ibáñez *et al.*, 2012), or corresponding canonical transformations in classical systems (Deffner, Jarzynski, and del Campo, 2014). Given a Hamiltonian $H(t)$ that drives the wave function $|\psi(t)\rangle$, the unitarily transformed state $|\psi'(t)\rangle = \mathcal{U}^\dagger(t)|\psi(t)\rangle$ is driven by the Hamiltonian (the primes here distinguish the picture, they do not represent derivatives)

$$H'(t) = \mathcal{U}^\dagger(H - K)\mathcal{U}, \tag{26}$$

$$K = i\hbar\dot{\mathcal{U}}\mathcal{U}^\dagger. \tag{27}$$

If we set $\mathcal{U}(0) = \mathcal{U}(t_f) = 1$, then the wave functions coincide at the boundary times $|\psi(0)\rangle = |\psi'(0)\rangle$ and $|\psi(t_f)\rangle = |\psi'(t_f)\rangle$. If, in addition, $\dot{\mathcal{U}}(0) = \dot{\mathcal{U}}(t_f) = 0$, then also the Hamiltonians coincide at boundary times $H(0) = H'(0)$ and $H(t_f) = H'(t_f)$.

Note that here the alternative Hamiltonian form (26) and the state $|\psi'(t)\rangle$ are not just convenient mathematical transforms of $H(t)$ or $|\psi(t)\rangle$ representing the same physics as in conventional interaction or Heisenberg picture transformations. Instead, at intermediary times, $H'(t)$ and $H(t)$ represent indeed different (laboratory) drivings, and $|\psi(t)\rangle$ and $|\psi'(t)\rangle$ different dynamical states. This was emphasized by S. Ibáñez *et al.* (2012) by calling the different alternatives "multiple Schrödinger pictures."

The art is to find a useful $\mathcal{U}(t)$ to make $H'(t)$ feasible. This approach was applied in many works; see, e.g., Hollenberg (2012), Takahashi (2015), Agundez *et al.* (2017), and Sels and Polkovnikov (2017), and several experiments (Bason *et al.*, 2012; Zhang *et al.*, 2013; An *et al.*, 2016; Du *et al.*, 2016). Deffner, Jarzynski, and del Campo (2014) applied it to generate feasible (i.e., involving local potentials in coordinate space, independent of momentum) Hamiltonians for scale-invariant dynamical processes.

When $H(t)$ is a linear combination of generators G_a of some Lie algebra,

$$[G_b, G_c] = \sum_{a=1}^{N} \alpha_{abc} G_a, \tag{28}$$

where the α_{abc} are the structure constants, $\mathcal{U}$ may be constructed by exponentiating elements of the algebra and imposing the vanishing of the unwanted terms (Martínez-Garaot *et al.*, 2014). To carry out the transformation an element G of the Lie algebra of the Hamiltonian is chosen,

$$\mathcal{U}(t) = e^{-ig(t)G}, \tag{29}$$

where $g(t)$ is a real function to be set. This type of unitary operator $\mathcal{U}(t)$ constitutes a "Lie transform." Note that K in Eq. (27) becomes $-\hbar\dot{g}(t)G$ and commutes with G so H' is given by

$$\mathcal{U}^{\dagger}(H-K)\mathcal{U} = e^{igG}(H-K)e^{-igG}$$
$$= H - \hbar\dot{g}G + ig[G,H] - \frac{g^2}{2!}[G,[G,H]]$$
$$- i\frac{g^3}{3!}[G,[G,[G,H]]] + \cdots, \tag{30}$$

which depends only on G, H, and its nested commutators with G, so it stays in the algebra. If we can choose G and $g(t)$ so that the undesired generator components in $H(t)$ cancel out and the boundary conditions for $\mathcal{U}$ are satisfied, the method provides a feasible, alternative shortcut. A simple example for the two-level Hamiltonian is given in Appendix A. Martínez-Garaot *et al.* (2014) and Kang *et al.* (2018) provided more examples.

Interaction pictures.—Frequently the CD terms are found formally in a transformed picture, I in Fig. 4, which is intended only as a mathematical aid. The effective Hamiltonian H_I in this picture, without the CD term, represents the same physics as some original Hamiltonian H_S in the Schrödinger picture S in Fig. 4. Once the CD term is added we get a new Hamiltonian H_I' that when transformed back gives $H_{S'}$. It happens often that simple-looking auxiliary terms in the transformed frames become difficult to implement in the laboratory frame. In Sec. III.G we comment on some N-body models with easily solvable CD terms in a convenient transformed frame but hard to realize in the lab frame. Alternative unitary transformations $U_{\tilde{\varphi}}$, different from the one used to go between the I and S pictures U_{φ}, may help to solve the problem, giving from $H_{I'}$ feasible shortcuts driven by a new lab frame Hamiltonian $H_{S''}$. Ibáñez *et al.* (2015) worked out this alternative route for two-level systems when the rotating wave approximation is not applicable; see also Ibáñez, Peralta Conde *et al.* (2011), Chen and Wei (2015), and H. Li *et al.* (2017). Physics beyond the rotating wave approximation is of much current interest due to the increasing use of strong fields and microwave frequencies, for example, in NV centers.

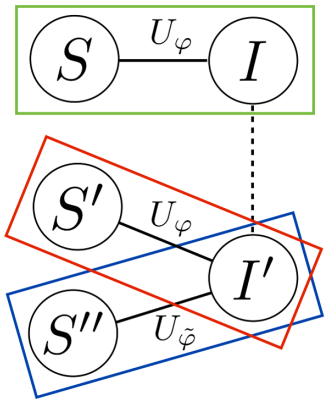

FIG. 4. Schematic relation between different Schrödinger and interaction pictures. Each node corresponds also to different Hamiltonians. The rectangular boxes enclose nodes that represent the same underlying physics. The solid lines represent unitary relations for the linked states and the dashed line represents a nonunitary addition of an auxiliary term to the Hamiltonian.

b. Schemes that focus on one state

A simplifying assumption that helps one to find simpler decoupling terms is to focus on only one state, typically the ground state $|0(t)\rangle$ or a subset of states. Explicit exact forms of the driving that uncouples that state were worked out quite early (Demirplak and Rice, 2008), see Eq. (25), and more recently for systems described in coordinate space in Patra and Jarzynski (2017b) or in a discrete basis (Setiawan *et al.*, 2017). As for approximate schemes, Opatrný and Mølmer (2014) proposed to add to $H_0(t)$ the Hamiltonian $H_B(t) = \sum_k^K f_k(t)T_k$ using only feasible interactions (i.e., available experimentally) T_k, where the $f_k(t)$ are amplitudes found by minimizing the norm of $(H_B - H_{CD})|0(t)\rangle$. A related approach uses the Lyapunov control theory (Ran *et al.*, 2017). Similarly, Chen, Xia *et al.* (2016) and Chen *et al.* (2017) achieved feasible auxiliary Hamiltonians by adding adjustable Hamiltonians that nullify unwanted nonadiabatic couplings for specific transitions.

c. Effective counterdiabatic field

In Petiziol *et al.* (2018, 2019) $H_0(t) = \sum_k u_k(t)H_k$ is written as before in terms of control functions $u_k(t)$ and available time-independent control Hamiltonians H_k. Using control theory arguments it is found that H_{CD} necessarily belongs to the corresponding dynamical Lie algebra, i.e., the smallest algebra that contains the $-iH_k$ and the nested commutators. As well, the action of H_{CD} can be approximated by using only the initially available Hamiltonians in an "effective counterdiabatic" Hamiltonian $H_E = \sum e_k(t)H_k$. To implement H_E in Petiziol *et al.* (2018 , 2019), the control functions $e_k(t)$ are chosen as periodic functions of period T with the form of a truncated Fourier expansion $\sum_k \mathcal{A}_k \sin(k\omega t) + \mathcal{B}_k \cos(k\omega t)$, where $\omega = 2\pi/T$.

The coefficients are determined by setting the first terms of the Magnus expansion generated by H_E to match those of the desired evolution stroboscopically at multiples of T and interpolating smoothly in between. Avoided crossing problems and entanglement creation are addressed with this technique. Note alternative uses of the Magnus expansion in the WAHWAH technique of Schutjens *et al.* (2013), aimed at producing fast pulses to operate on a qubit without interfering with other qubits in frequency-crowded systems, and in Claeys *et al.* (2019).

d. Dressed-states approach

CD driving is generalized by Baksic, Ribeiro, and Clerk (2016) by considering a dressed-states approach which uses three different dynamical pictures. In this summary the notation and even the terminology differs from Baksic, Ribeiro, and Clerk (2016); see Table I.

First consider a Schrödinger picture description where the driving Hamiltonian is $H_0(t) + H_c(t)$ with reference Hamiltonian $H_0(t)$ as in Eq. (7), and driven wave function $|\psi(t)\rangle$. $H_c(t)$ will be found later so that the total Hamiltonian satisfies some conditions. Then a first rotating picture defined by $|\psi_I(t)\rangle = U(t)^{\dagger}|\psi(t)\rangle$ is introduced, where $U(t) = \sum_n |n(t)\rangle\langle n|$ and the $|n\rangle$ are time independent. A simple choice is $|n\rangle = |n(0)\rangle$ that insures $U(0) = U(t_f) = 1$. Since $|n(t)\rangle$ are instantaneous (adiabatic) eigenstates of $H_0(t)$

TABLE I. Scheme for "dressed-state" driving (Baksic, Ribeiro, and Clerk, 2016).

Picture	Wave function	Unitary transformation	Hamiltonian
Schrödinger	$\psi(t)$		$H = H_0 + H_c$
First rotating picture ("adiabatic")	$\psi_I(t) = U^\dagger \psi(t)$	$U = \sum_n \lvert n(t)\rangle\langle n\rvert$	$H_I = i\hbar \dot{U}^\dagger U + U^\dagger H U$
Second rotating picture ("dressed")	$\psi_{II}(t) = V^\dagger \psi_I(t)$	$V = \sum_n \lvert \tilde{n}(t)\rangle\langle n\rvert$	$H_{II} = i\hbar \dot{V}^\dagger V + V^\dagger H_I V$

we may naturally call this picture the "adiabatic frame" with driving Hamiltonian $H_I(t)$; see Table I. Then a second rotating frame is introduced as $|\psi_{II}(t)\rangle = V(t)^\dagger |\psi_I(t)\rangle$, with $V(t) = \sum_n |\tilde{n}(t)\rangle\langle n|$, driven by $H_{II}(t)$. $\{|\tilde{n}(t)\rangle\}$ are called dressed states and it is assumed that $V(0) = V(t_f) = 1$. The method to generate shortcuts is to choose $V(t)$, i.e., the functions $|\tilde{n}(t)\rangle$ and H_c so that $H_{II}(t)$ is diagonal in the basis $\{|n\rangle\}$, $H_{II}(t) = \sum_n |n\rangle E_n^{II}(t)\langle n|$. Back to the Schrödinger picture this means that no transitions occur among states $U(t)V(t)|n\rangle = U(t)|\tilde{n}(t)\rangle$.

$V(t)$ is chosen to ensure that $H_c(t)$ is feasible. The two nested transformations make the method more involved and less intuitive than standard CD driving. To gain insight note that if $V(t) = 1$ for all t the method reduces to standard CD driving. One can think of V as a way to add flexibility to the inverse engineering so as to drive states in the Schrödinger picture along uncoupled $U(t)V(t)|n\rangle$ vectors rather than along vectors $U(t)|n\rangle = |n(t)\rangle$. The latter are given, up to phases, once $H_0(t)$ is specified, whereas $U(t)V(t)|n\rangle$ may still be manipulated to find a convenient $H_c(t)$ and possibly minimize the occupancy of some state to be avoided, e.g., because of spontaneous decay (Baksic, Ribeiro, and Clerk, 2016).

For applications see Baksic *et al.* (2017), Coto *et al.* (2017), Liu *et al.* (2017), Wu, Ji, and Zhang (2017b), B. B. Zhou *et al.* (2017), and X. Zhou *et al.* (2017).

e. Variational approach

Motivated by difficulties to diagonalize $H_0(t)$ and the nonlocalities in the exact counterdiabatic Hamiltonian in many-body systems, Kolodrubetz *et al.* (2017) and Sels and Polkovnikov (2017) developed a variational method to construct approximate counterdiabatic Hamiltonians without using spectral information. The starting point in Sels and Polkovnikov (2017) is a unitary transformation $U[\lambda(t)] = \sum_n |n[\lambda(t)]\rangle\langle n|$ to rotate the state $|\psi(t)\rangle$ that evolves under a time-dependent Hamiltonian $H_0[\lambda(t)]$, to the moving frame state $|\tilde{\psi}(t)\rangle = U^\dagger[\lambda(t)]|\psi(t)\rangle$, which satisfies the effective Schrödinger equation

$$i\hbar \partial_t |\tilde{\psi}\rangle = \{\tilde{H}_0[\lambda(t)] - \dot{\lambda}\tilde{A}_\lambda\}|\tilde{\psi}\rangle, \tag{31}$$

where $\tilde{H}_0$ is diagonal in the $|n\rangle$ basis and $\tilde{A}_\lambda$ is the adiabatic "gauge potential" in the moving frame,

$$\tilde{H}_0[\lambda(t)] = U^\dagger H_0[\lambda(t)]U = \sum_n E_n(\lambda)|n\rangle\langle n|,$$
$$\tilde{A}_\lambda = i\hbar U^\dagger \partial\lambda U. \tag{32}$$

All nonadiabatic transitions are produced by the gauge potential. In the counterdiabatic approach the system is driven by the Hamiltonian

$$H(t) = H_0 + \dot{\lambda}A_\lambda, \tag{33}$$

where $A_\lambda = U\tilde{A}_\lambda U^\dagger = i\hbar(\partial_\lambda U)U^\dagger$ such that in the moving frame $H_0^{\text{eff}} = \tilde{H}_0$ is diagonal and no transitions are allowed. Up to now we have only introduced a new notation and terminology in Eqs. (31)–(33).[2] In the adiabatic limit $|\dot{\lambda}| \to 0$ the Hamiltonian (33) reduces to the original one $H(t) = H_0(t)$. After differentiating the first equation in Eq. (32), the gauge potential satisfies (Jarzynski, 2013)

$$i\hbar(\partial_\lambda H_0 + F_{ad}) = [A_\lambda, H_0], \tag{34}$$

where $F_{ad} = -\sum_n \partial_\lambda E_n(\lambda)|n(\lambda)\rangle\langle n(\lambda)|$ is the adiabatic force operator. Since, by construction, F_{ad} commutes with H_0, Eq. (34) implies that

$$[i\hbar\partial_\lambda H_0 - [A_\lambda, H_0], H_0] = 0, \tag{35}$$

where the difficult-to-calculate force has been eliminated. This equation can be used to find the adiabatic gauge potentials directly without diagonalizing the Hamiltonian. Moreover, solving this equation is analogous to minimizing the Hilbert-Schmidt norm of the operator

$$G_\lambda = \partial_\lambda H_0 + \frac{i}{\hbar}[A_\lambda^*, H_0] \tag{36}$$

with respect to A_λ^*, where A_λ^* is a trial gauge potential. For an application to prepare ground states in a lattice gauge model, see Hartmann and Lechner (2018).

Potential problems with this scheme are that it may be difficult to know what local operators should be included in the variational basis, and moreover their practical realizability is not guaranteed. To solve these two difficulties, Claeys *et al.* (2019) expanded the gauge potential in terms of nested commutators of the Hamiltonian H_0 and the driving term $\partial_\lambda H_0$, even if these do not close a Lie algebra. Since the commutators also arise in the Magnus expansion in Floquet systems, they can be realized up to arbitrary order using Floquet engineering, i.e., periodical driving (Boyers *et al.*, 2018). The expansion coefficients can be calculated either analytically or variationally. The method can be adapted to suppress excitations in a known frequency window. Application examples were provided for a two- and a three-level system, where one, respectively, two terms

[2]We assumed for simplicity a dependence on time via a single parameter λ. A more general dependence on a vector $\boldsymbol{\lambda}$ is worked out by Deffner, Jarzynski, and del Campo (2014) and Nishimura and Takahashi (2018) which leads to a decomposition of the CD term and a "zero curvature condition" among the CD components.

returned the exact gauge potential, and to a many-body spin chain, where a limited number of terms and an approximate gauge potential resulted in a drastic increase in fidelity. Further useful properties of the expansion are that it relates the locality of the gauge potential to the order in the expansion, and that it remains well defined in the thermodynamic and classical limits.

f. Counterdiabatic Born-Oppenheimer dynamics

Duncan and del Campo (2018) proposed to exploit the separation of fast and slow variables using the Born-Oppenheimer approximation. Simpler CD terms (compared to the exact CD term) for the fast and slow variables can be found in two steps avoiding the diagonalization of the full Hamiltonian. The method is tested for two coupled harmonic oscillators and a system of two charged particles.

g. Constant CD-term approximation

Oh and Kais (2014) proposed, in the context of the adiabatic Grover's search algorithm implemented by a two-level system, to substitute the exact CD term by a constant term. This method improves the scaling of the nonadiabatic transitions with respect to the running time. J. Zhang *et al.* (2018) performed an experiment with a single trapped ion choosing the constant term with the aid of a numerical simulation.

In a different vein Santos and Sarandy (2018) discussed the conditions for $H_0(t)$ and phase choice necessary in the unitary evolution operator (11) to implement an exact constant driving.

C. Invariants and scaling laws

Dynamical invariants and invariant-based engineering constitute a major route to design STA protocols. The basic reason, already sketched in Eqs. (5) and (6), is that, in linear systems, determining the desired dynamics amounts to setting dynamical invariants of motion, and the Hamiltonian may in principle be found from them. This connection is quite general and is also valid classically (Lewis and Leach, 1982), but it is mostly applied for systems in which the Hamiltonian form and corresponding invariants are known explicitly as functions of auxiliary parameters that satisfy auxiliary equations consistent with the dynamical equation and the invariant.

1. Lewis-Riesenfeld invariants

Originally proposed in 1969, a Lewis-Riesenfeld invariant (Lewis and Riesenfeld, 1969) for a Hamiltonian $H(t)$ is a Hermitian operator $I(t)$ which satisfies

$$\frac{dI}{dt}=\frac{\partial I}{\partial t}+\frac{i}{\hbar}[H,I]=0, \tag{37}$$

so that the expectation values for states driven by $H(t)$ are constant in time. Since $I(t)$ is a constant of motion it has time-independent eigenvalues. If $|\phi_n(t)\rangle$ is an instantaneous eigenstate of $I(t)$, a solution of the Schrödinger equation $i\hbar\partial_t|\psi_n(t)\rangle=H(t)|\psi_n(t)\rangle$ can be constructed as $|\psi_n(t)\rangle=e^{i\alpha_n(t)}|\phi_n(t)\rangle$. Here $\alpha_n(t)=(1/\hbar)\int_0^t\langle\phi_n(s)|[i\hbar\partial_s-H(s)]|\phi_n(s)\rangle ds$ is the Lewis-Riesenfeld phase. Hence a general solution to the Schrödinger equation can be written as

$$|\psi(t)\rangle=\sum_n c_n|\psi_n(t)\rangle, \tag{38}$$

where the c_n are independent of time.

These invariants were originally used to solve for the state driven by a known time-dependent Hamiltonian (Lewis and Riesenfeld, 1969). In shortcuts to adiabaticity this idea is reversed (Chen, Ruschhaupt *et al.*, 2010) and the Hamiltonian is found from a prescribed state evolution. Formally, a time evolution operator of the form

$$U=\sum_n e^{i\alpha_n(t)}|\phi_n(t)\rangle\langle\phi_n(0)| \tag{39}$$

implies a Hamiltonian $H(t)=i\hbar\dot{U}U^\dagger$. This is the essence of invariant-based inverse engineering.

For a given Hamiltonian there are many possible invariants. For example, the density operator describing the evolution of a system is a dynamical invariant. The choice of which particular invariant to use is made on the basis of mathematical convenience. Invariants have also been generalized to non-Hermitian invariants and Hamiltonians (Gao, Xu, and Qian, 1992; Lohe, 2009; Ibáñez, Martínez-Garaot *et al.*, 2011), as well as open systems (see Sec. V).

A connection to adiabaticity is asymptotic. In the limit of long operation times (i.e., adiabatic), Eq. (37) becomes $[H,I]\approx 0$ and the dynamics prescribed by invariant-based engineering will approach adiabatic dynamics driven by H. Hence for long times, $H(t)$ and $I(t)$ have approximately a common eigenbasis for all times.

Other relations to adiabaticity do not need long times nor common bases for $H(t)$ and $I(t)$ at all times. In particular, demanding only that the invariant and the Hamiltonian commute at the start and the end of the process, i.e., $[I(0),H(0)]=[I(t_f),H(t_f)]=0$, the eigenstates of the invariant and the Hamiltonian coincide at initial and final times, but may differ with each other at intermediate times because the commutativity is not imposed. If no level crossings take place, the final state will keep the initial populations for each nth level, as in an adiabatic process, but in a finite (short, faster-than-adiabatic) time. This leaves freedom to choose how the state evolves in the intermediate time and then use Eq. (37) to find the Hamiltonian that drives such a state evolution. The flexibility can be exploited to improve the stability of the schemes against noise and systematic errors; see Sec. II.H.

The relation of the invariant-based approach to CD driving (Chen, Torrontegui, and Muga, 2011) implies a different connection to adiabaticity. So far we have not mentioned in this section any "reference" $H_0(t)$, but by reinterpreting $|\phi_n(t)\rangle$ as eigenvectors of $H_0(t)$, and the Lewis-Riesenfeld phases as adiabatic phases, an implicit $H_0(t)$ operator may be written down using Eq. (20). Hence an implicit $H_{CD}(t)$ follows from subtraction, $H_{CD}(t)=H(t)-H_0(t)$. In invariant-based engineering, however, these implicit operators are not really used and do not play any role in practice. As a consequence of the different emphases and construction

recipes for $H(t)$, given some initial and final Hamiltonians, STA protocols designed via CD or invariant approaches are often very different.

Lie algebras.—As first noted by Sarandy, Duzzioni, and Serra (2011), invariant-based inverse engineering can also be formulated in terms of dynamical Lie algebras. The assumption of a Lie structure is also used to classify and construct dynamical invariants for four-level or smaller nontrivial systems for specific applications (Güngördü *et al.*, 2012; Herrera *et al.*, 2014; Kiely *et al.*, 2016). The approaches by Martínez-Garaot *et al.* (2014) and Petiziol *et al.* (2018), already discussed, also make use of the Lie algebraic structure.

Torrontegui, Martínez-Garaot, and Muga (2014) provided a bottom-up construction procedure of the Hamiltonian using invariants and Lie algebras. Let us assume that the Hamiltonian of a system $H(t)$ and the invariant $I(t)$ can be written as linear combinations of Hermitian operators G_a (generators),

$$H(t)=\sum_{a=1}^{N}h_a(t)G_a,\qquad I(t)=\sum_{a=1}^{N}f_a(t)G_a, \tag{40}$$

that form a Lie algebra closed under commutation; see Eq. (28). Inserting these forms into Eq. (37), we get that

$$\dot{f}_a(t)-\sum_{b=1}^{N}\mathcal{A}_{ab}(t)h_b(t)=0, \tag{41}$$

where the $N\times N$ matrix $\mathcal{A}$ is defined by

$$\mathcal{A}_{ab}\equiv\frac{1}{i\hbar}\sum_{c=1}^{N}\alpha_{abc}f_c(t), \tag{42}$$

and the α_{abc} are the structure constants. In vector form,

$$\partial_t\vec{f}(t)=\mathcal{A}\vec{h}(t), \tag{43}$$

where the vectors $\vec{f}(t)$ and $\vec{h}(t)$ represent the invariant and Hamiltonian, respectively. The inversion trick is to first choose the auxiliary functions $\vec{f}(t)$ (and therefore the state evolution) and infer $\vec{h}(t)$ from this. Technically the inversion requires introducing a projector $\mathcal{Q}$ for the null subspace of $\mathcal{A}$ and the complementary projector $\mathcal{P}$. In $\mathcal{P}$ subspace a pseudoinverse matrix can be defined, and the $\mathcal{Q}$ component of $\vec{h}$ is chosen to make the resulting Hamiltonian realizable (Torrontegui, Martínez-Garaot, and Muga, 2014). Examples for two- [SU(2) algebra] and three-level systems (with the four-dimensional algebra U3S3) were provided. Levy *et al.* (2018) reformulated this formalism in terms of the density operator and used it to design robust control protocols against the influence of different types of noise. In particular, they developed a method to construct a control protocol which is robust against dissipation of the population and minimizes the effect of dephasing.

2. Examples of invariant-based inverse engineering

Lewis-Riesenfeld invariants have been used to design state transfer schemes in two-level (Ruschhaupt *et al.*, 2012; Martínez-Garaot *et al.*, 2013; Kiely and Ruschhaupt, 2014), three-level (Chen and Muga, 2012a; Kiely and Ruschhaupt, 2014; Benseny *et al.*, 2017), and four-level systems (Güngördü *et al.*, 2012; Herrera *et al.*, 2014; Kiely *et al.*, 2016), or Hamiltonians quadratic in creation and annihilation operators (Stefanatos and Paspalakis, 2018a). They are also useful to design motional dynamics in harmonic traps or otherwise. Many more applications specific for different system types may be found in Sec. III. Here we provide two basic examples, the two-level model and the Lewis-Leach family of potentials for a particle of mass m moving in 1D.

a. Two-level system

We now present an example of a two-level system with a Hamiltonian given by

$$H(t)=\frac{\hbar}{2}\begin{pmatrix}-\Delta(t) & \Omega_R(t)-i\Omega_I(t)\\ \Omega_R(t)+i\Omega_I(t) & \Delta(t)\end{pmatrix}, \tag{44}$$

and an invariant of the form

$$I(t)=\frac{\hbar}{2}\begin{pmatrix}\cos[\theta(t)] & \sin[\theta(t)]e^{-i\alpha(t)}\\ \sin[\theta(t)]e^{i\alpha(t)} & -\cos[\theta(t)]\end{pmatrix}. \tag{45}$$

From the equation that defines the invariant, Eq. (37), $\theta(t)$ and $\alpha(t)$ must satisfy

$$\dot{\theta}=\Omega_I\cos\alpha-\Omega_R\sin\alpha, \tag{46}$$

$$\dot{\alpha}=-\Delta-\cot\theta(\Omega_R\cos\alpha+\Omega_I\sin\alpha). \tag{47}$$

The eigenvectors of $I(t)$ are

$$|\phi_+(t)\rangle=\begin{pmatrix}\cos(\theta/2)e^{-i\alpha/2}\\ \sin(\theta/2)e^{i\alpha/2}\end{pmatrix}, \tag{48}$$

$$|\phi_-(t)\rangle=\begin{pmatrix}\sin(\theta/2)e^{-i\alpha/2}\\ -\cos(\theta/2)e^{i\alpha/2}\end{pmatrix}, \tag{49}$$

with eigenvalues $\pm\hbar/2$. The angles α and θ can be thought of as spherical coordinates on the Bloch sphere. The general solution of the Schrödinger equation is then a linear combination of the eigenvectors of $I(t)$, i.e., $|\Psi(t)\rangle=c_+e^{i\kappa_+(t)}|\phi_+(t)\rangle+c_-e^{i\kappa_-(t)}|\phi_-(t)\rangle$, where $c_\pm\in\mathbb{C}$ and

$$\dot{\kappa}_\pm(t)=\frac{1}{\hbar}\langle\phi_\pm(t)|[i\hbar\partial_t-H(t)]|\phi_\pm(t)\rangle.$$

Therefore, it is possible to construct a particular solution

$$|\psi(t)\rangle=|\phi_+(t)\rangle e^{-i\gamma(t)/2}, \tag{50}$$

where $\gamma=\pm2\kappa_\pm$ and

$$\dot{\gamma} = \frac{1}{\sin\theta}(\Omega_R \cos\alpha + \Omega_I \sin\alpha). \tag{51}$$

Using Eqs. (46), (47), and (51) we can retrieve the physical quantities in terms of the auxiliary functions,

$$\Omega_R = \cos\alpha \sin\theta\dot{\gamma} - \sin\alpha\dot{\theta}, \tag{52}$$

$$\Omega_I = \sin\alpha \sin\theta\dot{\gamma} + \cos\alpha\dot{\theta}, \tag{53}$$

$$\Delta = -\cos\theta\dot{\gamma} - \dot{\alpha}. \tag{54}$$

If the functions α, γ, and θ are chosen with the appropriate boundary conditions, different state manipulations are possible. For example, $\theta(0) = 0$ and $\theta(t_f) = \pi$ imply perfect population inversion at a time t_f. Note the freedom to interpolate along different paths.

b. Lewis-Leach family

Consider a one-dimensional Hamiltonian $H = p^2/2m + V(q,t)$ with potential (Lewis and Leach, 1982)

$$V(q,t) = -F(t)q + \frac{m}{2}\omega^2(t)q^2 + \frac{1}{\rho(t)^2}U\left[\frac{q - q_c(t)}{\rho(t)}\right] + g(t). \tag{55}$$

These Hamiltonians have a quadratic in momentum invariant

$$I = \frac{1}{2m}[\rho(p - m\dot{q_c}) - m\dot{\rho}(q - q_c)]^2 + \frac{1}{2}m\omega_0^2\left(\frac{q - q_c}{\rho}\right)^2 + U\left(\frac{q - q_c}{\rho}\right), \tag{56}$$

provided the functions ρ, q_c, ω, and F satisfy the auxiliary equations

$$\ddot{\rho} + \omega^2(t)\rho = \frac{\omega_0^2}{\rho^3},$$
$$\ddot{q_c} + \omega^2(t)q_c = F(t)/m, \tag{57}$$

with ω_0 a constant. The first equation is known as the Ermakov equation (Ermakov, 1880), while the second is the Newton equation of motion for a forced harmonic oscillator. They can be found by inserting the quadratic-in-p invariant, Eq. (56), into Eq. (37). The properties of such invariants have also been formulated in terms of Feynman propagators (Dhara and Lawande, 1984).

For this family of Hamiltonians we can explicitly calculate the Lewis-Riesenfeld phase,

$$\alpha_n(t) = -\frac{1}{\hbar}\int_0^t dt'\left[\frac{\lambda_n}{\rho^2} + \frac{m[(\dot{q_c}\rho - q_c\dot{\rho})^2 - \omega_0^2 q_c^2/\rho^2]}{2\rho^2} + g\right], \tag{58}$$

and the eigenvectors in coordinate representation,

$$\phi_n(q,t) = \exp\left\{\frac{im}{\hbar}[\dot{\rho}q^2/2\rho + (\dot{q_c}\rho - q_c\dot{\rho})q/\rho]\right\}\rho^{-1/2}\Phi_n\left(\frac{q - q_c}{\rho}\right), \tag{59}$$

where $\Phi_n(\sigma)$ is a solution of the stationary Schrödinger equation

$$\left[-\frac{\hbar^2}{2m}\frac{\partial^2}{\partial\sigma^2} + \frac{1}{2}m\omega_0^2\sigma^2 + U(\sigma)\right]\Phi_n = \lambda_n\Phi_n, \tag{60}$$

with $\sigma = (q - q_c)/\rho$. This quadratic invariant has been instrumental in designing many of the schemes which manipulate trapping potentials for expansions, compressions, transport, launching, stopping, or combined processes. It is key, for example, to manipulate the motion of trapped ions, see Sec. III.A, and in proposals to implement STA-based interferometry (Dupont-Nivet, Westbrook, and Schwartz, 2016; Martínez-Garaot, Rodriguez-Prieto, and Muga, 2018).

Designing first the function $\rho(t)$ which determines the wave function width, and $q_c(t)$ (a classical particle trajectory), the force $F(t)$ and $\omega(t)$ can be determined using Eq. (57). The boundary values of the auxiliary functions at the time limits are fixed to satisfy physical conditions and commutativity of H and the invariant. The nonunique interpolation is usually done with polynomials or trigonometric functions.

Expansions.—Invariant-based inverse engineering for Lewis-Leach Hamiltonians was first implemented by Chen, Ruschhaupt *et al.* (2010) to cool down a trapped atom by expanding the trap. Expansions using invariant-based engineering were first implemented with ultracold atoms in a pioneering experiment on STA techniques by Schaff *et al.* (2010) and Schaff, Capuzzi *et al.* (2011). Such cooling protocols have also been envisioned to optimize sympathetic cooling (Choi, Onofrio, and Sundaram, 2011; Onofrio, 2016). For very short processes, $t_f < 1/(2\omega_f)$, where ω_f is the trap frequency at the final time, $\omega^2(t)$ may become negative during some time interval. While this implies a transient repulsive potential, the atoms always remain confined (Chen, Ruschhaupt *et al.*, 2010). A repulsive potential may or may not be difficult to implement depending on the physical setting. For example, the analysis by Torrontegui *et al.* (2018) suggested that it is viable for trapped ions.

Compared to the simplicity of invariant-based engineering, the CD approach for expansions or compressions provides, for an H_0 characterized by some predetermined time-dependent frequency $\omega(t)$, a nonlocal, cumbersome counterdiabatic term $H_{CD} = -(pq + qp)\dot{\omega}/(4\omega)$ (Muga *et al.*, 2010). However, a unitary transformation produces a new shortcut with local potential and modified frequency (Ibáñez *et al.*, 2012)

$$\omega' = \left[\omega^2 - \frac{3\dot{\omega}^2}{4\omega^2} + \frac{\ddot{\omega}}{2\omega}\right]^{1/2}, \tag{61}$$

see further connections among the two Hamiltonians in del Campo (2013) and Mishima and Izumida (2017).

So far we have considered only one-dimensional motion. Formally, the three coordinates in an ideal harmonic trap are

uncoupled so expansion or transport processes can be treated independently. However, in many cold atom experiments changing the intensity of a laser beam simultaneously affects the longitudinal and transversal frequencies (Torrontegui, Chen, Modugno, Ruschhaput *et al.*, 2012).

Transport.—Designing particle transport has been another major application of the invariant (56) (Torrontegui *et al.*, 2011; Ness *et al.*, 2018; Tobalina, Alonso, and Muga, 2018); see also Secs. II.G and III.A. Note that U in Eq. (55) is arbitrary. Setting $\omega = \omega_0 = 0$, and $\rho = 1$, $F = m\ddot{q}_c$ plays the role of a "compensating force" that cancels the inertial effects of a moving $U[q - q_c(t)]$ so that the wave function stays at rest in the frame moving with q_c.[3] $q_c(t)$ can be chosen as an arbitrary function connecting the desired initial and final trap positions. The same solution is reached applying fast forward (Masuda and Nakamura, 2010), or using unitary transformations combined with the CD approach (Ibáñez *et al.*, 2012), which in principle provides the difficult-to-realize term $H_{CD} = p\dot{q}_c$.[4]

Deffner, Jarzynski, and del Campo (2014) discussed more generally that for Hamiltonians of the form

$$H_0 = \frac{p^2}{2m} + \frac{1}{\gamma^2} U\left(\frac{q-f}{\gamma}\right) \tag{62}$$

the (nonlocal) CD term is

$$H_{CD} = \frac{\dot{\gamma}}{2\gamma}[(q-f)p + p(q-f)] + \dot{f}p, \tag{63}$$

and found the generic unitary transformation that provides the local auxiliary terms that appear in Eq. (55). More general cases for multiparticle systems are discussed in the following section.

Tobalina *et al.* (2017) used the invariants to design shortcuts to adiabaticity for nonrigid driven transport and to launch particles in harmonic and general potentials. Compared to rigid transport, nonrigid transport requires a more demanding manipulation, but it also provides a wider range of control opportunities, for example, to achieve narrow velocity distributions in a launching process, suitable for accurate ion implantation or low-energy scattering experiments.

3. Scaling laws

For many-body systems constructing the Lewis-Riesenfeld invariant is in general much more involved. Takahashi (2017b) avoided this difficulty for an infinite-range Ising model in a transverse field by constructing an invariant using a mean-field *Ansatz*. However, another approach is to exploit scaling laws. If the Hamiltonian fulfills certain scaling laws one can determine the invariant in a similar manner as in Sec. II.C.2.b. Specifically the Hamiltonian

$$H(t) = \sum_{i=1}^{N}\left\{\frac{\mathbf{p}_i^2}{2m} + U[\mathbf{q}_i, \lambda(t)]\right\} + \epsilon(t)\sum_{i<j} V(\mathbf{q}_i - \mathbf{q}_j) + \sum_{i=1}^{N}\left[-\frac{m}{2}\frac{\ddot{\gamma}}{\gamma}(\mathbf{q}_i - \mathbf{f})^2 - m\ddot{\mathbf{f}}\cdot\mathbf{q}_i\right], \tag{64}$$

describing N interacting particles with the following scaling laws (Deffner, Jarzynski, and del Campo, 2014):

$$U[\mathbf{q}, \lambda(\mathbf{t})] = U_0\{[\mathbf{q} - \mathbf{f}(t)]/\gamma(t)\}/\gamma(t)^2,$$
$$V(\kappa\mathbf{q}) = \kappa^{-\alpha}V(\mathbf{q}),$$
$$\epsilon(t) = \gamma(t)^{\alpha-2}, \tag{65}$$

where $U_0(\mathbf{q}) = U[\mathbf{q}, \lambda(0)]$, has the invariant

$$I = \sum_{i=1}^{N}\frac{1}{2m}[\gamma(\mathbf{p}_i - m\dot{\mathbf{f}}) - m\dot{\gamma}(\mathbf{q}_i - \mathbf{f})]^2 + \sum_{i=1}^{N} U_0\left(\frac{\mathbf{q}_i - \mathbf{f}}{\gamma}\right) + \sum_{i<j} V\left(\frac{\mathbf{q}_i - \mathbf{q}_j}{\gamma}\right). \tag{66}$$

The method based on Lewis-Riesenfeld invariants is not applicable to nonlinear equations such as the Gross-Pitaevskii equation, but the presence of scaling laws can still prove beneficial for inverse engineering. Scaling solutions for the Gross-Pitaevskii equation were first noticed by Castin and Dum (1996) and Kagan, Surkov, and Shlyapnikov (1996) and were exploited to perform STA expansions in harmonic traps by Muga *et al.* (2009). For example, the 1D equation

$$i\hbar\partial_t\psi(x,t) = \left[-\frac{\hbar^2}{2m}\frac{\partial^2}{\partial x^2} + \frac{1}{2}m\omega^2(t)x^2 + g(t)|\psi(x,t)|^2\right]\psi(x,t), \tag{67}$$

with $g(t) = g_0/\rho(t)$ has scaling solutions of the form

$$\psi(x,t) = \rho^{-1/2}e^{im\dot{\rho}x^2/2\hbar\rho}e^{-i\mu\tau(t)/\hbar}\Psi(x/\rho, 0) \tag{68}$$

provided that the following consistency equations, including the Ermakov equation, are fulfilled:

$$\ddot{\rho} + \omega(t)^2\rho = \frac{\omega_0^2}{\rho^3},$$
$$\tau(t) = \int_0^t \frac{dt'}{\rho^2(t')}, \tag{69}$$

and $\Psi(y,\tau)$ satisfies

[3]For rigidly moving harmonic traps, a formal alternative to the compensating force is to set $U = 0$ and $F = m\omega_0^2 q_0(t)$, keeping $\omega(t) = \omega_0$ as the trap frequency (Torrontegui *et al.*, 2011). The two routes may be shown to be equivalent up to a gauge time-dependent term; see, e.g., Tobalina, Alonso, and Muga (2018).

[4]See, however, An *et al.* (2016) and Sec. III.E for a possible realization. Note that CD terms like $-(pq + qp)\dot{\omega}/(4\omega)$ or $p\dot{q}_c$ anticommute with the time reversal operator Θ (Sels and Polkovnikov, 2017). Microscopic irreversibility holds by changing the sign of the external forces in the backward trajectories (Campisi, Hänggi, and Talkner, 2011). In the two examples above this means to change $\dot{\omega} \to -\dot{\omega}$ and $\dot{q}_c \to -\dot{q}_c$.

$$i\hbar\frac{\partial\Psi}{\partial\tau}=-\frac{\hbar^2}{2m}\frac{\partial^2\Psi}{\partial y^2}+\frac{m\omega_0^2}{2}y^2\Psi+g_0|\Psi|^2\Psi. \tag{70}$$

Different dimensions imply different scalings. In 1D and 3D traps, the STA scaling solutions for the frequency change are found for either a simultaneous change of the time dependence of the coupling or a Thomas-Fermi type of regime, whereas 2D traps are privileged in this respect since none of these conditions are needed.

These methods were realized experimentally for trapped Bose-Einstein condensates (Schaff, Song *et al.*, 2011; Rohringer *et al.*, 2015). Scaling solutions also exist for a class of many-body systems including interacting quasi-1D Bose gases (Gritsev, Barmettler, and Demler, 2010) and were applied to construct shortcuts for a square box (del Campo and Boshier, 2012), and other trapping potentials (del Campo, 2013; Deffner, Jarzynski, and del Campo, 2014).

Inverse engineering the transport of condensates was worked out by Torrontegui, Chen, Modugno, Schmidt *et al.* (2012) using as an *Ansatz* the scaling provided by invariant theory for linear dynamics. Scaling has also been used to design STA protocols for the fast expansion of a condensate in an optical lattice (Yuce, 2012), possibly pumped from a reservoir (Ozcakmakli and Yuce, 2012).

Fermi gas.—Papoular and Stringari (2015) put to work a new class of exact scaling solutions for 3D "unitary," Fermi gases and 2D weakly interacting Bose gases in anisotropic time-dependent harmonic traps with initial and final traps having the same frequency ratios. These solutions may be useful to implement a microscope for quantum defects hosted by the cloud, avoiding the strong distortion due to free expansion. The proposal of Papoular and Stringari (2015) was realized experimentally by Deng, Chenu *et al.* (2018) and Deng, Diao *et al.* (2018) for a 3D Fermi gas "at unitarity."

4. Connection with Lax pairs

Lax pairs were originally introduced by Peter Lax in 1968 (Lax, 1968). A completely integrable nonlinear partial differential equation (PDE) can be associated with a Lax pair and Lax pairs have been used to find the solution $u(x,t)$ of the corresponding nonlinear PDE. The key objective was to construct a pair of linear differential operators $L=L(u)$, $M=M(u)$ in such a way that the equation

$$\partial_t L(u)+[L(u),M(u)]=0 \tag{71}$$

is fulfilled if and only if u is a solution of the initial nonlinear PDE. Let $\psi(t,x)$ be the eigenvectors of $L(u)$,

$$L(u)\psi=\lambda\psi, \tag{72}$$

where it follows from Eq. (71) that the eigenvalues λ must be time independent. It also follows from Eq. (71) that

$$\partial_t\psi=M(u)\psi. \tag{73}$$

This transforms the problem of solving the nonlinear PDE for $u(x,t)$ to that of solving the linear equation (71) [respectively, the linear equations (72) and (73)] which is often easier to solve than the initial nonlinear PDE.

The relation between Lax pairs and shortcuts with a counterdiabatic Hamiltonian was first noted by Okuyama and Takahashi (2016). They considered systems for which H_0 is the invariant for $H=H_0+H_{CD}$ (see Sec. II.B). From the equation defining the invariant the counterdiabatic Hamiltonian can be determined by

$$\partial_t H_0=\frac{i}{\hbar}[H_0,H_{CD}]. \tag{74}$$

By comparing Eqs. (71) and (74), the connection with Lax pairs is given by setting $L=H_0$ and $M=-(i/\hbar)H_{CD}$. Okuyama and Takahashi (2016) first considered $H_0=p^2+u(x,t)$ and H_{CD} containing third order in p terms. This results in the nonlinear Korteweg–de Vries equation for the physical potential $u(x,t)$. The advantage is that a complete set of solutions for this nonlinear equation can now be found. Based on these solutions, the exact counterdiabatic term for a particle in a hyperbolic Scarf potential was determined, and unitary transformations were applied to generate feasible auxiliary Hamiltonians avoiding the cubic-in-p term. They discussed a spin lattice as a second example. When considering instead that the invariant takes the form $\gamma^2(t)H_0$ and H_{CD} includes up to first orders in p, as in Eq. (63), the scale-invariant potential (62) follows. It is also possible to extend the approach to non-scale-invariant systems.

A different but similar route is to regard Lewis-Riesenfeld invariants (Lewis and Riesenfeld, 1969) and Lax pairs (the invariants were proposed 1 yr after the Lax pairs) as two sides of the same coin (Kiely and Ruschhaupt, 2019), relating Eqs. (37) and (74) by the alternative connection $L=I$ and $M=-(i/\hbar)H$. This approach facilitates extending the domain of invariant-based shortcuts, for example, using cubic-in-p invariants with feasible interactions.

D. Variational methods

We have already discussed an STA variational approach in Sec. II.B.2.e (Kolodrubetz *et al.*, 2017; Sels and Polkovnikov, 2017) for CD driving. Here we review other variational proposals.

Takahashi (2013a, 2015) reformulated invariant-based engineering or counterdiabatic approaches in terms of a quantum brachistochrone variational problem, with the action

$$S=\int_0^T dt(\mathcal{L}_T+\mathcal{L}_S+\mathcal{L}_C) \tag{75}$$

and Lagrangians corresponding to the constraints for the process time ($\mathcal{L}_T$), the Schrödinger equation ($\mathcal{L}_S$), and additional experimental constraints ($\mathcal{L}_C$). This formulation is used to examine the stability of the driving, noting that processes are stable against variations in operators which commute with H_{CD} and unstable against variations in those that anticommute with it. This work has been extended to classical, stochastic finite-sized systems described by a continuous-time master equation to find an optimal transition-rate matrix (Takahashi and Ohzeki, 2016).

A different variational approach was worked out by Li, Sun, and Chen (2016) and J. Li *et al.* (2018). These works considered a BEC trapped in a harmonic trap. Quantum dynamical equations follow by minimizing the action defined from a Lagrangian density, using some *Ansatz* for the wave function. This allows one to cope with systems that would otherwise be difficult to treat (e.g., with no scaling laws available). However, the quality of the approximate dynamics strongly depends on the *Ansatz* chosen.

Li, Sun, and Chen (2016) used this approach to control matter waves in harmonic traps. Using as an *Ansatz* a bright solitary wave solution, approximate auxiliary equations analogous to Eqs. (57) are found. The Newton equation for the wave center remains the same, whereas the Ermakov equation is modified to include a term that depends on the nonlinear coupling parameter. Using only a time-dependent control of this parameter via a Feschbach resonance, the soliton wave function can be compressed or expanded in nonadiabatic time scales with high fidelity.

Applying the same concepts, an efficient quantum heat engine running an Otto cycle with a condensate as its working medium was proposed by J. Li *et al.* (2018). The engine strokes are done on a short timescale ensuring a large power output and high efficiency. Also, Fogarty *et al.* (2019) applied the variational approach to design the time-dependent interaction strength between two ultracold atoms so as to create entangled states.

E. Fast forward

The so-called FF approach was first derived to accelerate a given quantum dynamics by mimicking the effect of an FF button in an audio or video player (Masuda and Nakamura, 2008). The original idea was to use a scaling transformation $\tau = \alpha t$, for some constant α (inhomogeneous scalings are also possible) so that the solutions $\psi_0(\tau)$ of $i\hbar\partial_\tau\psi_0(\tau) = H(\tau)\psi_0(\tau)$ are just scaled in time as $\psi_0(\tau) = \psi_\alpha(t)$ with respect to the solutions of $i\hbar\partial_t\psi_\alpha(t) = \alpha H(\alpha t)\psi_\alpha(t)$. This concept works formally and in some discrete Hamiltonians it is experimentally viable. However, if H includes a kinetic energy it implies that the mass should be changed (Bernardo, 2019). Masuda and Nakamura (2008) solved this problem by modifying the potential but not the mass.

1. The original formalism

Consider the time-dependent Schrödinger equation

$$i\hbar\frac{\partial\psi_0(\mathbf{r},t)}{\partial t} = -\frac{\hbar^2}{2m}\Delta\psi_0(\mathbf{r},t) + V_0(\mathbf{r},t)\psi_0(\mathbf{r},t) \tag{76}$$

in a time interval $[0,T]$ with real potential V_0. To speed up the dynamics keeping the potential real, a nontrivial phase factor that depends on the coordinates has to be added to the FF wave function,

$$\psi_{FF}(\mathbf{r},t) = \psi_0(\mathbf{r},\Lambda(t))e^{i\varphi(\mathbf{r},t)}, \tag{77}$$

driven by the FF potential

$$V_{FF}(\mathbf{r},t) = -\hbar\ddot{\Lambda}\Sigma(\mathbf{r},\Lambda(t)) - 2\hbar[\dot{\Lambda}-1]\partial_t\Sigma(\mathbf{r},\Lambda(t)) - \frac{\hbar^2}{2m}(\dot{\Lambda}^2-1)[\partial_{\mathbf{r}}\Sigma(\mathbf{r},\Lambda(t))]^2 + V_0(\mathbf{r},\Lambda(t)). \tag{78}$$

The phase is given by $\varphi(\mathbf{r},t) = [\dot{\Lambda}-1]\Sigma(\mathbf{r},\Lambda(t))$, where Σ is the phase of the reference wave function $\psi_0(\mathbf{r},t) = \tilde{\psi}_0(\mathbf{r},t)\exp[i\Sigma(\mathbf{r},t)]$. Imposing $\Lambda(0)=0$, $\Lambda(t_f)=T$, $\dot{\Lambda}(0) = \dot{\Lambda}(t_f) = 1$, and $\ddot{\Lambda}(0) = \ddot{\Lambda}(t_f) = 0$ implies that $V_{FF}(\mathbf{r},0) = V_0(\mathbf{r},0)$ and $V_{FF}(\mathbf{r},t_f) = V_0(\mathbf{r},T)$. Moreover, the additional phase $\varphi(\mathbf{r},t)$ vanishes at the boundary of the time interval $[0,t_f]$. For $\dot{\Lambda} > 1$, the dynamics is accelerated while it is slowed down for $0 < \dot{\Lambda} < 1$. A negative $\dot{\Lambda}$ corresponds to a time reversed evolution.

The transposition of these results to speed up an adiabatic evolution is not direct because the adiabatic evolution holds only for an infinitely slow process that needs infinite magnification factors. A first but too naive approach consists of considering the adiabatic wave function as a candidate for applying the previous fast-forward formalism. If the system is in the nth eigenstate $\phi_n(\mathbf{r},\lambda)$ associated with the eigenvalue $E_n(\lambda)$, where λ accounts for the parameters, the corresponding adiabatic wave function reads

$$\psi_{\mathrm{ad}}(\mathbf{r},t,\lambda(t)) = \phi_n(\mathbf{r},\lambda(t))e^{-i\varphi_{\mathrm{dyn}}(t)+i\varphi_{\mathrm{ad}}(t)}, \tag{79}$$

where $\varphi_{\mathrm{dyn}}(t) = \int_0^t E_n(\lambda(t'))dt'/\hbar$ is the dynamical phase. The direct route fails and a renormalization is needed modifying both the wave function and the Hamiltonian in a consistent manner to ensure that the wave function remains valid for a finite change of the parameters (Masuda and Nakamura, 2010).

To highlight the smallness of the change of parameter, Masuda and Nakamura (2010) introduced the constant rate $\varepsilon \ll 1$ associated with $\lambda \to \lambda + \delta\lambda$ where $\delta\lambda = \varepsilon t$. A finite change of the parameter λ during the time interval $[0,t_f]$ is given by

$$\lambda(\Lambda(t_f)) - \lambda(0) = \varepsilon\Lambda(t_f). \tag{80}$$

The expression for the FF potential to drive the regularized wave function

$$\psi^{(\mathrm{reg})}(\mathbf{r},t,\lambda(t)) = \phi_n(\mathbf{r},\lambda(t))e^{-i\varphi_{\mathrm{dyn}}(t)+i\varepsilon\delta\theta(\mathbf{r},t)} \tag{81}$$

finally reads (Masuda and Nakamura, 2010)

$$V_{FF}(\mathbf{r},t) = \dot{\Lambda}\varepsilon\delta V[\mathbf{r},\tilde{\lambda}_t] + V_0[\mathbf{r},\tilde{\lambda}_t] - \hbar\ddot{\Lambda}\varepsilon\delta\theta[\mathbf{r},\tilde{\lambda}_t] - \hbar\dot{\Lambda}^2\varepsilon^2\left.\frac{\partial\delta\theta}{\partial\lambda}\right|_{\mathbf{r},\tilde{\lambda}_t} - \frac{\hbar^2}{2m_0}\dot{\Lambda}^2\varepsilon^2(\nabla\delta\theta)^2, \tag{82}$$

with $\tilde{\lambda}_t = \lambda(\Lambda(t))$, and

$$0 = |\phi_n|^2 \Delta\delta\theta + 2\mathrm{Re}[\phi_n \nabla\phi_n^*] \cdot \nabla\delta\theta + \frac{2m}{\hbar}\mathrm{Re}[\phi_n \partial_\lambda \phi_n^*],$$
$$\delta V = -\hbar \mathrm{Im}\left[\frac{\partial_\lambda \phi_n}{\phi_n}\right] - \frac{\hbar^2}{m}\mathrm{Im}\left[\frac{\nabla\phi_n}{\phi_n}\right] \cdot \nabla\delta\theta. \tag{83}$$

As an application, consider the 1D transport of a wave function with a moving confining potential $V_0(x,t) = U(x-\varepsilon t)$. We readily find $\delta V = 0$ and $\delta\theta = mx/\hbar$ for all n. The fast-forward potential is now n independent and reads

$$V_{FF}(x,t) = U(x - x_0(t)) - mx\ddot{x}_0, \tag{84}$$

with $x_0(t) = \varepsilon\Lambda(t)$ and terms that depend only on time have been dropped. This result is exactly the one found by the compensating force approach within invariant-based inverse engineering (Torrontegui *et al.*, 2011), see Sec. II.C.2.b: the inertial forces in the frame attached to the moving potential are compensated for by an appropriate uniform time-dependent force.

Let us underline some conceptual and methodological similarities and differences with the CD approach: even if the adiabatic states $\phi_n(\mathbf{r}, \lambda(\mathbf{t}))$ are used as a reference in the construction, now the auxiliary potential in general depends on the specific nth wave function used (except in the previous example and for the Lewis-Leach family as discussed later), and the dynamical wave function differs along the dynamics with the adiabatic function more strongly than just by a (constant in $\mathbf{r}$) phase factor, because of the position-dependent phases in Eq. (81). Moreover, the FF method leads by construction to local and real potentials. By contrast, the CD recipe may lead to auxiliary nonlocal terms that depend on the momentum.

2. Streamlined fast-forward approach

The original fast-forward approach is somewhat involved. A simpler, more direct "streamlined version" of fast forward was proposed by Torrontegui, Martínez-Garaot *et al.* (2012) and further developed further by Torrontegui, Martínez-Garaot *et al.* (2013) and Martínez-Garaot *et al.* (2016) without making explicit use of a slow reference adiabatic process. Kiely *et al.* (2015) extended the streamlined version for a charged particle in an electromagnetic field.

This streamlined version is essentially inverse engineering. For this discussion we use a 1D setting. The key simplification is to directly inverse engineer the potential $V(x,t)$ from the given (desired) $\psi(x,t) = \rho(x,t)e^{i\phi(x,t)}$ wave function in the Schrödinger equation, imposing $V(x,t)$ to be local,

$$V(x,t) = \frac{1}{\psi(x,t)}\left(i\hbar\frac{\partial\psi(x,t)}{\partial t} + \frac{\hbar^2}{2m}\frac{\partial^2\psi(x,t)}{\partial x^2}\right). \tag{85}$$

Using the representation (ρ and ϕ real)

$$\psi(x,t) = \rho(x,t)e^{i\phi(x,t)}, \tag{86}$$

and imposing $\mathrm{Im}[V(x,t)] = 0$, we get a continuity equation

$$\frac{1}{\rho}\frac{\partial\rho}{\partial t} + \frac{\hbar}{2m}\left(\frac{2}{\rho}\frac{\partial\phi}{\partial x}\frac{\partial\rho}{\partial x} + \frac{\partial^2\phi}{\partial x^2}\right) = 0, \tag{87}$$

that links ρ and ϕ. In particular, if $\rho(x,t)$ is given, $\phi(x,t)$ cannot be arbitrary. The expression for the potential then reads

$$V(x,t) = -\hbar\frac{\partial\phi}{\partial t} + \frac{\hbar^2}{2m}\left[\frac{1}{\rho}\frac{\partial^2\rho}{\partial x^2} - \left(\frac{\partial\phi}{\partial x}\right)^2\right]. \tag{88}$$

Equation (87) can be integrated formally,

$$\frac{\partial\phi}{\partial x} = -\frac{mu(x,t)}{\hbar}, \tag{89}$$

where u plays the role of a "hydrodynamic velocity,"

$$u(x,t) = \frac{1}{\rho^2(x,t)}\frac{\partial}{\partial t}\left(\int_0^x \rho^2(x',t)dx'\right). \tag{90}$$

The potential $V(x,t)$ can therefore be inferred from $\rho(x,t)$ as

$$V(x,t) = m\frac{\partial}{\partial t}\int_0^x u(x',t)dx' + \frac{\hbar^2}{2m}\frac{1}{\rho(x,t)}\frac{\partial^2\rho(x,t)}{\partial x^2} - \frac{1}{2}mu^2(x,t) - \hbar\dot{\phi}_0(t), \tag{91}$$

where $\phi_0 \equiv \phi(x=0,t)$. This is the central result by Martínez-Garaot *et al.* (2016).

While the freedom to choose $\rho(x,t)$ is very welcome for applications that go beyond the speedup of adiabatic processes, for example, a transfer between the ground and the first excited state of a harmonic oscillator, ρ may of course also be chosen as an adiabatic function. Then connections to the other STA approaches can be made. An important fact is that for the Lewis-Leach family of Hamiltonians, the fast-forward potential becomes n independent (Torrontegui, Martínez-Garaot *et al.*, 2012; Patra and Jarzynski, 2017b) and the method provides the terms found in invariant-based inverse engineering. As well, the local FF potentials may be unitarily related to the nonlocal CD Hamiltonians. Moreover, Patra and Jarzynski (2017b) noticed the following connection with CD driving: The generally state-dependent Hamiltonian

$$H_{CD}(n) = -\frac{pu_n + u_n p}{2}, \tag{92}$$

where u_n is the hydrodynamic velocity for the nth adiabatic state, acts on the (parallel transported, real) $\langle x|n(t)\rangle$ exactly as H_{CD} does. They also introduced an acceleration flow field $a(x,t) = -\partial u/\partial t + u\partial u/\partial x$ so that the FF potential for a real function $\rho(x,t)$ corresponding to some eigenstate of H_0, which includes kinetic energy and a reference potential $V_0(x,t)$, may be written compactly as

$$V(x,t) = V_0(x,t) - m\int_0^x a(x',t)dx'. \tag{93}$$

FF potentials may have divergences due to wave function nodes. Nevertheless, Martínez-Garaot *et al.* (2016)

demonstrated that in a transition from ground to excited states, truncating the potential is a viable approximation.

3. Generalizations and terminology

Masuda and Rice (2016) reviewed FF and CD approaches focusing on applications in molecular systems. The FF method was extended to finite-dimensional Hilbert space with applications to drive two-level (Takahashi, 2014) and three-level systems (Masuda and Rice, 2016), or two-spin systems (Setiawan *et al.*, 2017) and spin clusters with different geometries (Setiawan *et al.*, 2019). In a finite Hilbert space, the auxiliary potential may be constrained by some criterion (e.g., to be diagonal). In particular, Setiawan *et al.* (2017) found different state-dependent CD terms.

FF was applied to manipulate Bose-Einstein condensates in optical lattices (Masuda, Nakamura, and del Campo, 2014; Masuda and Rice, 2014; Masuda, Nakamura, and Nakahara, 2018), to accelerate the STIRAP protocol (Masuda and Rice, 2015a, 2016), or to investigate the fast generation of entanglement in spin systems (Setiawan *et al.*, 2017). The extension to the classical realm was discussed by Jarzynski *et al.* (2017); see Sec. VII.A.

The method was also used to control a charged quantum particle that interacts with electromagnetic fields (Masuda and Nakamura, 2011; Kiely *et al.*, 2015; Masuda and Rice, 2015c). In Kiely *et al.* (2015) the fields found via invariant-based engineering and (streamlined) FF, to change the radial spread of the particle state in a Penning trap, are shown to be equivalent. Khujakulov and Nakamura (2016) and Nakamura *et al.* (2017) accelerated the tunneling of a charged particle treating the wave function phase differently than Masuda and Nakamura (2010).

We conclude the section with a comment on terminology. Some [see, e.g., Bukov, Sels, and Polkovnikov (2019) and Villazon, Polkovnikov, and Chandran (2019)] qualify as FF any Hamiltonian $H[\lambda(t)]$ for which no terms are added and only the parameter λ (possibly multidimensional) is shaped in time to get to target states with unit fidelity. While this notion is in agreement with some of the results of the FF methodology previously described, it generally covers a different domain. For example, Masuda and Rice (2015a, 2016) set a discrete FF approach where actually an additional control parameter with respect to the CD driving term is added.

F. FAQUAD and related approaches

Fast quasiadiabatic (FAQUAD) and related approaches depart from the core of paradigms discussed so far in that they are intended from the start as approximate methods to balance two conflicting aims: shortening the process time and keeping the process as adiabatic as possible with respect to the actual Hamiltonian, not with respect to a reference Hamiltonian. For Hamiltonians that depend on one control parameter $\lambda(t)$, the strategy is to distribute its rate of change $\dot{\lambda}$ so that diabatic transitions are equally likely along the process. In this way $\dot{\lambda}$ slows down at and near avoided crossings but allows for fast changes away from them to make diabatic transitions weak along the whole process.

The specific methods differ on the following: the exact recipe used to distribute diabaticity "homogeneously" from $t=0$ to t_f, which leads to different $\lambda(t)$, and on the spectral information needed to implement them. This latter aspect sets a hierarchy of complementary approaches: the maximum information corresponds to FAQUAD, which needs the eigenfunctions and eigenvalues; the local adiabatic, the uniform adiabatic, or the parallel adiabatic transfer approaches imply an intermediate level which only requires eigenvalues; finally, phenomenological approaches may be based on knowing only the location of avoided crossings (Amin, 2008; Xing-Xin *et al.*, 2013). Complex systems and, in particular, many-body systems to implement quantum adiabatic computing and quantum annealing constitute a natural domain and motivation to develop effective methods that need little or no spectral information (Albash and Lidar, 2018; Tian, 2018). Of course there is also a domain of simpler systems with more information-consuming approaches that are useful and applicable.

FAQUAD.—The idea of keeping the adiabaticity parameter constant along trap expansions, i.e., such that $\dot{\omega}/\omega^2 = c \ll 1$, had been applied in a number of works (Kastberg *et al.*, 1995; Chen, Ruschhaupt *et al.*, 2010; Bowler *et al.*, 2012; Torrontegui, Chen, Modugno, Ruschhaput *et al.*, 2012; Martínez-Garaot *et al.*, 2013) and was generalized for other systems in the FAQUAD approach developed by Martínez-Garaot, Ruschhaupt *et al.* (2015). In the simplest two-level scenario with instantaneous eigenvalues $E_{1,2}(t)$ and eigenvectors $\phi_{1,2}(t)$,

$$\hbar\left|\frac{\langle\phi_1(t)|\partial_t\phi_2(t)\rangle}{E_1(t)-E_2(t)}\right| = \hbar\left|\frac{\langle\phi_1(t)|\partial H/\partial t|\phi_2(t)\rangle}{[E_1(t)-E_2(t)]^2}\right| = c, \quad (94)$$

and, as $\lambda=\lambda(t)$, the chain rule gives

$$\dot{\lambda} = \mp\frac{c}{\hbar}\left|\frac{E_1(\lambda)-E_2(\lambda)}{\langle\phi_1(\lambda)|\partial_\lambda\phi_2(\lambda)\rangle}\right| = \mp\frac{c}{\hbar}\left|\frac{[E_1(\lambda)-E_2(\lambda)]^2}{\langle\phi_1(\lambda)|\partial H/\partial\lambda|\phi_2(\lambda)\rangle}\right|, \quad (95)$$

where $\mp$ applies to a monotonous decrease or increase of $\lambda(t)$. Equation (95) must be solved with the boundary conditions $\lambda(0)$ and $\lambda(t_f)$, which fixes c and the integration constant. This technique has been applied to accelerate processes described by two- and three-level systems such as cotunneling and splitting of two bosons in a double well, see Fig. 5, to generate macroscopically entangled states in a Tonks-Girardeau gas (Martínez-Garaot, Palmero *et al.*, 2015), to design optical waveguide devices (Chung, Lee, and Tseng, 2017; Liu and Tseng, 2017; Martínez-Garaot, Muga, and Tseng, 2017), and quantum neural networks (Torrontegui and García-Ripoll, 2019).

Other approaches.—In the "parallel adiabatic transfer" technique (Guérin, Thomas, and Jauslin, 2002; Guérin, Hakobyan, and Jauslin, 2011) the level gap is required to be constant, which prevents it from being applicable when the initial and final gaps are different.

The "uniform adiabatic" method developed by Quan and Zurek (2010) relies on a comparison of transition and relaxation time scales and proposes, instead of Eq. (95),

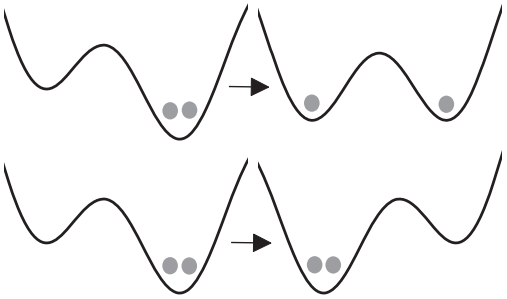

FIG. 5. Splitting and cotunneling operations on two interacting bosons performed by FAQUAD. From Martínez-Garaot, Ruschhaupt *et al.*, 2015.

$$\dot{\lambda} = \mp \frac{c_{UA}}{\hbar} \left| \frac{[E_1(\lambda) - E_2(\lambda)]^2}{\partial [E_1(\lambda) - E_2(\lambda)]/\partial \lambda} \right|. \tag{96}$$

The "local adiabatic" approach (Roland and Cerf, 2002; Richerme *et al.*, 2013) gives an equation similar to Eq. (95), without the factor $\langle \phi_1(\lambda)|\partial H/\partial\lambda|\phi_2(\lambda)\rangle$. This leads to a different constant c and time dependence of the parameter $\lambda(t)$, and therefore different minimal times. There are many works applying the local adiabatic method in the context of adiabatic quantum computation (Albash and Lidar, 2018). For the Grover problem to find a marked item in an unsorted database of N items, the schedule provided by the local adiabatic approach provides the best asymptotic scaling of the time needed with respect to N (Albash and Lidar, 2018). Schaller, Mostame, and Schützhold (2006) generalized the local adiabaticity condition taking into account high-order powers of $E_1(\lambda) - E_2(\lambda)$. Moreover, Wiebe and Babcock (2012) and Kieferová and Wiebe (2014) proposed a method combining linear local adiabaticity and the boundary cancellation methods. In boundary cancellation methods (Morita, 2007; Rezakhani, Pimachev, and Lidar, 2010) the diabatic transitions at the time boundaries are suppressed by imposing vanishing derivatives at the boundaries $\dot{H}[\lambda(t)] = 0$ at $t = 0$ and $t = t_f$. Recently, Stefanatos and Paspalakis (2019a, 2019b) proposed a modified FAQUAD protocol in which the adiabaticity parameter c is not held constant but follows a simple "on-off" modulation found by optimal control theory.

Martínez-Garaot, Ruschhaupt *et al.* (2015) compared local adiabatic, uniform adiabatic, and FAQUAD approaches, also with a π pulse and a linear ramp, for a two-level population inversion. The model uses a bare basis $|1\rangle = \binom{1}{0}$ and $|2\rangle = \binom{0}{1}$, so that a time-dependent state is $|\Psi(t)\rangle = b_1(t)|1\rangle + b_2(t)|2\rangle$ and

$$H_0 = \begin{pmatrix} 0 & -\sqrt{2}J \\ -\sqrt{2}J & U - \Delta \end{pmatrix}, \tag{97}$$

where the bias $\Delta = \Delta(t)$ is the control parameter, and $U > 0$, $J > 0$ are constant. The goal is to drive the eigenstate from $|\phi_1(0)\rangle = |2\rangle$ to $|\phi_1(t_f)\rangle = |1\rangle$. To design the reference adiabatic protocol Martínez-Garaot, Ruschhaupt *et al.* (2015) imposed on $\Delta(t)$ the boundary conditions $\Delta(0) \gg U$, J, and $\Delta(t_f) = 0$. The FAQUAD protocol is shown in Fig. 6(a) compared to a linear-in-time $\Delta(t)$ and a

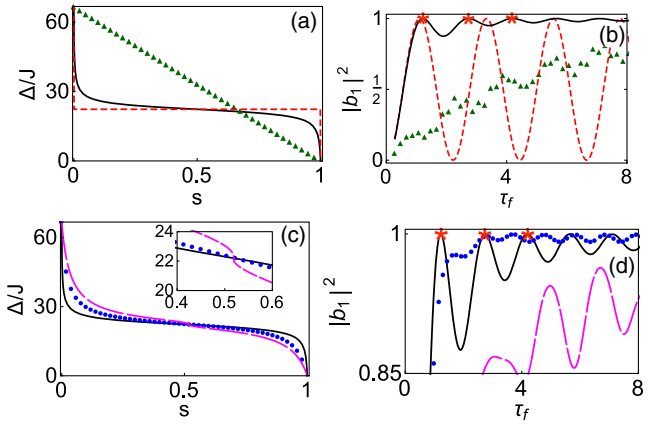

FIG. 6. (a) Bias vs $s = t/t_f$ for linear-in-time bias (green triangles), π pulse (short-dashed red line), and FAQUAD (solid black line). (b) Final ground state population $|b_1(t_f)|^2$ vs $\tau_f = Jt_f/\hbar$ for linear-in-time bias (green triangles), π pulse (short-dashed red line), and FAQUAD (solid black line). (c) Bias vs s for FAQUAD (solid black line), local adiabatic approach (blue dots), and uniform adiabatic approach (long-dashed magenta line). The inset amplifies a kink of the uniform adiabatic approach. (d) $|b_1(t_f)|^2$ vs $\tau_f = Jt_f/\hbar$ for FAQUAD (solid black line), local adiabatic approach (blue dots), and uniform adiabatic approach (long-dashed magenta line). The stars in (b) and (d) correspond to integer multiples of the characteristic FAQUAD timescale $2\pi/\Phi$. $\Delta(0)/J = 66.7$, $U/J = 22.3$. From Martínez-Garaot, Ruschhaupt *et al.*, 2015.

constant $\Delta = U$. The final ground state populations $|b_1(t_f)|^2$ versus the dimensionless final time $\tau_f = Jt_f/\hbar$ are shown in Fig. 6(b). For $\Delta = U$ between 0 and t_f, Rabi oscillations occur [short-dashed red line in Fig. 6(b)] due to interference between two dressed states. By contrast the FAQUAD process is quasiadiabatic and is dominated by one dressed state. The existence of special process times with perfect fidelity can be also understood as an interference phenomenon with characteristic period $T = 2\pi/\Phi$, the minimal time for fidelity one, where $\Phi = (\hbar/t_f)\int_0^{t_f} dt E_{\text{gap}}(t)$ and E_{gap} is the gap between instantaneous levels. Figure 6(b) also shows the poorer results of the linear ramp for $\Delta(t)$. Figures 6(c) and 6(d) compare FAQUAD, local adiabatic, and uniform adiabatic approaches. FAQUAD gives the best behavior at short times, and the local adiabatic method achieves better population stability after a few oscillations.

G. Optimal control and shortcuts to adiabaticity

Optimal control theory is a widely used method (Pinch, 1993; Kirk, 2004) to find control parameter trajectories that minimize a given cost function (global constraint) and obey some specific boundary conditions. According to the Pontryagin maximum principle, such extremal solutions satisfy the equations of a generalized Hamiltonian system. When more constraints are imposed, the quantity to be minimized should be adapted with some weights for the different constraints. Optimal control theory analytically yields solutions only for low-dimensional systems. Very often the OCT solutions are found by discretizing the problem and

implementing numerical approaches such as dynamic programming, the gradient ascent, or Krotov algorithms.

In contrast, STA techniques are not built, in general, upon a minimization principle. However, they serve a similar objective, to drive the system toward the desired states in a short amount of time. The solutions found for the parameter trajectories are by construction typically analytical, continuous, and well adapted to introduce many local constraints (for instance the successive derivative at the initial and final time of the dynamical quantity of interest). Directly comparing both approaches is therefore somewhat misleading. Actually, a class of STA solutions depending on a free parameter can be used to minimize a given cost function yielding results close to those of optimal control theory.

In fact there are many examples in which STA and OCT methods are usefully combined to get nearly optimal protocols by minimizing a cost function of interest or to accommodate for extra constraints in a reduced space made of analytical solutions originating from an STA approach. Such a hybrid strategy has been explicitly worked out to engineer spinlike systems (Hegerfeldt, 2013; Sun, Saxena, and Sinitsyn, 2017; B. B. Zhou *et al.*, 2017), to minimize final excitation after a fast transport in the presence of anharmonicities (Torrontegui, Chen, Modugno, Schmidt *et al.*, 2012; Zhang *et al.*, 2016), to ensure fast transport with extra relevant constraints (e.g., minimum transient energy, bounded trap velocity, or bounded distance from the trap center) (Chen *et al.*, 2011; Torrontegui *et al.*, 2011; Stefanatos and Li, 2014; Alonso *et al.*, 2016; Amri *et al.*, 2018), to ensure a fast and robust shuttling of an ion with noise (Lu, Muga *et al.*, 2014), to perform fast expansions (Salamon *et al.*, 2009; Stefanatos, Ruths, and Li, 2010; Stefanatos, 2013, 2017b; Lu, Chen *et al.*, 2014; Boldt, Salamon, and Hoffmann, 2016; Plata *et al.*, 2019), or to drive a many-body Lipkin-Meshkov-Glick system (Campbell *et al.*, 2015).

Mortensen *et al.* (2018) combined the perturbative approach to enhance robustness described in Sec. II.H with optimal control. A cost function is defined to achieve low peak laser power and stability against systematic error (or scaling) of the control functions. Shortcut schemes for the Λ system were found which minimize this function. This strategy is less computationally expensive than other optimal control methods, since the Schrödinger equation does not need to be solved for every run. Normally the fidelity is part of the cost function, but this is unnecessary for STA methods.

To transport a particle in a harmonic trap of angular frequency ω_0, OCT provides a minimum transport time t_f for a fixed transport distance d using a "bang-banglike" solution for which the acceleration is changed abruptly from a constant value $\omega_0^2\delta$ to the opposite value $-\omega_0^2\delta$ at $t_f/2$ and where the relation between the final time and the parameters is $t_f = (2/\omega_0)(d/\delta)^{1/2}$ (Chen *et al.*, 2011). This kind of solution was implemented experimentally to transport a cold cloud of atoms trapped in a moving optical tweezer in twice the oscillation period (Couvert *et al.*, 2008).

The challenges and prospects of optimal control theory for quantum systems which overlap with those of shortcuts to adiabaticity are discussed in the review articles by Glaser *et al.* (2015) and Koch (2016).

H. Robustness

Adiabatic processes possess a natural robustness to parameter variations. As long as the parameters vary slowly enough, there are many smooth adiabatic paths to the same final result, ignoring phases. However, this robustness does not apply to all imperfections, for example, adiabatic wave packet splitting is very sensitive to asymmetries in the potential (Torrontegui, Martínez-Garaot *et al.*, 2013). Indeed adiabatic drivings are prone to decoherence, excitations, and particle loss, due to the accumulation of noisy perturbations during long process times. STA methods prove useful as they reduce the detrimental cumulative effect of noise, but they require specific control of the parameters for intermediate times, so in general will not have such a natural stability against smooth parameter variations.

Nevertheless, the flexibility of STA methods can be exploited to improve robustness against external influences and imperfections. Within the class of control schemes that work perfectly in the ideal, noiseless setting, the objective is to find the most robust one versus the relevant imperfections or noises, singled out or combined, of a given experiment.

1. Error sensitivity and its optimization using perturbation theory

In several works [see, e.g., Choi, Onofrio, and Sundaram (2012) and Torrontegui, Chen, Modugno, Schmidt *et al.* (2012)], the effect of perturbations and imperfections on STA protocols is analyzed. We can go further and actively improve or even maximize the robustness of the control schemes.

The starting point to do so (Ruschhaupt *et al.*, 2012) is to first design a class of shortcut schemes which fulfill the wanted control task with fidelity one without perturbations. The next step is to define an error sensitivity $q \geq 0$ with respect to the relevant error source; this is done by using perturbation theory to define a series expansion of the fidelity $F(\lambda)$ in terms of the error parameter, q being (minus) the coefficient of the quadratic term. Depending on the nature of the error, systematic or stochastic, q may be found using a Schrödinger equation or a master equation.

This principle was applied to many physical systems and different sources of errors and imperfections. In the following, we review some of these works beginning with the simple example of a two-level system.

a. Illustrative example: Control of a two-level system

Ruschhaupt *et al.* (2012) examined population inversion in a two-level quantum system subjected to different systematic and noisy errors. The starting point is a two-level Hamiltonian

$$H_0(t) = \frac{\hbar}{2}\begin{pmatrix} -\Delta(t) & \Omega_R(t) - i\Omega_I(t) \\ \Omega_R(t) + i\Omega_I(t) & \Delta(t) \end{pmatrix}. \quad (98)$$

Following the invariant-based inverse engineering, see Sec. II.C.2, the control parameters $\Omega_R(t)$, $\Omega_I(t)$, and $\Delta(t)$ can be calculated from the auxiliary functions θ, α, and γ via Eqs. (52), (53), and (54), with the boundary conditions $\theta(0) = 0$ and $\theta(T) = \pi$. By realizing these control functions exactly the population would be inverted in the unperturbed,

error-free case along a family of solutions for the parameter paths.

For systematic errors, for example, if atoms at different positions are subjected to slightly different fields due to the Gaussian profile of the laser, the actual, experimentally implemented Hamiltonian is $H_0+\beta H_1$, where $H_1(t)=H_0(t)|_{\Delta\equiv 0}$ and β is the dimensionless amplitude of the relative systematic error in Ω_R and Ω_I. To give a specific example, consider now only systematic errors in the Rabi frequency. Using time-dependent perturbation theory, the population to be in the excited state $P_2(\beta)$ can be expressed as $P_2(\beta)=P_2(0)-q_S\beta^2+\cdots$, where the noise sensitivity is found to be

$$q_S=-\frac{1}{2}\frac{\partial^2 P_2}{\partial\beta^2}\bigg|_{\beta=0}=\left|\int_0^{t_f} dt e^{-i\gamma}\dot{\theta}\sin^2\theta\right|. \tag{99}$$

One simple choice that gives $q_S=0$ is

$$\Omega_R=\frac{\pi}{t_f}\sqrt{1+16\sin^6\left(\frac{\pi t}{t_f}\right)},\qquad \Omega_I=0,$$
$$\Delta=-\frac{8\pi}{t_f}\sin\left(\frac{\pi t}{t_f}\right)\sin\left(\frac{2\pi t}{t_f}\right)\frac{1+4\sin^6(\pi t/t_f)}{1+16\sin^6(\pi t/t_f)}. \tag{100}$$

We can now consider amplitude noise. We assume that Ω_R and Ω_I are affected independently with the same strength parameter λ^2. This is motivated by the assumption that in principle two lasers may be used to implement the real and imaginary parts of the Rabi frequency with the same intensity. The corresponding master equation with only noise error (no systematic error) is

$$\frac{d}{dt}\rho=-\frac{i}{\hbar}[H_0,\rho]-\frac{\lambda^2}{2\hbar^2}([H_{2R},[H_{2R},\rho]]+[H_{2I},[H_{2I},\rho]]), \tag{101}$$

where $H_{2R}(t)=H_0(t)|_{\Delta\equiv\Omega_I\equiv 0}$, and $H_{2I}(t)=H_0(t)|_{\Delta\equiv\Omega_R\equiv 0}$. Note that STA methods for systems explicitly coupled to an external bath are discussed in further detail in Sec. VII.D. The noise sensitivity q_N is defined as

$$q_N:=-\frac{\partial P_2}{\partial(\lambda^2)}\bigg|_{\lambda=0},$$

where $P_2=\langle 2|\rho(t_f)|2\rangle$ is the probability of the excited state at final time t_f, i.e., $P_2\approx 1-q_N\lambda^2$. Using time-dependent perturbation theory for the master equation, this sensitivity can again be calculated in terms of the auxiliary functions which define the invariant and the state evolution. The transient values of these functions can then be optimally chosen to minimize q_N, while keeping the boundary conditions fixed to ensure perfect state transfer without noise.

In Fig. 7, two STA schemes optimized for noise-error, respectively, systematic error are shown; see Ruschhaupt *et al.* (2012) for details. Clearly, different sources of imperfection need different optimized STA schemes. For a recent combination of this perturbative approach with optimal control theory in the context of topologically protected gates see Ritland and Rahmani (2018).

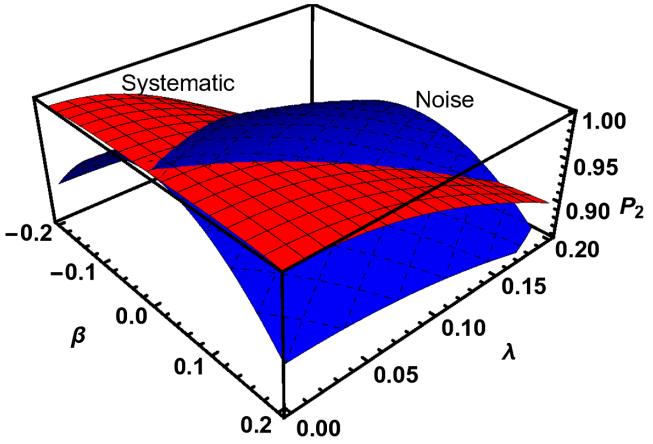

FIG. 7. Excitation probability P_2 vs noise error (strength λ) and systematic error parameter (strength β). Noise error optimized STA (blue) and systematic error optimized STA (red). Adapted from Ruschhaupt *et al.*, 2012.

b. Optimization using perturbation theory in other settings

The optimization of robustness of shortcut schemes using the perturbative approach has been applied to many different systems and systematic error and noise types. Dephasing noise and systematic frequency shift for the two-level system have been examined by Lu *et al.* (2013), where $\Gamma_d:=\gamma_d\sigma_z$ is the noise operator (Sarandy, Duzzioni, and Moussa, 2007), whereas Ruschhaupt and Muga (2014) addressed bit-flip noise, with $\Gamma_b:=\gamma_b\sigma_x$ being the noise operator. The perturbative approach has also been used to work out stable single- and two-qubit gates (Santos, 2018), and to designed schemes to suppress unwanted transitions (Kiely and Ruschhaupt, 2014; Yu *et al.*, 2018; Y. Yan *et al.*, 2019). It may also be combined with optimal control theory (Mortensen *et al.*, 2018); see Sec. II.G. There are as well many works studying and improving robustness in transport problems with respect to anharmonicities (Chen *et al.*, 2011; Torrontegui *et al.*, 2011; Zhang, Chen, and Guéry-Odelin, 2015; Zhang *et al.*, 2016), and noise (Lu, Muga *et al.*, 2014; Lu, Ruschhaupt, and Muga, 2018); see Sec. III.A.

The results of Ruschhaupt *et al.* (2012) were extended by Daems *et al.* (2013) in two ways. First, higher derivatives in the error were also considered, and second, the optimization of the auxiliary function was done by starting with an *Ansatz* with free parameters which were optimized numerically [while it was still possible to derive the optimal scheme by Ruschhaupt *et al.* (2012) analytically]. In addition, the absolute systematic error in the detuning was examined. The results of Daems *et al.* (2013) for population inversion have been used experimentally to rephase atomic coherences in a $Pr^{3+}:Y_2SiO_5$ crystal (Van-Damme *et al.*, 2017) and also applied to create a superposition state with a controlled relative phase in a two-level system (Ndong *et al.*, 2015).

Dirac systems.—An application of the perturbative technique was demonstrated for Dirac systems (Song *et al.*, 2017).

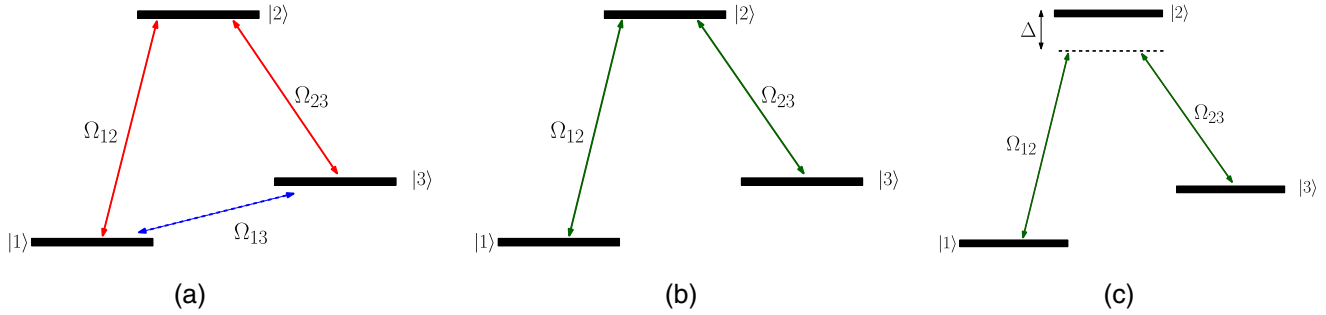

FIG. 8. Different strategies for STA in three-level systems. (a) Apply counterdiabatic STA: initial couplings (red, solid lines), additional required STA coupling (blue, dotted line). (b) Apply invariant-based inverse engineering STA: modified STA couplings (green, solid lines). (c) Detuned couplings: use STA techniques after mapped to a two-level system: modified STA couplings (green, solid lines).

A plethora of natural or artificial systems obey the Dirac equation in certain conditions, with a proper reinterpretation of symbols. The new physical platforms for Dirac dynamics (trapped ions, optics, superconducting circuits) are easier to manipulate than relativistic particles. In trapped ions, for example, the effective (simulated) mass, speed of light, or electric field may be changed in time. This rich simulation scenario opens prospects for finding and implementing new or exotic effects and carrying out fundamental studies. Shortcuts to adiabaticity offer a suitable framework for the task (Muga, Simón, and Tobalina, 2016). For example, Deffner (2016) used the fast-forward technique to suppress production of pairs (transitions among positive and negative energy solutions) in fast processes.

The goal of Song *et al.* (2017) was instead to induce a fast and robust population inversion among the bare levels on a $(1+1)$-dimensional Dirac equation for a charged particle simulated by ultracold trapped ions, designing a simulated electric field α_t. The problem is that the coupling between momentum and internal levels in the Dirac equation changes with the momentum. For each plane wave, there is a momentum-dependent Hamiltonian,

$$H_{p_0} = \begin{pmatrix} mc^2 & cp_0 + \alpha_t \\ cp_0 + \alpha_t & -mc^2 \end{pmatrix}, \tag{102}$$

but a robust population inversion should be independent of the momentum within the momentum spread of the wave packet. This is achieved by considering the p_0-dependent part in Eq. (102) as a perturbation and designing the time dependences of the other elements in the Hamiltonian using the approach by Ruschhaupt *et al.* (2012).

2. Other approaches

Guéry-Odelin and Muga (2014) used a Fourier method to find transport protocols (for either a single particle or BEC) which are robust with respect to spring-constant errors; see more details in Sec. VII.B.2. It exploits the fact that the final excitation energy can be expressed as the Fourier transform of the trap acceleration (Reichle *et al.*, 2006). It avoids perturbation approximations and can also be applied to transport noninteracting particles of different species. Its connection to flatness based control in mathematics is discussed in Sec. VII.B.2.

The use of perturbation theory or iterative methods is also avoided by Zhang, Chen, and Guéry-Odelin (2017) and Levy *et al.* (2018). Using the fast-forward approach (see Sec. II.E) a magnetic field is determined which prescribes specific stable dynamics of a single or two interacting spins (Zhang, Chen, and Guéry-Odelin, 2017). Levy *et al.* (2018) designed protocols for both a two-level system and a harmonic oscillator, which are stable against Markovian noise sources. They are designed using dynamical invariants and are made robust by enforcing that the invariant approximately commutes with the noise operator during the process.

The effect of the environment can also be reduced by choosing the phases in the noise-free evolution operator $U(t) = \sum_n e^{i\xi_n(t)}|n(t)\rangle\langle n(0)|$ to design the driving Hamiltonian (Santos and Sarandy, 2018).

Boyers *et al.* (2018) proposed protocols based on "Floquet engineering" with periodic drivings, where the coefficients are adjusted by matching an effective Floquet Hamiltonian found by a Magnus expansion with CD-driving Hamiltonians. For a qubit inversion the method is resilient to noise because the spectral bandwidth of the protocol (centered around the Floquet frequency) is separated from the spectral bandwidth of the noise around zero as long as the noise is perturbative with respect to the driving.

I. Three-level systems

Few-level models are essential to understand and manipulate actual or artificial atoms. We have presented several examples of shortcuts applied to two-level models and in this section we review three-level models. STIRAP is a basic adiabatic method of reference [see Vitanov *et al.* (2017) for a recent review] to transfer population among the two ground states of a Λ configuration (or the extreme states in ladder systems) without populating the excited state. Being an adiabatic process, it can be sped up with STA techniques. Here are three possible STA approaches to STIRAP speedup; see Fig. 8.

1. Apply counterdiabatic shortcuts to the full three-level Λ system

We assume a three-level Λ system consisting of two "ground levels" $|1\rangle$ and $|3\rangle$ and a central excited level $|2\rangle$ coupled with time-dependent terms Ω_{12} and Ω_{23}. We refrain

from specifying by now the exact nature of these couplings which will depend very much on the system. The first strategy is to apply the counterdiabatic STA technique directly to this Λ system to speed up the STIRAP transfer. This strategy leads to an additional coupling between the two levels $|1\rangle$ and $|3\rangle$ (Unanyan *et al.*, 1997; Demirplak and Rice, 2003; Chen, Lizuain *et al.*, 2010). The improved robustness of STA schemes compared with different STIRAP protocols was shown by Giannelli and Arimondo (2014), and the effect of decay and dephasing was studied by Issoufa and Messikh (2014), who observed that the latter has more effect on the final fidelity than the former. The robustness of this scheme with respect to energies fluctuations, e.g., due to collisions of a solute with a solvent, was examined by Masuda and Rice (2015b).

In practice the additional coupling Ω_{13} can be implemented in some but not in all systems, e.g., because of selection rules due to symmetry of the states or the necessary phase of the term. In fact, Vitanov and Drewsen (2019) proposed a method for efficient optical detection and separation of chiral molecules based on the phase sensitivity of the approach.

An example of a physical system to which this first strategy was applied is "spatial adiabatic passage" (Menchon-Enrich *et al.*, 2016) in which three wells play the role of the three internal states. The additional imaginary coupling may be implemented using a magnetic field that induces a complex tunneling term (Benseny *et al.*, 2017). In nitrogen-vacancy electronic spins, this additional coupling was experimentally implemented mechanically via a strain field (Amezcua, Golter, and Wang, 2017; Kölbl *et al.*, 2019). In a superconducting transmon with a three-level ladder configuration, the auxiliary field to induce a fast transition from the ground to the second excited state was achieved with a two-photon microwave pulse to circumvent the forbidden transition (Vepsäläinen, Danilin, and Paraoanu, 2018).

As a generalization, a discrete FF approach can be set to accelerate the STIRAP protocol with an additional control parameter with respect to the CD solution (Masuda and Rice, 2015a, 2016). The following text discusses alternative STA routes when the new required coupling is not easy to implement or too weak, e.g., a magnetic dipole transition.

2. Applying invariant-based inverse engineering shortcuts to the full three-level Λ system

The second strategy is to apply the invariant-based inverse engineering to the Λ system. Chen and Muga (2012) applied this strategy to a Hamiltonian with resonant couplings that imply an $SU(2)$ dynamical symmetry and built different protocols that may or may not populate level $|2\rangle$, without the need for an additional coupling between $|1\rangle$ and $|3\rangle$. Interestingly, to achieve the same fidelity, less intensity is required when the intermediate level $|2\rangle$ is populated. This means that protocols that populate level $|2\rangle$ may be considered as useful alternatives for certain systems and sufficiently short process times. Moreover, Chen and Muga (2012) put forward the concept of invariant-based "multimode driving," where the dynamical state is a combination of invariant eigenstates rather than just one of them as had been customary in previous works.

Related to this approach are also the speeded-up STIRAP protocols based on the dressed-state approach by Baksic, Ribeiro, and Clerk (2016), which were used in experiments with nuclear spins (Coto *et al.*, 2017; B. B. Zhou *et al.*, 2017).

3. Using STA techniques after mapping to a two-level system

The third strategy is based on mapping or approximate the three-level system to a two-level system and then applying two-level STA techniques. In particular, when the middle level $|2\rangle$ is detuned it can be adiabatically eliminated. The counterdiabatic techniques of STA can then be applied to this effective two-level system and the resulting pulses can be mapped back to the three-level system. No additional coupling is required between the metastable states $|1\rangle$ and $|3\rangle$, and the existing couplings are only modified. This approach was exploited theoretically by Li and Chen (2016) and, using cold ^{87}Rb atoms, experimentally implemented by Du *et al.* (2016).

J. Motional states mapped into a discrete system

In trapped systems a simplifying route to apply shortcuts to control motional degrees of freedom is to first discretize the quantum system into a finite number of localized states that could be time dependent. Then the previous methods can be applied. Ideally the resulting STA protocol should be translated to the original setting to check its performance, or resistance to noise and perturbations, although this step is not always realized.

We provide here some examples of approximations in terms of two, three, and four states.

- Two states: Wave packet splitting operations were modeled by systems of two time-dependent states by Torrontegui, Martínez-Garaot *et al.* (2013), and multiplexing or demultiplexing of harmonic oscillator vibrational states by Martínez-Garaot *et al.* (2013). Two-level models are also used to study spin dynamics in a quantum dot with spin-orbit coupling (SOC) (Ban *et al.*, 2012b).
- Three states: In spatial adiabatic passage, analogous to STIRAP (Vitanov *et al.*, 2017), a particle may tunnel between three wells. The system is approximated by a three-state system and shortcuts may be applied (Benseny *et al.*, 2017). Martínez-Garaot *et al.* (2014) provided other examples, such as wave packet splitting in three wells or operations on two-interacting bosons in two wells.
- Four states: Kiely *et al.* (2016) and Kiely, Muga, and Ruschhaupt (2018) modeled the motion of an ultracold atom in a lattice by a four-state system and applied invariant-based STA techniques to create exotic angular momentum states of ultracold atoms in an optical lattice. In Li, Chen *et al.* (2018) the four-level model takes into account both motional and internal aspects, representing up and down spin states in two different wells.

III. APPLICATIONS IN QUANTUM SCIENCE AND TECHNOLOGY

This section is organized by system type. A number of tables group together articles, otherwise dispersed in different sections, according to transversal criteria: "gates" in Table II,

TABLE II. Quantum logic gates designed using STA methods. CD: counterdiabatic driving; OCT: optimal control theory; QED: quantum electrodynamics; QZD: quantum Zeno dynamics; N*V*: nitrogen vacancy.

Reference	Gate type	System	Method
Martinis and Geller (2014)	Phase	Superconducting Xmon transmon	Optimization
Song, Xia, and Song (2014)	Toffoli	Cavity QED	QZD + invariants
Santos and Sarandy (2015)	Universal gates	N qubits	CD driving
Chen, Xia, Chen, and Song (2015)	Phase	Cavity QED	QZD + invariants
Liang, Wu *et al.* (2015)	Phase	Cavity QED	QZD + invariants
Liang, Song *et al.* (2015)	CNOT	Cavity QED	QZD + invariants
Liang, Ji *et al.* (2015)	Swap	Cavity QED	QZD + invariants
Zhang *et al.* (2015)	Non-Abelian geometric	Superconducting transmon	CD driving
Santos, Silva, and Sarandy (2016)	N qubit	Four-level	CD driving
X.-K. Song, Zhang, Ai *et al.* (2016)	One- and two-qubit holonomic	NV centers	CD driving
Liang *et al.* (2016)	Non-Abelian geometric	NV centers	CD driving
Palmero *et al.* (2017)	Two-qubit phase	Two trapped ions	Invariants
Du *et al.* (2017)	Non-Abelian geometric	NV centers	CD driving
Wu, Ji, and Zhang (2017a)	CNOT	Cavity QED	QZD + dressed-state scheme
Santos (2018)	Single- and two-qubit	Two- and four-level	Inverse engineering
Liu *et al.* (2018)	Non-Abelian geometric	NV centers	Invariants
Wang *et al.* (2018)	Single-qubit	Superconducting Xmon qubit	CD driving
Shen and Su (2018)	Two-qubit controlled phase	Two Rydberg atoms	Invariants
Ritland and Rahmani (2018)	Majorana	Top transmon	OCT for noise canceling
Li, Chen *et al.* (2018)	One-qubit gate and transport	Double quantum dot	Inverse engineering
T. Yan *et al.* (2019)	Non-Abelian geometric	Superconducting Xmon qubit	CD driving
Lv *et al.* (2019)	Noncyclic geometric	Two-level atom	CD driving
Santos *et al.* (2019)	Single-qubit	Nuclear magnetic resonance	CD driving
Qi and Jing (2019)	Single- and double-qubit holonomic	Rydberg atoms	CD driving

LMG-like models in Table III, "transport" in Table IV, and "experiments" in Table V.

A. Trapped ions

Trapped ions constitute one of the most developed physical platforms to implement fundamental quantum phenomena and quantum information processing. Since many ions in a single trap are difficult to control, a way toward large-scale computations with many qubits is a divide-and-conquer scheme (Wineland *et al.*, 1998; Kielpinski, Monroe, and Wineland, 2002), where ions are shuttled around in multisegmented Paul traps, while keeping just a few ions in each processing site. Apart from shuttling, complementary operations such as separating and merging ion chains, trap rotations, and expansions or compressions of ion chains are needed. Coulomb interactions and controllable external effective potentials created by radio frequency or dc electrodes determine the motion of the ions and the corresponding Hamiltonians, which can be approximated by quadratic forms near equilibrium.

1. Dynamical normal modes

Dynamical normal modes are a useful generalization of ordinary normal modes for time-dependent, quadratic Hamiltonians (Palmero *et al.*, 2014) or in the small-oscillations regime for nonharmonic ones. They are independent harmonic motions which describe the dynamics of an effective time-dependent harmonic oscillator. Dynamical normal modes help to describe the motion in a simple way but also to inverse engineer the potentials to achieve fast motions without final excitation. The invariant-based engineering of the time

TABLE III. Works where STA methods are applied to LMG-like models.

Reference	Reference Hamiltonian	Comment
Juliá-Díaz *et al.* (2012)	$U(t)J_z^2 - 2JJ_x$	Invariants, large N.
Yuste *et al.* (2013)	$UJ_z^2 - 2J(t)J_x$	Invariants, time-dependent mass
Takahashi (2013b)	$-(2/N)[J_x(t)S_x^2 - J_y(t)S_y^2 + \gamma S_y^2] - 2h(t)S_z$	Large N, CD
Campbell *et al.* (2015)	$-(2/N)(S_x^2 + \gamma S_y^2) - 2h(t)S_z$	Approximate CD
Opatrný *et al.* (2016)	$A_c(t)H_c + A_n(t)H_n$; $H_c = \vec{c}\cdot\vec{J}$, $H_n = (J_z - nI)^2$	Approximate CD
Hatomura (2017)	$-[(2J)/N]S_z^2 - 2\Gamma(t)S_x - 2hS_z$	Mean field, CD
Takahashi (2017b)	$f(t)\{-[(2J)/N]S_z^2 - 2hS_z\} - 2\Gamma(t)S_x$ $-f(t)[(2J)/N]S_z^2 - 2\Gamma_x(t)S_x - 2\Gamma_y(t)S_y$ $f(t)(-\sum J_{ij}\sigma_i\sigma_j^2 - 2hS_z) - 2\Gamma(t)S_x$	Mean field, invariants
Hatomura (2018)	$-[(2J)/N]S_z^2 - 2\Gamma_x(t)S_x$	Mean field, CD

TABLE IV. List of papers on STA-mediated transport. CD: counterdiabatic driving; IE: inverse engineering; OCT: optimal control theory; FF: fast forward; Exp.: experiment.

Reference	Method	System
Couvert *et al.* (2008)	Fourier-based IE (Exp.)	Cold atoms in moving optical tweezers
Masuda and Nakamura (2010)	FF	1 particle in arbitrary trap
Torrontegui *et al.* (2011)	Invariants, compensating-force, bang-bang	1 particle
Chen *et al.* (2011)	Invariants + OCT	1 particle harmonic transport
Torrontegui, Chen, Modugno, Schmidt *et al.* (2012)	Invariants + OCT	BEC
Sun *et al.* (2012)	Bang-bang (Exp.)	Load in a 2D planar overhead mechanical crane
Bowler *et al.* (2012)	Fourier transform (Exp.)	1, 2, or 9 ions in Paul trap
Walther *et al.* (2012)	Optimized drivings (Exp.)	1 or 2 ions in Paul trap
S. Ibáñez *et al.* (2012)	Unitary transformations	1 particle in harmonic trap
Palmero *et al.* (2013)	Invariants	2 ions in anharmonic traps
Stefanatos and Li (2014)	OCT	1 particle
Lu, Muga *et al.* (2014)	Invariants + perturbation theory + OCT	1 ion
Fürst *et al.* (2014)	OCT + compensating force	1 ion in Paul trap
Palmero *et al.* (2014)	Invariants	Mixed-species ion chains in Paul trap
Guéry-Odelin and Muga (2014)	Fourier method	1 particle or BEC
Pedregosa-Gutierrez *et al.* (2015)	Numerical simulations	Large ion clouds
Lu *et al.* (2015)	Invariants	2 ions of different mass
Zhang, Chen, and Guéry-Odelin (2015)	Inverse engineering	1 particle in anharmonic trap
Kamsap *et al.* (2015)	Numerical simulations	Large ions clouds
Martínez-Garaot, Palmero *et al.* (2015)	FAQUAD, compensating-force	1 particle
Alonso *et al.* (2016)	Bang-bang (Exp.)	1 ion
Zhang *et al.* (2016)	Invariants + OCT	Cold atoms
Okuyama and Takahashi (2016)	Lax pairs + local CD	Solitonlike potentials
An *et al.* (2016)	CD and CD + unitary transformation (Exp.)	Simulated transport of 1 ion
Funo *et al.* (2017)	CD	1 ion in Paul trap
Tobalina *et al.* (2017)	Invariants	1 ion in a nonrigid trap
Li, Zhang, and Chen (2017)	Trigonometric protocols	Cold atoms in anharmonic traps
Torrontegui *et al.* (2017)	Invariants	Load in mechanical crane
Dowdall *et al.* (2017)	Pauli blocking	Ultracold Fermi gases
González-Resines *et al.* (2017)	Invariants	Load in mechanical crane
Corgier *et al.* (2018)	Inverse engineering	BECs in atom chips
Kaufmann *et al.* (2018)	Invariants (Exp.)	1 ion in Paul trap
Lu, Ruschhaupt, and Muga (2018)	Invariants	1 ion
Tobalina, Alonso, and Muga (2018)	OCT + compensating-force	1 ion in Paul trap
Ness *et al.* (2018)	Invariants (Exp.)	Cold atoms in optical dipole trap
Chen, Jiang *et al.* (2018)	Inverse engineering	Spin-orbit-coupled BECs
Li, Chen *et al.* (2018)	Inverse engineering	Qubit in double quantum dots
Amri *et al.* (2018)	OCT & STA	BECs in atom chips

dependence of the potentials is a natural route to that end. An important difference with respect to inverse engineering a single harmonic oscillator is that several time-dependent harmonic oscillators for the different dynamical modes have to be engineered simultaneously with common control functions.

For example, to transport a chain of two ions, the position of the external harmonic trap is a common control function, and we cannot engineer a different trap position for each mode. The way to solve this type of inversion problem is to increase the number of adjustable parameters in the *Ansätze* for the auxiliary functions, see Sec. II.C.2.b, so that all the boundary conditions of the auxiliary functions of all modes are satisfied simultaneously, either exactly or via minimization subroutines.

Dynamical normal modes have been used to speed up, via invariants, the transport of two or more (possibly different) ions (Palmero *et al.*, 2013, 2014; Lu *et al.*, 2015) and to design trap expansions or compressions of ion chains in a common trap (Palmero, Martínez-Garaot, Alonso *et al.*, 2015), ion separation (Palmero, Martínez-Garaot, Poschinger *et al.*, 2015), and two-ion phase gates driven by spin-dependent forces (Palmero *et al.*, 2017). However, for some operations a point transformation[5] to define the dynamical modes does not exist.

For 2D systems the condition that an uncoupling point transformation exists is simply that the principal axes of the equipotential ellipses, see Fig. 9, do not rotate in the laboratory frame (Lizuain, Palmero, and Muga, 2017). If the ellipses are translated, expanded, or compressed, dynamical normal modes may be defined via point transformations. An operation for which the point transformation does not exist in

[5]In a point transformation new coordinates depend only on old ones.

TABLE V. Experiments using STA methods. CD: counterdiabatic driving; IE: inverse engineering; OL: optical lattice; STIRAP: stimulated Raman adiabatic passage; N*V*: nitrogen vacancy; FAQUAD: fast quasiadiabatic dynamics.

Reference	System	Operation	Method
Couvert *et al.* (2008)	Ultracold atoms	Transport	Fourier-based IE
Bason *et al.* (2012)	Two-level Landau-Zener system (BEC in OL)	Population inversion	CD + unitary transformation
Bowler *et al.* (2012)	Trapped ions (1, 2) Trapped ion chain (9 ions)	Transport Separation	Fourier transform FAQUAD
Sun *et al.* (2012)	Overhead crane	Transport	Bang-bang
Walther *et al.* (2012)	1 and 2 ions	Transport	Optimized drivings
Richerme *et al.* (2013)	14 spins in linear trap (Ising model)	Adiabatic quantum simulation	Local adiabatic
Zhang *et al.* (2013)	N*V* center in diamond	Assisted adiabatic passage	CD and accelerated CD
Ruster *et al.* (2014)	2 ions	Separation	Implement a function for equilibrium distance
Kamsap *et al.* (2015)	Large ion clouds	Transport	Numerical simulations
Rohringer *et al.* (2015)	1D BEC	Expansion or compression	Scaling
Alonso *et al.* (2016)	Trapped ion	Transport	Bang-bang
Du *et al.* (2016)	Three-level Rb	STA-STIRAP	CD + unitary transform
Martínez *et al.* (2016)	Brownian particle in optical potential	Equilibration	Engineered swift equilibration
An *et al.* (2016)	Trapped ion	Simulated transport	CD and unitarily equivalent protocols
Navez *et al.* (2016)	Atoms in state-dependent "moving buckets"	Interferometer	Choose convenient timing
Guo and Chu (2017)	Optical waveguides	Demultiplexing	Invariant-based IE
Z. Zhang *et al.* (2017)	Superconducting phase qubit	Measure Berry phase	CD
Chupeau, Ciliberto *et al.* (2018)	Brownian particle in quadratic potential	Control of temperature	Inverse engineering
Cohn *et al.* (2018)	2D array of 70 ions in Penning trap	Create highly entangled state	Bang-bang
Deng, Diao *et al.* (2018)	Anisotropic Fermi gas	Expansion or compression	Scaling
Kaufmann *et al.* (2018)	Trapped ion	Transport	Invariant-based IE
Ness *et al.* (2018)	Ultracold K atoms in optical lattice	Transport	Invariants
Smith *et al.* (2018)	Two-level in $^{171}Yb^{+}$	Qubit rotations	CD
Wang *et al.* (2018)	Superconducting Xmon qubit	Quantum gates	CD
Hu *et al.* (2018)	Trapped $^{171}Yb^{+}$ ion	Speed up Landau-Zener	Optimized-phase CD
Z. Zhang *et al.* (2018)	Superconducting Xmon qubit	Measure work statistics	CD
Zhou, Jin, and Schmiedmayer (2018)	BEC	Prepare BEC in bands of OL	Optimized pulse sequences
Faure *et al.* (2018)	RC circuit	Change stationary regime	Inverse engineering
Boyers *et al.* (2018)	N*V* center	Qubit population inversion	Floquet engineering of Hamiltonian components
Kölbl *et al.* (2019)	N*V* center	Control of dressed states	CD
T. Yan *et al.* (2019)	Xmon superconducting qutrit	Holonomic gates	CD
Vepsäläinen, Danilin, and Paraoanu (2019)	Transmon	STA-STIRAP	CD
Santos *et al.* (2019)	NMR of a Cloroform molecule	Single-qubit gates	CD driving

general is the separation of two different ions in an external potential $\alpha(t)x^2+\beta(t)x^4$, except when the ratio $\beta^3(t)/\alpha^5(t)$ is a constant. Similarly, for the rotation of a two-dimensional anisotropic trap holding one ion there is no point transformation leading to normal modes. A way out is to compensate for the inertial potential proportional to the angular momentum with an effective magnetic field. This is similar to the inertial force compensation with a homogeneous force in transport; see Sec. II.C.2.b. Finally, it is also possible to consider generalized transformations mixing coordinates and momenta (Lizuain *et al.*, 2019).

2. Ion transport

Among the different operations on ions addressed by STA methods, ion transport is the most studied both theoretically (Palmero *et al.*, 2013, 2014; Fürst *et al.*, 2014; Lu, Muga *et al.*, 2014; Lu *et al.*, 2015; Pedregosa-Gutierrez *et al.*, 2015; Li, Zhang, and Chen, 2017; Lu, Ruschhaupt, and Muga, 2018; Tobalina, Alonso, and Muga, 2018) and experimentally in Paul traps (Bowler *et al.*, 2012; Walther *et al.*, 2012; Kamsap *et al.*, 2015; Alonso *et al.*, 2016; An *et al.*, 2016; Kaufmann *et al.*, 2018). The first two experiments were done simultaneously in Boulder (Bowler *et al.*, 2012), using a Fourier transform technique, and Mainz (Walther *et al.*, 2012), optimizing some driving protocols, to transport one or two ions diabatically for 300 to 400 μm on a 5 to 10 μs timescale (a few oscillation periods) achieving final excitations below one motional quantum. Later, Kamsap *et al.* (2015) transported large ion clouds using numerical simulations to control the dynamics. In 2016, other shortcut techniques were used to improve transport experiments, for example, the bang-bang method using nanosecond switching of the trapping potentials by Alonso *et al.* (2016). The experiment by An *et al.* (2016)

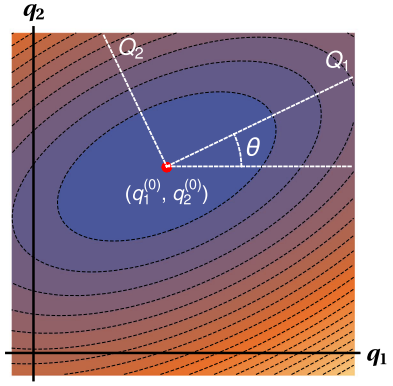

FIG. 9. Schematic representation of isopotential curves of a mass-weighted potential in the two-dimensional configuration space of laboratory-frame coordinates q_1 and q_2. These curves are ellipses centered at the moving equilibrium position $(q_1^{(0)}, q_2^{(0)})$ with the orientation of the principal axes given by the angle θ. The dynamical normal mode coordinates are Q_1 and Q_2. From Lizuain, Palmero, and Muga, 2017.

simulated CD-driven transport in an interaction picture with respect to the harmonic oscillation and also performed the compensating force approach as unitarily equivalent transport in the interaction picture. The driving forces were induced optically rather than by varying voltages of control electrodes. Finally Kaufmann *et al.* (2018) used invariant-based inverse engineering to design ion transport and measured internal infidelities less than 10^{-5}, an important prerequisite for the success of quantum-information-processing schemes that rely on ion transport.

On the theoretical side, Fürst *et al.* (2014) used optimal control theory and the compensating force approach to analyze the transport of an ion in realistic conditions for state-of-the-art miniaturized ion traps. Given the simplicity of the approach and results, they considered the compensating force to be the method of choice for current experimental settings. Anharmonicity was found to play no significant role. This paper sets the relation between the desired trap trajectory and the voltages applied in the control electrodes. The model was later applied by Tobalina, Alonso, and Muga (2018) to analyze the energy cost of ion transport.

Lu, Muga *et al.* (2014) and Lu, Ruschhaupt, and Muga (2018) analyzed the effect of different colored noises on single-atom transport and how to mitigate their effect. Dynamical and static sensitivities are distinguished according to their dependence or independence with trap motion. They behave in opposite ways with respect to transport duration, which implies a transition between the dominance of the dynamical sensitivity at short times and of the static one at large times. The crossover is important as it demonstrates that the widespread expectation that shorter STA times are always more robust versus noise (a behavior that holds for the static but not for the dynamic sensitivity) is not necessarily true and that optimal times exist with respect to robustness. Li, Zhang, and Chen (2017) proposed trigonometric protocols that minimize the classical excitation due to anharmonicities within a perturbative approach.

Two-ion transport was addressed by Palmero *et al.* (2013, 2014). Also, Lu *et al.* (2015) designed optimal transport of two ions under slow spring-constant drifts. Designing fast transport of two different ions is challenging because the simple compensating force approach is not possible if only forces induced by the electrodes are applied. They depend only on the charges, whereas the compensating forces should depend on the mass (Palmero *et al.*, 2014). Dynamical normal modes can however be defined so the problem is solved using invariants (Palmero *et al.*, 2014). Two-ion transport may also be performed with "spin-dependent" optically induced forces that may be different for different internal states. An interesting application is the implementation of fast phase gates in which different phases are imprinted depending on the internal states because of the different motions induced. The invariant-based design of the ion trajectories guarantees a robust phase because of its geometric nature and its independence on the motional state (Palmero *et al.*, 2017). Similar ideas may be applied to design a single-ion driven interferometer to measure unknown small forces (Martínez-Garaot, Rodriguez-Prieto, and Muga, 2018). Interferometry driven by STA trajectories (using ions or neutral atoms) (Navez *et al.*, 2016; Martínez-Garaot, Rodriguez-Prieto, and Muga, 2018) offers, compared to the usual schemes where the systems evolve freely along separated branches, the possibility to control the timing and the sensitivity, the absence of wave packet dispersion, and robustness versus initial motional states.

3. Other operations

Fast ion separation.—Separating two ions, or more generally a chain, is a delicate operation and STA-enhanced experiments (Bowler *et al.*, 2012; Ruster *et al.*, 2014) provide excitations above one motional quantum per ion. Bowler *et al.* (2012) used a FAQUAD approach, and Ruster *et al.* (2014) optimized control parameters. In theoretical works (Home and Steane, 2005; Nizamani and Hensinger, 2012; Kaufmann *et al.*, 2014; Palmero, Martínez-Garaot, Poschinger *et al.*, 2015) the control process is modeled as a time-dependent evolution of the parameters in the external confinement potential $\alpha(t)x^2 + \beta(t)x^4$. The difficulties come from the change of sign of $\alpha(t)$ from positive (in the initial trap) to negative values (to form the central barrier). When the harmonic confinement vanishes, the values of β are bounded by experimental limitations. Thus the confinement becomes weak, levels get close to each other, and the ions suffer heating. If the ions are different, further difficulties arise as a consequence of the general absence of normal modes based on point transformations (Lizuain, Palmero, and Muga, 2017), as commented on previously; see Sec. III.A.1.

Ion expansions and compressions.—Palmero, Martínez-Garaot, Alonso *et al.* (2015) analyzed by invariant-based inverse engineering how to expand or compress ion chains of equal or unequal ions, and Torrontegui *et al.* (2018) studied how to speed up a single-ion heat pump. This work analyzed the possibility to implement repulsive potentials. They are found to be feasible in the radial direction by turning of the radio-frequency drive and relying on the direct-current (cap) electrodes. Earnshaw's theorem does not allow for absolute minima so that a minimum in the axial direction of the trap corresponds to a maximum in the radial direction.

Penning traps.—Shortcuts have been applied as well to Penning traps: Kiely *et al.* (2015) designed via invariants a

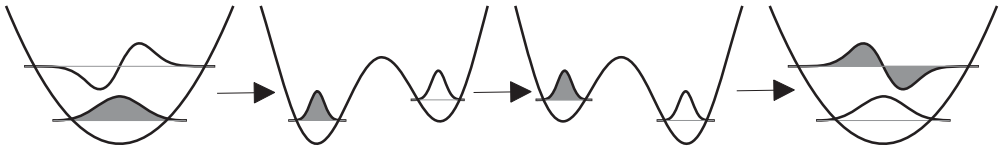

FIG. 10. Vibrational level inversion by STA processes based on trap deformations: demultiplexing, bias inversion, and multiplexing. From Martínez-Garaot *et al.*, 2013.

nonadiabatic change of the magnetic field strength to change the radial spread without final excitations, and Cohn *et al.* (2018) implemented experimentally a protocol to produce entangled states in a Dicke model realized in a two-dimensional array of trapped ions.

Rotations.—Palmero *et al.* (2016) provided invariant-based shortcuts to perform fast rotations of an ion in a 1D trap.[6] Lizuain *et al.* (2019) designed fast rotations of a 2D anisotropic trap to produce a rotated version of an arbitrary initial state when the two normal frequencies are commensurate.

B. Double wells

A double well is a useful potential to test fundamental quantum physics and applications in interferometry or quantum and classical information processing. Shortcuts using invariants have been proposed for several operations involving double wells and motional states, for example, to split one-particle wave functions in linear or nonlinear settings (Torrontegui, Martínez-Garaot *et al.*, 2013; Martínez-Garaot *et al.*, 2016), to speed up the cotunneling of two interacting bosons (Martínez-Garaot, Ruschhaupt *et al.*, 2015), to split ion chains as discussed in Sec. III.A.3, or to model the erasure of a bit with a Brownian particle (Boyd *et al.*, 2018). Applications involving many-body systems are reviewed in Sec. III.G. Other STA operations in double wells are vibrational-state inversion and multiplexing or demultiplexing.

Vibrational mode multiplexing is the spatial separation of the vibrational modes of a harmonic trap. For the first two modes the separation is done by smoothly transforming the harmonic trap into a biased double well. Martínez-Garaot *et al.* (2013) maped the STA process from a two-level model into a realizable potential in coordinate space designing the time dependence of two control parameters. A fast inversion of the double-well bias, so that the lower well becomes the upper one and vice versa, can be performed by noticing that the operation, in an independent-well regime, amounts to a transport process, so that the compensating force approach can be applied (Martínez-Garaot, Palmero *et al.*, 2015) to design the time dependence of the bias. Combining sequentially multiplexing, bias inversion, and demultiplexing leads to a fast inversion of vibrational levels using only a transient trap deformation and no excited internal states; see Fig. 10. Interestingly, there is no adiabatic path connecting the ground and the excited states, but a combination of STA processes leads to the desired state. The explanation is that inverting the bias is in fact adiabatic within the approximation of independent wells, in other words, during a timescale which is short compared to the duration of the process.

Bücker *et al.* (2011, 2013) independently performed motional-state inversions by shaking anharmonic potentials guided by an OCT algorithm to produce twin atom beams and interferometry applications, but a smooth STA-based deformation similar to Fig. 10 has not yet been implemented experimentally.

C. Cavity quantum electrodynamics

Entangled state preparation in cavity quantum electrodynamics.—In cavity quantum electrodynamics atoms and light are confined such that the quantum states of the atom are protected by allowing only controllable transitions compatible with the modes of the cavity and thus isolating the atom from any electromagnetic environment other than the cavity itself. These systems have recently opened up new prospects to implement large-scale quantum computation and to generate nonclassical states.

An early proposal to produce entangled states faster than adiabatically by moving atoms in and out of an optical cavity was provided by Marr, Beige, and Rempe (2003): the proposal was to use cavity leakage to stabilize the desired adiabaticlike time evolution by damping away population in unwanted states. However, a consequence is that the success rate decreases.

In the post-2010 era the use of shortcuts to inverse engineer the dynamics of two atoms inside a cavity was first discussed by Lu, Xia, Shen, Song, and An (2014). They used the counterdiabatic driving formalism to create maximal entanglement between the two atoms but, due to the complexity of the resulting counterdiabatic Hamiltonian, they had to introduce an alternative, physically feasible Hamiltonian that needs auxiliary internal levels, an extra laser field, and an extra cavity mode. The same group tried a different strategy using invariants to accelerate the state transfer between two three-level atoms in a cavity quantum electrodynamics (QED) system (Lu, Xia, Shen, and Song, 2014).

Y.-H. Chen *et al.* (2014a) used invariants combined quantum Zeno dynamics (QZD) to simplify the dynamics and speed up the population transfer between two atoms trapped in a cavity. The quantum Zeno effect inhibits transitions by frequent measurements so that the system evolves in the so-called Zeno subspace (Facchi and Pascazio, 2002). This quantum Zeno dynamics can also be achieved via a strong continuous coupling (Facchi and Pascazio, 2002). In particular, Muga *et al.* (2008) discussed the mapping between discrete and continuous interactions. Following Y.-H. Chen *et al.* (2014a), many other papers have used the QZD approximation to decouple different Hilbert

[6]Video in https://www.youtube.com/watch?v=ToQXnd_FdUw.

subspaces by assuming that the atom-cavity coupling is much larger than the driving field Rabi frequencies. The simplified effective Hamiltonians were controlled with the use of different STA techniques to design fast and robust protocols against decoherence produced by atomic spontaneous emission and cavity leakage; see, for example, Wu, Ji, and Zhang (2017b). Chen *et al.* (2014b) extended the idea of combining QZD and STA methods to control the dynamics of atoms trapped in distant cavities connected through a fiber.

A requirement for the success of quantum mechanics in information processing tasks is scalability toward multiparticle ($N > 2$) setups. The macroscopic character of cavity QED setups favors the interaction among qubits and thus scalability. Numerous setups and control designs have been proposed to generate large entangled states using STA methods and the QZD assumption, in particular, large-N entangled W states (Huang, Zhong, and Chen, 2015; Chen, Huang *et al.*, 2016; Huang, Chen, and Wang, 2016b; Kang *et al.*, 2016a, 2016b; Song and Chen, 2016; Z. Wang *et al.*, 2016; Yu *et al.*, 2017; Yang *et al.*, 2018), or Greenberger-Horne-Zeilinger (GHZ) states (Chen, Xia, Song, and Chen, 2015; Huang *et al.*, 2016; Huang, Chen, and Wang, 2016a; Shan *et al.*, 2016; Ye *et al.*, 2016; Xu *et al.*, 2017; X. Zhang *et al.*, 2017). Moreover, using the QZD scheme several presented various STA setups to create 3D entanglement between atoms individually trapped in distant optical cavities connected by a fiber (Liang, Su *et al.*, 2015; Lin *et al.*, 2016; Wu, Ji, and Zhang, 2016; Wu, Song *et al.*, 2016) or between two atoms trapped in a single cavity (He *et al.*, 2016; Yang *et al.*, 2017).

Shortcuts have also been proposed to generate other less common entangled states, such as large NOON states of two sets of Λ atoms in distant cavities using invariants (C. Song *et al.*, 2016), and, using CD driving, a three-atom singlet in a common cavity (Z. Chen *et al.*, 2016), tree-type 3D entangled states (Wu, Ji, and Zhang, 2016; Wu, Su, Ji, and Zhang, 2017), two-atom qutrit entanglement (Peng *et al.*, 2017), or maximally entangled states of two Rydberg atoms (Zhao *et al.*, 2017).

Other applications.—Different STA-enhanced quantum gates were designed within the QZD condition. For example, invariant-based inverse engineering was used to develop Toffoli gates (Song, Xia, and Song, 2014), phase gates (Chen, Xia, Chen, and Song, 2015; Liang, Wu *et al.*, 2015), CNOT gates (Liang, Song *et al.*, 2015), or swap gates (Liang, Ji *et al.*, 2015). Wu, Ji, and Zhang (2017a) used the dressed-state method (Baksic, Ribeiro, and Clerk, 2016) to design a fast CNOT gate in a cavity QED system which consists of two identical five-level atoms in two single-mode optical cavities connected by a fiber.

Shortcuts have been proposed as well to produce single photons on demand in an atom-cavity system approximated by three levels (Shi and Wei, 2015). A system of distant nodes in two-dimensional networks (cavities with a Λ-type atom) was approximated by a three-level Λ system in Zhong (2016) and then STA techniques were applied to achieve fast information transfer.

Optomechanical systems.—Shortcuts have been applied as well to optomechanical systems. One of the early applications of the invariant-based approach by Chen, Ruschhaupt *et al.* (2010) was to cool down a mechanical resonator in a cavity optomechanical system with external optical fields (Li, Wu, and Wang, 2011).[7] For more recent applications, see X. Zhou *et al.* (2017), Chen, Shi *et al.* (2018), and H. Zhang *et al.* (2018).

D. Superconducting circuits

Superconducting circuits have recently made rapid progress and become a leading architecture for quantum technologies (Wendin, 2017). In this context STA techniques were independently developed under the names "derivative removal by adiabatic gate" for single qubits (Motzoi *et al.*, 2009) and weak anharmonicity with average Hamiltonian (Schutjens *et al.*, 2013) for multiqubit setups and multilevel systems (qutrits); see also Theis, Motzoi, and Wilhelm (2016), Lu *et al.* (2017), and Theis *et al.* (2018) and the discussion in Sec. II.B.1, focusing on avoiding unwanted transitions to spectrally neighboring energy levels.

Other techniques for sped-up manipulations take into account the peculiarities of the experimental settings, such as small nonlinearities in the qubits (implying that unwanted transitions are not necessarily off resonant), or a need for smooth pulses (versus square pulses common in nuclear magnetic resonance). In particular, Martinis and Geller (2014) considered a two-level model where only the σ_z term changes to achieve fast gates with the σ_x term constant in $H = H_x\sigma_x + H_z\sigma_z$. Relating the error in the gate operation to the Fourier transform of the properly scaled rate of change of the polar angle $\theta = \arctan(H_x/H_z)$, optimal protocols were found, minimizing the integrated error for any time larger than some chosen time.

Other works apply the standard STA methods, in particular, CD driving, to transfer information between distant nodes of flux qubits in annular and radial superconducting networks (Kang, Shi *et al.*, 2017), to complete Bell-state analysis for two superconducting-quantum-interference-device qubits (Kang, Chen *et al.*, 2017), or to measure the Berry phase (Z. Zhang *et al.*, 2017) in a phase qubit.

Further applications of CD shortcuts include the proposal or realization of gates. Zhang *et al.* (2015) proposed holonomic one- and two-qubit gates based on four-level systems in superconducting transmons. Experiments were performed to implement single-qubit quantum gates in a superconducting Xmon system (Wang *et al.*, 2018) with a hybrid CD + DRAG approach, and non-Abelian geometric gates with a ladder three-level system (T. Yan *et al.*, 2019). Superconductors also play a role as a possible platform to realize topological quantum information processing based on "braiding" non-Abelian quasiparticles. Karzig *et al.* (2015) explored CD protocols to realize these braiding operations in finite time.

Interfacing different architectures to make better use of their optimal features may be important to jump from proof of principle to practical technologies. In particular, superconducting circuits may be combined with optomechanical systems producing hybrid quantum systems. X. Zhou *et al.* (2017) proposed a protocol to efficiently convert microwave to

[7]Zhang, Li, and Feng (2013) proposed instead electromechanical cooling.

optical photons, enabling the transmission of information through optical fibers with minimal loss. One more application of shortcuts in superconducting circuits is to create photonic cat states. Stored in high-Q resonators these states could lead to efficient universal quantum computing (Puri, Boutin, and Blais, 2017).

E. Spin-orbit coupling

Discrete models.—Coherent spin manipulation in quantum dots via electric, magnetic, and spin-orbit coupling control is one of the avenues to solid-state based quantum information. STA methods have been proposed to speed up operations and fight decoherence also in this context. In particular, STA are welcome to speed up double quantum dots with SOC control, since strong fields nontrivially slow down the operations involving spin-orbit coupling and tunneling (Khomitsky, Gulyaev, and Sherman, 2012).

The interplay between motional and spin degrees of freedom is typically modeled by an effective discrete Hamiltonian where STA techniques are applied. The physics behind the model, however, makes the exercise nontrivial, as the different matrix elements are not always controllable independently by the available external manipulations. An example of these physical constraints and a way out was provided by Ban *et al.* (2012a, 2012b), in which the spin dynamics in a quantum dot with spin-orbit coupling and a weak magnetic field is controlled by time-dependent external electric fields only. The dependence of the effective 2×2 Hamiltonian on the electric field makes a CD approach nonviable with electric control. However, invariant-based inverse engineering is applicable and circumvents the difficulty.

Two electrons in a double dot offer more freedom since different electric fields can be applied to each dot. Thus CD driving combined with a unitary transformation could be applied to induce fast singlet-triplet transitions (Ban and Chen, 2014), again within a 2×2 Hamiltonian modeling.

Synthetic spin-orbit coupling in ultracold atoms and condensates is also of interest to control internal and motional states. Invariant-based protocols to simultaneously control the internal (related to its pseudospin-1/2) and motional states of a spin-orbit-coupled BEC in Morse potential have also been studied by Ban *et al.* (2015) by a 2×2 effective Hamiltonian.

A 4×4 Hamiltonian was used in Li, Chen *et al.* (2018) to model and design the transport of a qubit encoded in the electron spin among two quantum dots, performing simultaneously an arbitrary qubit rotation (gate). The transfer may be extended sequentially to a chain of dots. These processes need time-dependent control of the spin-orbit and interdot tunneling couplings. The dynamical engineering of the four-level system applies the technique developed by Li, Martínez-Cercós *et al.* (2018) based on the geometry of 4D rotations.

Models with a continuum.—Models that retain motional (1D, in x direction) and internal degrees of freedom of the electron without discretization began with Čadež, Jefferson, and Ramšak (2013), who considered an electron with spin-orbit coupling in a moving harmonic quantum dot,

$$H(t)=\frac{p_x^2}{2m^*}+\frac{m^*\omega^2}{2}[x-\xi(t)]^2+p_x(\alpha\sigma_y-\beta\sigma_x), \quad (103)$$

where m^* is the effective electron mass, $\xi(t)$ is the time-dependent position of the harmonic trap, and α and β are Rashba and Dresselhaus spin-orbit couplings. The dynamics of this model is exactly solvable via invariants, and fast bang-bang trap trajectories leading to spin control (e.g., spin flip) without final excitation were found for $\beta=0$. In Čadež, Jefferson, and Ramšak (2014), β is fixed to zero while α remains time dependent. The dynamics can still be found exactly and expressions are given for dynamical and geometrical phases in closed-loop trajectories of the control parameters. Chen, Jiang *et al.* (2018) translated these ideas to synthetic spin-orbit couplings in BECs and applied inverse engineering of $\xi(t)$ and $\alpha(t)$ ($\beta=0$) from auxiliary Newton-like equations for the center-of-mass position of the condensate and its spin precession. Again spin is flipped fast by proper design of the controls.

Controllable linear-in-momentum interactions to implement direct (not unitarily transformed) CD-driven transport in the lab frame, i.e., with the form $H_{CD}=p_x\alpha(t)$, with $\alpha=\dot{q}_c$, see Torrontegui *et al.* (2011) and Sec. II.C.2.b, may in principle be implemented by synthetic spin-orbit coupling for one of the spin components (Tobalina, Alonso, and Muga, 2018). Note that the change of sign for the other component is crucial to determine the possible applications. This dependence precludes, for example, transporting a qubit, but it is useful to set different paths in interferometry (Martínez-Garaot, Rodriguez-Prieto, and Muga, 2018).

F. Nitrogen-vacancy centers

Quantum information processing with NV centers is appealing because of the possibility to operate with qubits at room temperature. Yet, decoherence is still a problem and several STA protocols have been implemented in experiments or proposed theoretically.

The counterdiabatic driving approach was applied to design "universal" sets of fast and robust non-Abelian geometric gates: X.-K. Song, Zhang, Ai *et al.* (2016) proposed to use four NV centers around a whispering-gallery mode microsphere cavity, while Liang *et al.* (2016) made use of a single NV center coupled to a ^{13}C nuclear spin both modeled as two-level systems. Du *et al.* (2017) proposed a three-level scheme for the NV center where two of the couplings are due to microwave fields, and the third coupling is mechanically induced.

Experiments have shown the flexibility of NV centers to implement STA protocols for discrete systems: Kleißler, Lazariev, and Arroyo-Camejo (2018) implemented one-qubit holonomic gates proposed by Liang *et al.* (2016) in an effective two-level system driven by a microwave field with controllable, time-dependent detuning, Rabi frequency, and phase; Liu *et al.* (2018) used the eigenbasis of the dynamical invariant $I(t)$ associated with $H(t)$ as the auxiliary basis for constructing geometrical gates; and in B. B. Zhou *et al.* (2017), stimulated Raman adiabatic passage in a three-level system was sped up using dressed-state driving in terms of the original controls of the reference Hamiltonian.

The possibility of physically implementing two microwave couplings and one mechanical coupling among three levels is one of the interesting features of STA applied to NV centers (Amezcua, Golter, and Wang, 2017; Du *et al.*, 2017). Thanks to this structure Kölbl *et al.* (2019) used CD protocols experimentally to implement the initialization, readout, and coherent control of three-level dressed states. These states offer efficient coherence protection, better than the one achieved by two-level systems.

G. Many-body and spin-chain models

Many-body systems display controllable emergent properties and phenomena potentially useful in metrology and quantum simulation or computation, as well as in applications such as quantum light generation, memory devices, or precise sensing and communications. Slowly varying control parameters is one of the key tools to prepare and manipulate quantum many-body systems. In particular, adiabaticity plays a central role in understanding or implementing the quantum Hall effect, topological insulators, adiabatic computing, certain quantum phases [see Bachmann, De Roeck, and Fraas (2017) and references therein], or to maximize entanglement (Dorner *et al.*, 2003).

This discussion sets a strong motivation for developing STA approaches in many-body systems. In some cases "exact" shortcuts may be found, for example, after having applied mean-field theories or semiclassical approximations for a large number of particles N, or due to exact solvability, as for self-similar dynamics for specific interactions (Muga *et al.*, 2009; del Campo, 2011, 2013; del Campo and Boshier, 2012; Deffner, Jarzynski, and del Campo, 2014). Rohringer *et al.* (2015) demonstrated scaling behavior and shortcuts for expansions and compressions of phase-fluctuating quasi-1D Bose gases and more recently Deng, Chenu *et al.* (2018) and Deng, Diao *et al.* (2018) in a three-dimensional anisotropic "unitary Fermi gas."

Indeed, early STA experiments showed that many-body systems may benefit from STA techniques: expansions of clouds of cold thermal atoms were handled via invariants in the independent-atom approximation (Schaff *et al.*, 2010), and interacting Bose-Einstein condensates could be expanded fast using scaling in the mean-field approximation (Schaff, Capuzzi *et al.*, 2011; Schaff, Song *et al.*, 2011).

However, adiabaticity is often problematic for many-body systems making STA challenging. The difficulties are illustrated by the "orthogonality catastrophe": two ground states for two slightly different values of a control parameter λ may become orthogonal in the thermodynamic limit so that "strict" adiabaticity breaks down in essentially zero time. For certain drivings this occurs even with a finite gap. Milder definitions of adiabaticity are possible (Bachmann, De Roeck, and Fraas, 2017) referring to local variables rather than to the global N-body wave function.

The difficulties to implement adiabatic drivings are also evident in phase transitions across a quantum critical point, which lead to excitations for any finite crossing rate of the parameter. CD drivings can be found for the family of models which are solvable by a transformation into independent fermions, as for the 1D Ising model in a traverse field (del Campo, Rams, and Zurek, 2012),[8]

$$H = -\sum_{n=1}^{N} (\sigma_n^x \sigma_{n+1}^x + g\sigma_n^z). \tag{104}$$

After a Jordan-Wigner transformation, the Hamiltonian is decomposed into a series of independent Landau-Zener Hamiltonians for which the counterdiabatic driving is known. However, in spin space H_{CD} is highly nonlocal; it involves long-range, multibody interactions, and is increasingly important and divergent near the critical point (del Campo, Rams, and Zurek, 2012; del Campo, 2013; Damski, 2014, 2015; del Campo and Sengupta, 2015; Duncan and del Campo, 2018). For specific models the nonlocality may be circumvented. Thus Okuyama and Takahashi (2016) achieved a local CD for the Toda lattice using the machinery of Lax pairs, and Takahashi (2013b) for the XY model used a "fixed-point condition" where $H_{CD} = 0$.

Systematic efforts have been done to find approximate shortcuts based on truncation of the CD terms (del Campo, Rams, and Zurek, 2012; Damski, 2014) by restricting the range of the interaction, imposing adiabaticity only locally via local interactions (Mukherjee, Montangero, and Fazio, 2016), or optimizing an approximate *Ansatz* for H_{CD} based on simple (in particular two-body) auxiliary fields. This optimization requires spectral and wave function knowledge that is available for finite systems of experimental interest (Saberi *et al.*, 2014). Such detailed information is however typically not available for larger systems so another major research thread is to avoid using explicit spectral information to construct the shortcut. A variational approach proposed by Sels and Polkovnikov (2017), see Sec. II.B.2, moved in that direction. In particular, the aim of adiabatic computing is to find the ground state, which encodes the solution of a computational problem, by adiabatic following, precisely because it cannot be calculated. Yoshimura and Freericks (2015) proposed to apply a method to estimate the probability to be in the ground state from time-dependent measurements without knowing the Hamiltonian or its eigenfunctions, in order to optimize approximate shortcuts. Another phenomenological way out for some applications may be to optimize control parameters experimentally. For example, Cohn *et al.* (2018) proposed an optimization of a bang-bang protocol for the external parameter to produce entangled states in a Dicke model realized in a two-dimensional array of trapped ions in a Penning trap.

Josephson junctions and Lipkin-Meshkov-Glick-like models.—Much work has been done to apply shortcuts to many-body models which are either similar to or particular cases of the Lipkin-Meshkov-Glick (LMG) model

$$H_{\mathrm{LMG}} = \hbar[\Omega J_z + W(J_x^2 + J_y^2) + V(J_x^2 - J_y^2)], \tag{105}$$

[8]Another solvable model, where the CD driving involves as well many-body interactions, is the one-dimensional Kitaev honeycomb model (Kyaw and Kwek, 2018). It was proposed to generate highly entangled "cluster states" needed to implement "measured based quantum computation."

where

$$J_x = \tfrac{1}{2}(a^\dagger b + a b^\dagger),$$

$$J_y = \frac{1}{2i}(a^\dagger b - a b^\dagger),$$

and

$$J_z = \tfrac{1}{2}(a^\dagger a - b^\dagger b)$$

are "pseudospin" operators, with a and b being annihilation operators for two sites or two internal states. The same type of Hamiltonian appears in spin models where the operators J_α are to be interpreted as global angular momentum operators, usually denoted instead by $S_\alpha = (1/2)\sum_i \sigma_\alpha^i$, $\alpha = x$, y, and z, where σ^i is the Pauli spin operator for site i. Table III depicts some of the original Hamiltonians for which shortcuts were developed.

Bosonic Josephson junctions were treated by Juliá-Díaz *et al.* (2012) to generate spin-squeezed states. The junction was modeled with a two-site Bose-Hubbard Hamiltonian; see Table III. The ground state for $U > 0$ (antiferromagnetic LMG model) is unique. In the large-N limit and in the Fock basis of boson imbalance between the two wells the system may be treated semiclassically, i.e., considering a continuous rather than discrete population imbalance, for time dependent $U(t)$ and fixed J. The model simplifies to a single particle in an oscillator with time-dependence frequency. Invariants can then be used to design shortcuts and produce spin-squeezed states. A similar approach was later applied when the time dependence is in J, which is better suited for "internal junctions" where the connected states are not at different locations but in different internal states (Yuste *et al.*, 2013).

Other works have treated the two-site Bose-Hubbard Hamiltonian for low particle numbers, specifically $N = 2$: Opatrný and Mølmer (2014) proposed it as a toy model for a transition between a superfluid (maximally delocalized) state and a Mott-insulator ground state and explained the difficulties to physically implement the CD Hamiltonian[9]; Martínez-Garaot *et al.* (2014) applied Lie-algebraic methods to this problem, see Sec. II.B.2.a, to get STA without experimentally unfeasible generators; and Stefanatos and Paspalakis (2018b) optimized shortcuts via optimal control to maximize entanglement.

[9]Suppose that A and B are feasible operators in same H_0 and that H_{CD} needs $[A, B]$, which is difficult to implement directly. According to the Baker-Hausdorff-Campbell formula, applying the sequence of operators $bB \to aA \to -bB \to -aA$, where a and b are coefficients, during time intervals Δt amounts to applying $iab[A, B]\Delta t$ for a time Δt, $e^{iaA\Delta t}e^{ibB\Delta t}e^{-iaA\Delta t}e^{-ibB\Delta t} = e^{-ab[A,B]\Delta t^2} + O(\Delta t^3)$. Thus, in principle implementing $ab\Delta t[A, B]$ is possible with $\pm aA$ and $\pm bB$, but the problem lies in the scaling of the coefficients with Δt. For a given target value of $c = ab\Delta t$, then $ab = c/\Delta t$, which leads to intense pulses. If high intensities are available the dynamics with H_0 becomes more adiabatic so that the CD term is not really needed (Opatrný and Mølmer, 2014).

Opatrný *et al.* (2016) looked for maximally spin-squeezed "Dicke states" for finite N approximating the CD terms as in Opatrný and Mølmer (2014) and discussed how to implement compensating terms that go beyond quadratic order in the collective spin operators by means of suitable time sequences switching between quadratic operators.

The negative nonlinear coupling coefficient (ferromagnetic model) was studied by Takahashi (2013b) by providing the CD term for the ground state in the large-N thermodynamic limit. It generally diverges at the critical point. However, protocols satisfying a "fixed-point" condition such that $H_{CD} = 0$ were shown to be feasible in some instances. Campbell *et al.* (2015) used approximate CD terms identified by retaining dominant few-body terms, that may be optimized, rather than calculated from spectral information, with the aid of the instantaneous ground state. By applying a small longitudinal field that avoids the critical point, a mean-field prescription was applied using invariant-based engineering by Takahashi (2017b), and counterdiabatic driving by Hatomura (2017). Hatomura (2018) applied the semiclassical large-N approximation to generate a CD term, which, corrected by finite-size terms, avoids divergence at the critical point to generate cat states. Formally the process amounts to performing a transition from a single to a double well assisted by CD driving. The effect of particle losses was studied by Hatomura and Pawłowski (2019).

State transfer.—Fast quantum state transfer in linear chains was also theoretically addressed with STA concepts and techniques. Agundez *et al.* (2017) used a CD approach plus unitary transformation in a spin chain and Z.-M. Wang *et al.* (2016) sped up a slow protocol by scaling up the Hamiltonian. A similar method was applied by Ren, Wang, and Gu (2017) to cut a chain into two pieces. Ban *et al.* (2019) proposed to inverse engineer the tunneling barriers to transfer two-electron entangled states from one edge of an array of quantum dots described by the Hubbard model to the other. Finally, Longhi (2017) proposed a nonadiabatic fast protocol of robust excitation transfer in a non-Hermitian Hatano-Nelson tight-binding linear chain assisted by gain and loss gradients to cancel nonadiabatic transitions providing a fast state transfer in coupled-resonator optical waveguide structures.

1D Tonks-Girardeau gases and fermionic systems.—Under 1D effective confinement, the control and dynamics of noninteracting fermions or Tonks-Girardeau gases can be studied with solvable models that ultimately rely on the Slater determinant built with orbitals for single particle dynamics. Shortcuts have been applied to them in several works with different aims: Martínez-Garaot, Ruschhaupt *et al.* (2015) with the aid of the FAQUAD approach and Schloss *et al.* (2016) using invariants devised protocols to prepare macroscopic entangled states (NOON states) stirring a Tonks-Girardeau gas on a ring. The observation that leaking between two occupied states does not influence the fidelity of the gas, and that only leaks into modes above the Fermi level do, was systematically exploited and developed by Dowdall *et al.* (2017) for more general objectives to control fermionic systems.

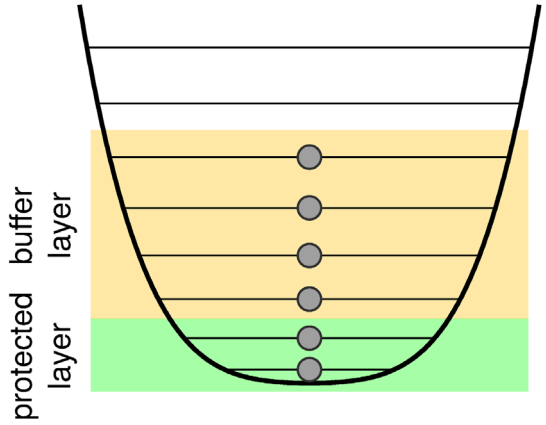

FIG. 11. To prevent transitions from the protected layer to higher-lying states during changes of the external parameters, a buffer layer of fermions is added. The Pauli principle prevents the protected fermions from accessing any level in the buffer zone. Adapted from Dowdall *et al.*, 2017.

Dowdall *et al.* (2017) proposed to use Pauli blocking for speeding up adiabatic evolution of the ground state of a number of "protected fermions" by using an additional layer of buffer particles; see Fig. 11. The protected fermions cannot make a transition to higher-lying excited states because these are occupied, and the fidelity for the final state of the protected particles increases with the number of buffer particles.

H. Metrology

Quantum systems offer, via interference, entanglement, and squeezing, many interesting possibilities for metrological applications and for improving measurement sensitivities. Allowing for time dependence in the Hamiltonian can only enhance the possibilities to find useful protocols (Pang and Jordan, 2017) so shortcuts to adiabaticity will also play an important role in metrology. We have already seen throughout the review several examples: In Sec. III.A we mentioned how STA-enhanced interferometry, in which the states are STA driven along the interferometer branches, can increase sensitivities and decrease decoherence effects. Also, Secs. III.C, III.D, and III.G provide examples where shortcuts are used to create in different platforms states of metrological interest such as spin-squeezed states, NOON states, and other entangled states.

Here we underline the strong link between CD driving and optimal protocols for quantum metrology. Pang and Jordan (2017) pointed out that fundamental precision limits valid for time-independent Hamiltonians can be dramatically violated with appropriate time-dependent control. In particular, the Fisher information, whose inverse square root limits the precision to measure some parameter g in the Hamiltonian H_g for arbitrary estimation strategies, can beat the limits valid for time-independent Hamiltonians. The information on g is transferred to a time evolution of a state measured at some time T. The upper bound for the Fisher information can be realized for superposition states whose components evolve at all times along the maximal and minimal eigenvalues of $\partial_g H_g(t)$. Here a slight modification of CD driving comes in handy. Similar to Sec. II.B, a Hamiltonian term $H_c(t)$ is added to $H_g(t)$ so that the dynamics follows exactly the eigenstates $|\psi_k(t)\rangle$ of $\partial_g H_g(t)$ [rather than the eigenstates of a zeroth Hamiltonian $H_0(t)$ as in regular CD driving]. Allowing for a freedom to choose phases $\theta(t)$ for each mode $H_{\rm tot} = H_g(t) + H_c(t)$ may be written as

$$H_{\rm tot} = -\sum |\psi_k(t)\rangle\dot{\theta}(t)\langle\psi_k(t)| + i\hbar\sum |\partial_t\psi_k(t)\rangle\langle\psi_k(t)|, \tag{106}$$

with exactly the same form as Eqs. (18) and (19), except for the meaning of the wave functions. The way to find g is in fact iterative, assuming first an estimate for g used to improve the estimate and so on. All this opens an exciting avenue since the possible difficulties to implement counterdiabatic driving terms as well as the arsenal of remedies described in Sec. II.B are applicable.

IV. THE ENERGY COST OF STA, ENGINES, AND THE THIRD LAW

A. Energy costs

In human affairs, shortcuts to reach a place or a goal may cost money or consume energy, although there is no universal recipe or law on the costs applicable to all circumstances. Some shortcuts are really for free, or almost, so they save time and resources, but others need a toll. Finding the "energy cost" of shortcuts to adiabaticity is a relevant and indeed, lately, popular goal. It is tempting to consider shortcuts to be energetically a free lunch since, by definition, the final energy is the same as for a slow adiabatic process. Many works, however, put forward different associated costs and imply that STA driving can hardly be free. In general the term "cost" has been used in a loose and heuristic way, without a fundamental analysis that justifies its suitability as an energy consumption. Actually most studies "define" rather than "find" the cost so that different definitions of cost given so far are not necessarily in conflict. As long as we put aside the propriety of the term, we may regard them as different aspects of the system energies or interactions, such as their evolution (transient values or time averages), excitations, fluctuations and flows, "intensities," or inequalities for several times and energies involved.

In an early study on the expansion and compression of a particle in a time-dependent harmonic oscillator (Chen and Muga, 2010), the cost was related to the time average of the particle energy. This average and its scaling with process time t_f depend strongly on the STA applied. If the shortcut makes use of a properly chosen $\omega(t)$ (e.g., designed via invariants) and no extra Hamiltonian terms, it was found by Euler-Lagrange optimization that for the nth eigenstate the time-averaged energy obeys $\bar{E}_n > (2n+1)\hbar/(2\omega_f t_f^2)$ for $(\omega_0/\omega_f)^{1/2} \gg 1$ and $t_f \ll (\omega_0\omega_f)^{-1/2}$, where ω_0 and ω_f are initial and final (angular) trap frequencies. Realizing this bound is indeed possible but at the price of infinite instantaneous power at boundary times (Cui, Chen, and Muga, 2016). The bound is relevant even in anharmonic traps since the trap depth D should be larger than $\bar{E}_n$, which sets a scaling

$t_f \gtrsim (\hbar/\omega_f D)^{1/2}$ for the minimal process time.[10] The time average of the standard deviation of the energy was found to scale also as t_f^{-2}, tighter than the bound $\gtrsim t_f^{-1}$ that follows from the Anandan-Aharonov (AA) relation (Anandan and Aharonov, 1990),

$$\tau \geq \frac{\hbar}{\overline{\Delta E}}\mathcal{L}, \tag{107}$$

setting $\tau = t_f$, where

$$\mathcal{L} = \arccos|\langle\psi(0)|\psi(\tau)\rangle|, \tag{108}$$

$$\overline{\Delta E} = \frac{1}{\tau}\int_0^\tau (\langle H^2\rangle - \langle H\rangle^2)^{1/2} dt. \tag{109}$$

This is one of the first applications of "quantum speed limits" to shortcuts to adiabaticity,[11] see Deffner and Campbell (2017). Many other applications have followed (Santos and Sarandy, 2015; Abah and Lutz, 2017; Campbell and Deffner, 2017) using AA and/or a Margoulis-Levitin–type of relation (Deffner and Lutz, 2013b). Note that a naive extension of the AA relation substituting $\overline{\Delta E}$ by the time-averaged energy $\langle H(t)\rangle$ is not valid in general for time-dependent Hamiltonians. Instead, a valid Margoulis-Levitin–type relation is (Deffner and Lutz, 2013a; Santos and Sarandy, 2015)

$$\tau \geq \hbar \frac{|\cos\mathcal{L} - 1|}{(1/\tau)\int_0^\tau |\langle\psi(0)|H|\psi(t)\rangle|}. \tag{110}$$

As a more recent example of other definitions, the average power computed as the total work divided by the process time was defined as the cost in Herrera *et al.* (2014). The cost has also been linked to the accumulated (Zheng *et al.*, 2016) or time-averaged (Santos and Sarandy, 2015, 2018; Coulamy *et al.*, 2016; Santos, Silva, and Sarandy, 2016) Frobenius norm of the Hamiltonian $\|H(t)\| = \sqrt{\mathrm{tr}[H(t)^2]}$ or of some nth power depending on the setting. This norm does not exist for many commonly found Hamiltonians such as the one for the harmonic oscillator. If it exists and $H = H_0 + H_{CD}$, the time average for H,

$$\Sigma_H(t_f) = \frac{1}{t_f}\int_0^{t_f} \sqrt{\mathrm{tr}[H_0^2 + H_{CD}^2]}dt,$$

is larger than the one for the reference protocol

$$\Sigma_0(t_f) = \frac{1}{t_f}\int_0^{t_f} \sqrt{\mathrm{tr}[H_0^2]}dt,$$

which suggests that CD driving always implies an additional cost. Choosing the phases $\xi_n(t)$ of the evolved states in the unitary evolution operator (11) has an impact on the energy cost. Specifically $\Sigma_H(t)$ is minimized by setting $\dot{\xi}_n(t) = -i\langle\dot{n}(t)|n(t)\rangle$ (Santos and Sarandy, 2018). In the framework of Eqs. (13)–(20) this amounts to applying H_{CD} alone, $H = H_{CD}$.

Zheng *et al.* (2016) and Campbell and Deffner (2017) defined differential costs, instantaneous or accumulated, in terms of the CD term only, ignoring H_0. In particular, existence problems are circumvented by considering the state-specific counterdiabatic term $H_{CD}^{[n]}$ in Eq. (25). Note that $\|H_{CD}^{[n]}\| = \hbar\sqrt{2\langle\dot{n}|\dot{n}\rangle}$ exists in systems where $\|H\|$ does not. Campbell and Deffner (2017) applied "quantum speed-limit inequalities" to driving by $H = H_0 + H_{CD}^{[n]}$ combining different norm types (trace norm and Frobenius norm). Interestingly, Demirplak and Rice already considered $\|H_{CD}\|$ and $\|H_{CD}^{[n]}\|$ as a measure of the "intensity" of the counterdiabatic terms and used them to find "minimal" CD terms. The state-specific $H_{CD}^{[n]}$ is thus less intense (costly) than the general purpose H_{CD} (Demirplak and Rice, 2008).

Other "differential costs" have been defined using different references. In an STA protocol driven by $H(t)$ with instantaneous eigenvalues $\mathsf{E}_n(t)$ and an initial state which is diagonal in the $|\mathsf{n}(t)\rangle$ eigenbasis of $H(t)$, with initial probabilities $p_n(0)$, del Campo, Goold, and Paternostro (2014) defined a work distribution and the corresponding average work as $\langle W\rangle = \sum_{k,n}[\mathsf{E}_k(t) - \mathsf{E}_n(0)]p_{nk}^t p_n^0$, which is $\langle H(t)\rangle - \langle H(0)\rangle$ for such states. $p_{nk}^t = |\langle\mathsf{k}(t)|U(t)|\mathsf{n}(0)\rangle|^2$ is the probability for the system to start at $|\mathsf{n}(0)\rangle$ and be found at $|\mathsf{k}(t)\rangle$ at time t. Similarly, they define the "adiabatic work" $\langle W_{ad}(t)\rangle = \sum[\mathsf{E}_n(t) - \mathsf{E}_n(0)]p_n^0$ and suggest as a "pragmatic" definition of cost the time average of the differential $\delta W(t) = \langle W(t)\rangle - \langle W_{ad}(t)\rangle$. A lower bound $\sim t_f^2$ for STA processes with inverse engineered time-dependent frequencies was found by Cui, Chen, and Muga (2016).

In CD-driven processes, the eigenenergies of $H(t)$, $\mathsf{E}_n(t)$ differ in general from the eigenenergies of $H_0(t)$, $E_n(t)$. Similarly, eigenstates of $H(t)$, $|\mathsf{n}(t)\rangle$, and $H_0(t)$, $|n(t)\rangle$ differ in general, although in most processes $H_{CD} = 0$ is imposed at $t = 0$ and t_f, so that the initial and final eigenvalues and eigenvectors of H_0 and H coincide. Funo *et al.* (2017) redefined $\langle W_{ad}(t)\rangle = \sum[E_n(t) - E_n(0)]p_n^0$ in terms of H_0 eigenvalues (this would agree with the previous definition at time t_f) and considered the work distributions

$$P[W(t)] = \sum_{k,n} p_n^0 p_{n\to k}^t \delta\{W(t) - [\mathsf{E}_k(t) - E_n(0)]\},$$
$$P_{ad}[W(t)] = \sum_n p_n^0 \delta[W(t) - W_{ad}^{(n)}], \tag{111}$$

where $W_{ad}^{(n)}(t) = E_n(t) - E_n(0)$. Since the initial state density operator is assumed diagonal in $\{|n(0)\rangle\}$ it will be diagonal in $\{|n(t)\rangle\}$ for all time because of the CD driving. As $\langle n(t)|H(t)|n(t)\rangle = \langle n(t)|H_0(t)|n(t)\rangle$ for all times, it follows that $\langle H(t)\rangle = \langle H_0(t)\rangle$ for all times and thus $\langle W(t)\rangle = \langle W_{ad}(t)\rangle$ during the process. As for the distributions, they

[10]The energy in CD driving scales differently. For example, choosing a linear ramp for the reference $\omega(t)$, $\bar{E}_n$ is independent of t_f, whereas the time-averaged variance [for all monotonous $\omega(t)$] goes as t_f^{-1}.

[11]The AA relation was later renamed a "Mandelstam-Tamm–type" relation, even if Mandelstam and Tamm did not consider time-dependent Hamiltonians (Mandelstam and Tamm, 1945).

coincide at boundary times $t = 0$ and t_f. Funo *et al.* (2017) also considered the work fluctuation with respect to the adiabatic trajectory

$$\delta(\Delta W)^2 = \sum_{m,n} p_n^0 p_{n\to m}^t [\mathsf{E}_m(t) - E_n(t)]^2,$$

and found that

$$t_f \geq \frac{\hbar \mathcal{L}[\rho(0), \rho(t_f)]}{\delta \bar{\Delta W}}, \tag{112}$$

where now $\mathcal{L}$ is the Bures length between initial and final (mixed) states. Funo *et al.* (2017) identified $\overline{\delta \Delta W}$ as the thermodynamic cost to implement the CD driving. The inequality (112) is tighter than the Aharonov-Anandan relation, which involves instead the fluctuation $\langle H^2(t)\rangle - \langle H(t)\rangle^2$, although the latter is of broader applicability, since it is not restricted to CD driving [nevertheless Bukov, Sels, and Polkovnikov (2019) conjectured, and validated for some models, that the quantum speed limit for all protocols is bounded by the quantum speed limit for CD protocols]. An experimental demonstration was carried out with an Xmon qubit (Z. Zhang *et al.*, 2018). These results were also extended to classical systems (Bravetti and Tapias, 2017). Funo, Shiraishi, and Saito (2019) studied a quantum speed limit for open quantum systems described by the Lindblad master equation. They found a "velocity term" that when the thermal relaxation is dominant compared to the unitary dynamics of the system is approximated by the energy fluctuation of the counterdiabatic Hamiltonian.

A related trade-off relation between time, entropy, and state distance was worked out by Takahashi (2017a) considering a canonical equilibrium state in density operator form $\rho(0)$, corresponding to a Boltzmann distribution with temperature T as the initial state. Removing the contact with the thermal bath, this evolves unitarily by $H(t) = H_0(t) + H_{CD}(t)$ into $\rho(0 \to t)$. Let $\rho(t)$ be the instantaneous equilibrium state corresponding to $H(t)$, and $\rho_0(t)$ the equilibrium state for H_0, both at the same temperature as the initial state. Using the Kullback-Leibler divergence, or relative entropy, from ρ_1 to ρ_2, $D_{KL} = \mathrm{tr}\rho_1 \ln \rho_1 - \mathrm{tr}\rho_1 \ln \rho_2$, Takahashi (2017a) found the "Pythagorean relation"

$$\begin{aligned} &D_{KL}(\rho(0 \to t) \| \rho(t)) \\ &\quad = D_{KL}(\rho(0 \to t) \| \rho_0(t)) + D_{KL}(\rho_0 \| \rho(t)), \end{aligned} \tag{113}$$

which is interpreted as a decomposition of entropy production. A trade-off relation previously mentioned follows from setting a lower bound to it.

Abah and Lutz (2017) considered STA expansions and compressions of a harmonic trap holding a particle in the context of microscopic quantum engines and refrigerators, see Fig. 12, making use only of different time dependences for $\omega(t)$. A reference Hamiltonian $H_0(t)$ is complemented by some modification term $H_{\mathrm{STA}}(t)$ [found by a unitary equivalence from a CD term as explained, e.g., by S. Ibáñez *et al.* (2012), see Sec. II.B.2.a and Eq. (61)], so that the resulting total $H(t)$ drives an STA process. They associated the energy

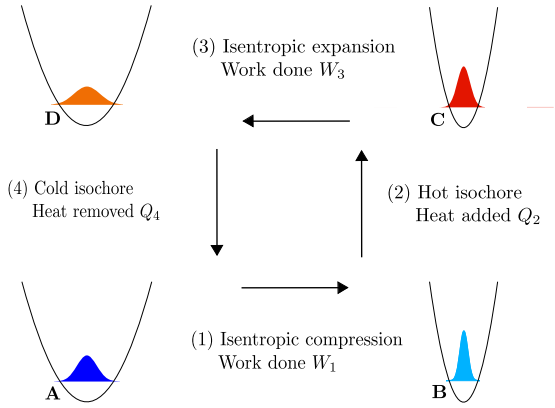

FIG. 12. Quantum Otto cycle for a particle in a harmonic oscillator. The colors are intended to represent the temperature ordering as (c) red, (d) orange, (b) light blue, and (a) deep blue. Adapted from Abah and Lutz, 2018.

cost with the time-averaged $\overline{\langle H_{\mathrm{STA}}\rangle}$. They also proposed to add these terms (one for the compression step $\overline{\langle H^1_{\mathrm{STA}}\rangle}$ and one for the expansion $\overline{\langle H^3_{\mathrm{STA}}\rangle}$) in the denominator of the efficiency of an Otto cycle to the heat added,

$$\eta = \frac{\text{work output}}{\text{heat added} + \overline{\langle H^1_{\mathrm{STA}}\rangle} + \overline{\langle H^3_{\mathrm{STA}}\rangle}}, \tag{114}$$

as an extra energy input. Thus this approach ignores the possible role of $H_0(t)$ in actual energy costs and leads to some paradoxical results. In particular, choosing $H(t) = H_0(t) + H_{\mathrm{STA}}(t)$ as the new reference $H_0'(t) = H(t)$, with frequency $\omega'(t)$ given by Eq. (61), no extra term is needed since $H_0'(t)$ is already a shortcut. The efficiency, being of a differential nature, would then have different values for the same process depending on how the Hamiltonian is partitioned (in one, $H_0' = H$, or two pieces, $H_0 + H_{\mathrm{STA}}$).

If the unitary transformation on H_{CD} is not performed (Abah and Lutz, 2018; Abah and Paternostro, 2018), the same type of modified efficiency is proposed with the time averaged $\overline{\langle H_{CD}\rangle}$ playing the role of $\overline{\langle H_{\mathrm{STA}}\rangle}$. However, $\langle H_{CD}(t)\rangle$ is zero by construction at all times for states diagonal in the eigenbasis of $H_0(t)$; see Eq. (14). Accordingly, all processes would have the same zero cost independently of the $H_0(t)$ chosen.

Several papers analyzed the effect of a control system (CS) (also termed driving or auxiliary system) coupled to the primary system (PS) of interest to set the STA driving and its influence on the energy cost. Calzetta (2018) pointed out that the time-dependent driving Hamiltonians in STA processes are typically semiclassical and thus approximate. For a simplified model with a particle in a harmonic oscillator whose frequency depends on a coordinate of a driving system and is subjected to quantum fluctuations, Calzetta estimated the excitation when the STA process is implemented on average. It grows inversely with process time, but also vanishes as the mass of the driving system increases. In a different vein, Horowitz and Jacobs (2015), for a model in which the mesoscopic PS system of interest is coupled to

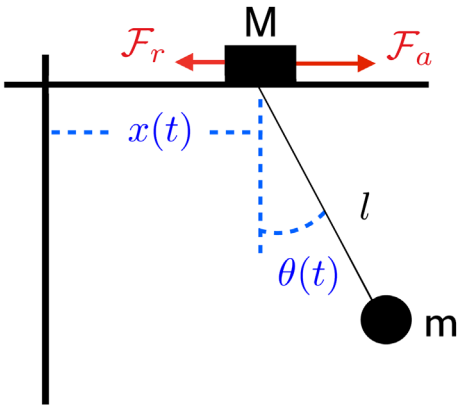

FIG. 13. Overhead crane composed of a load of mass m (the primary system PS) and a trolley of mass M (the control system CS) connected through a rope of constant length l. The solid red arrows represent the active force $\mathcal{F}_a$ and the friction force $\mathcal{F}_r$ acting on a rightward-moving trolley. Adapted from Torrontegui *et al.*, 2017.

dissipative Markovian noise processes and to an auxiliary control system connected to a thermal bath, argued that the minimal work to drive the system through a specified path of states is due to the need for the controller to compensate for the dissipation that tries to take the system away from the path. The exact formula depends on the Hamiltonian and state of the primary system for weak coupling but on the full Hamiltonian and state (including CS + PS) for strong coupling.

Torrontegui *et al.* (2017), Tobalina, Alonso, and Muga (2018), and Tobalina, Lizuain, and Muga (2019) also stressed the importance of the control system to find out true energy consumptions. The control system here is the equipment necessary to set the values of the control parameters of the primary system. This equipment is usually macroscopic and behaves classically. Even without direct dissipation of the primary system, implementing the driving will require energy consumption due to an external force, invested to change the energy of the global system (PS + CS) and to combat friction of the control system; see Sec. VII.B.1 and Fig. 13. Since STA processes are by definition fast, the arguments to justify minimal energy consumptions neglecting friction in the limit of slow motion (Landauer, 1961) are not of much value.[12] In a scenario with macroscopic control system and microscopic primary system, driving the control system along a predetermined path $x(t)$ is likely to be the dominant source of consumption, with the energy and backaction of the primary system being negligible in comparison, e.g., because of a large CS mass M compared to the PS mass m. These and other effects are indeed shown explicitly with models for transporting a classical load (Torrontegui *et al.*, 2017) or an ion in a multisegmented Paul trap (Tobalina, Alonso, and Muga, 2018; Tobalina, Lizuain, and Muga, 2019). A further relevant observation in these works is that in practice both positive and negative powers of the external force typically imply consumption, i.e., the energy given away by the system in "braking" time segments with a negative power is not stored and recovered at will in positive-power segments, although a phenomenological parameter is introduced to account for the possibility to perform, at least partially, energy-efficient regenerative braking. The models also show the importance of the control system to find the experimental gauge to determine the PS energy and corresponding power. For example, in a simple harmonic transport of a particle with Hamiltonian $p^2/(2m) + m\omega^2[x - x_0(t)]^2/2 + g(t)$, driven by the control function $x_0(t)$, the gauge function $g(t)$ does not affect the dynamics and so it is frequently ignored, but it may strongly affect the PS energy and corresponding power (Campisi, Hänggi, and Talkner, 2011; Tobalina, Lizuain, and Muga, 2019). A similar effect is found in expansions and compressions of an ion in a Paul trap, where the gauge term implies the opposite behavior to what could be naively expected, namely, an increase of energy during the expansion, and a decrease during the compression. It remains to be seen if smart engineering and design can equate the power of the external force to the PS power (this implies unrealistic assumptions in the worked out models, such as $M = 0$ and no friction), or at least make them proportional, as approximately realized in some model examples (Tobalina, Alonso, and Muga, 2018; Tobalina, Lizuain, and Muga, 2019). In any case further analysis of energy consumption, both fundamental and for STA processes in different systems (Impens and Guéry-Odelin, 2019), is needed.

B. Engines and refrigerators

A fundamental problem to design heat engine cycles is that maximal thermal efficiency (output work divided by the heat input from the hot bath) is achieved with slow processes that minimize losses but also imply negligible power output (output work divided by cycle time). Shortcuts appear at first sight to solve this problem as the adiabatic evolution can be mimicked in short times. STA-driven engines or refrigerators have been considered mostly for harmonic oscillators performing Otto cycles, see Fig. 12, with two isochoric (constant frequency) branches for contact with the hot and cold baths and thermally isolated compression or expansion branches where STA driving, as developed, e.g., in Salamon *et al.* (2009) and Chen, Lizuain *et al.* (2010), is applied.[13] For a recent review of the quantum Otto cycle for engines or refrigerators, see Kosloff and Rezek (2017).

Before the term shortcuts to adiabaticity existed, Ronnie Kosloff's group had already worked out "frictionless" bang-bang protocols for the isochoric strokes in which the adiabatic

[12]For an analysis of the work required by shortcuts to erase a bit in finite time beyond Landauer's bound, see Boyd *et al.* (2018). The model used is a Brownian particle in a double well potential. Instead of a trade-off between information and energy, as in Landauer's work, more complex trade-offs are found that depend on information and its robustness, energy, statistical bit-bias difference, size of the memory states, and speed.

[13]A version of the Otto cycle using single- and two-spin-1/2 systems was proposed by Çakmak and Müstecaplıoğlu (2018). An STA-enhanced Otto refrigerator based on a superconducting qubit with continuous coupling to two resonant circuits was analyzed by Funo *et al.* (2019).

state was recovered in the final time; see, e.g., Rezek *et al.* (2009) and Salamon *et al.* (2009). After 2010, two early studies on shortcuts applied to cycles were Torrontegui and Kosloff (2013), which examined the performance of a refrigerator subject to noise, and Deng *et al.* (2013), which addressed classical and quantum systems to boost work characteristics and overall heat engine performance.

Many other works followed and studied potential advantages or optimization of STA-driven processes (Tu, 2014; Xiao and Gong, 2014; del Campo, Goold, and Paternostro, 2014; Abah and Lutz, 2016, 2017). Some have tried to enhance the power output by considering not just STA but also many-body systems (Beau, Jaramillo, and del Campo, 2016; Chotorlishvili *et al.*, 2016; Jaramillo, Beau, and del Campo, 2016; Deng, Chenu *et al.*, 2018; Deng, Diao *et al.*, 2018), and nonlinear BECs (J. Li *et al.*, 2018) driven by STA found with variational methods (Li, Sun, and Chen, 2016). As well, Babajanova, Matrasulov, and Nakamura (2018) found the equations of state for FF dynamics in expanding cavities that contain an ideal Fermi gas, and Villazon, Polkovnikov, and Chandran (2019) proposed STA methods (unitarily transformed counterdiabatic driving) to manipulate both trap frequency and the coupling to the environment to realize fast approximate Otto engines operating near Carnot efficiency.

The role and design of STA methods in quantum engines and refrigerators is very much an open field where rather fundamental questions are still under scrutiny and debate. (Further aspects are discussed in Secs. IV.C and V.) For example, most studies systematically focus on the primary system only so that efficiencies and power computed with usual PS-based formulas are idealized limits that ignore CS effects discussed in the previous section. Some tentative proposals exist to modify the denominator (energy input) in the efficiency, such as taking into account time-averaged interactions of the terms added to the reference Hamiltonian to perform the STA (Abah and Lutz, 2017), energy dissipated by noise in the controls (Kosloff and Rezek, 2017), or energy consumptions to set the CS parameters (Tobalina, Lizuain, and Muga, 2019). Tobalina, Lizuain, and Muga (2019) pointed out that STA Otto engines based on a trapped ion are not ordinary engines. In the expansion stroke, the "piston," whose role is played by the harmonic trap, is not pushed by a hot ion, which exerts a negligible effect on the trap, but rather it is externally driven, in a fast manner specified by the STA protocol, by a controlled circuit that consumes and dissipates energy to do so, in fact, so much energy that the microscopic (PS) work output is far from compensating it. This may well happen for a broad domain of macroscopically controlled quantum systems. A way out might be that the quality of the microscopic work is worth the energy expense anyway, e.g., because of its effect on relevant degrees of freedom, but there is much to do to substantiate this hope in practice.

C. Third law

The third law of thermodynamics was formulated by Nernst as the impossibility to reduce any system to absolute zero in a finite number of operations; see Kosloff (2013) for a review. In the context of a quantum Otto heat pump it may be viewed as the vanishing of the cooling rate when the temperature of the cold bath approaches zero (Rezek *et al.*, 2009) and be quantified by the scaling law that relates the cooling rate and cold-bath temperature. The fundamental bottleneck is the time needed for the expansion branch. For a harmonic oscillator with a time-dependent frequency, the temperature of the equilibrium states connected adiabatically (i.e., slowly) or by STA is proportional to the frequency $\hbar\omega \propto kT$ to keep the average occupation number constant. Relevant questions are how fast we can lower ω and also finding scalings between the wanted times and the resources needed. The answers are not unique and depend on the method and constraints imposed. For expansions limited to a designed protocol for $\omega(t)$ minimal times exist if $\omega(t)$ is real and bounded. Simple bang-bang solutions for real ω give $t_f \sim \omega_c^{-1/2}$ (ω_c being the extreme, target value of ω in the expansion) (Rezek *et al.*, 2009; Salamon *et al.*, 2009; Stefanatos, 2017b). If $\omega(t)$ is not restricted and allowed to be imaginary, the expansion times can be formally arbitrarily short for any ω_c (Chen, Lizuain *et al.*, 2010). However, it is unrealistic to assume that arbitrarily fast processes are viable, as variously argued in Sec. IV.A. In particular, if the time average of the energy is supposed to be bounded, since the trap depth cannot be arbitrarily high, the same type of scaling arises (Chen and Muga, 2010). In fact more sophisticated bang-bang solutions, allowing for imaginary frequencies (Hoffmann *et al.*, 2011), or an arbitrary number of switches (Stefanatos, 2017a, 2017b) lead to faster processes.

V. OPEN QUANTUM SYSTEMS

In closed quantum systems, a slowly changing Hamiltonian can give rise to adiabatic dynamics as already discussed. By contrast, in open quantum systems, a slowly changing system Hamiltonian, or equivalently a long evolution time, does not necessarily guarantee adiabatic dynamics. In addition, the cumulative effect of dissipation increases with time. Shortcuts to adiabaticity in this context should therefore be defined with care. Interestingly, the control design of open quantum systems paves the way for the use of shortcuts in the emerging field of thermodynamics of quantum systems.

A. Concept of adiabaticity for open systems

A direct consequence of the coupling of the system with the environment is the need to redefine adiabaticity, as new elements and time scales appear compared to closed systems. Sarandy and Lidar (2005) generalized the adiabatic approximation to open systems for convolutionless master equations, i.e., master equations of the form $\dot{\rho}(t) = \mathcal{L}(t)\rho(t)$. Unlike closed systems, for which the Hamiltonian can always be diagonalized, the Lindblad superoperator $\mathcal{L}(t)$ of an open system is not necessarily diagonalizable and in general can be written only in Jordan normal form. Adiabaticity for open systems is subsequently defined as the regime for which the evolution of the state of a system takes place without mixing the various Jordan blocks. Alternatively, the adiabatic approximation in open systems can be formulated through an effective Hamiltonian approach (Yi *et al.*, 2007).

Further work about adiabaticity for open systems also includes the derivation of Markovian master equations suited

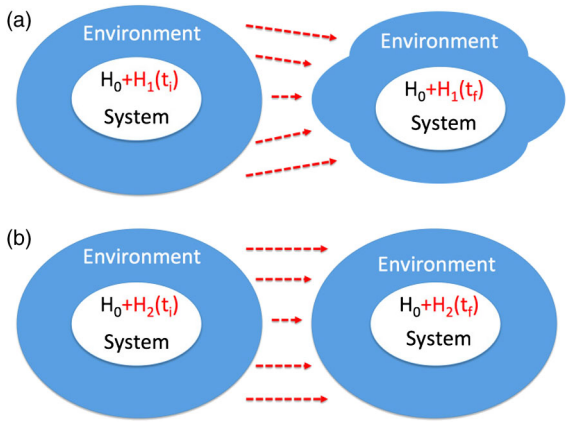

FIG. 14. Two kinds of control STA protocols of an open quantum system: (a) those involving a reservoir engineering in addition to Hamiltonian engineering, and (b) those relying only on Hamiltonian engineering.

for studying the time evolution of a system evolving slowly while coupled weakly to a thermal bath (Thunström, Åberg, and Sjöqvist, 2005; Pekola *et al.*, 2010; Albash *et al.*, 2012, 2015; Venuti *et al.*, 2016; Kiely, Muga, and Ruschhaupt, 2017), and the derivation of a link between the notion of adiabaticity for open system and the theory of noiseless subsystems (Oreshkov and Calsamiglia, 2010).

Hereafter, we address different strategies to implement STA protocols in the presence of a coupling with the environment. We first discuss techniques requiring a reservoir engineering, then focus on methods set up to mitigate the effect of a (nonmanipulated) environment; see Fig. 14. We conclude on a more specific class of open systems that can be described by non-Hermitian Hamiltonians.

B. Engineering the environment

Building on the work by Sarandy and Lidar (2005), the concept of a CD driving was generalized to open systems by working out the additional term to be superimposed to the Hamiltonian to guarantee an independent evolution of the different Jordan blocks of the Lindblad operator (Vacanti *et al.*, 2014). While this additional driving is unitary in some cases, in general it does not even provide a completely positive map.

A natural framework to extend the shortcuts to open systems is the explicit use of DFSs (S. L. Wu *et al.*, 2017). Consider that the coupling to the environment is accounted for by a Lindblad form

$$\mathcal{L}(t) = -\frac{i}{\hbar}[H,\rho] + \sum_k X_k \rho X_k^\dagger - \frac{1}{2}\{X_k^\dagger X_k, \rho\},$$

where the Lindblad operators may be time dependent. Similar to closed systems, the dynamical invariants of an open system provide us with both an intuitive physical framework and a set of tools to engineer quantum states (Ma, Cao, and Wu, 2017). In this perspective, it is useful to establish the modified equation for the invariant, which reads in this context

$$\partial_t I + \frac{i}{\hbar}[H,I] + \sum_k X_k^\dagger I X_k - \frac{1}{2}\{X_k^\dagger X_k, I\} = 0. \tag{115}$$

In contrast to closed systems, although $\langle I\rangle$ is still constant in time, its eigenvalues λ_n are no longer necessarily time independent. More precisely, all λ_n are time independent if I and X_k have a common basis of eigenvectors for all k.

However, it is possible to design a type of dynamical invariants for open quantum systems, in which a part of the eigenvalues is constant in time. By construction, the corresponding eigenstates are in the time-dependent DFSs. The interest of such subspace is that a quantum state evolves unitarily in it. By definition, the vectors of the DFS $\{|\Phi_1\rangle, |\Phi_2\rangle, \ldots, |\Phi_D\rangle\}$ are degenerate eigenstates of the Lindblad operators that obey the relation $X_k(t)|\Phi_j(t)\rangle = c_k(t)|\Phi_j(t)\rangle$ (Wu, Zhang, and Yi, 2015). A counterdiabatic driving Hamiltonian in the time-dependent DFS can be shown to be of the form (S. L. Wu *et al.*, 2017)

$$\tilde{H} = H(t) + \frac{i}{2}\sum_k (c_k^* X_k - c_k X_k^\dagger). \tag{116}$$

The driving based on invariants in the DFS can be equivalently worked out (Ma, Cao, and Wu, 2017). An important condition that needs to be fulfilled to control in time such quantum systems is the dynamical stability of the time-dependent DFS (S. L. Wu *et al.*, 2017). The application to few-spin systems was explicitly worked out by Ma, Cao, and Wu (2017) and S. L. Wu *et al.* (2017).

We note that another approach to set up the DFS consists of defining the invariant as a superoperator $\mathcal{I}$ that fulfills the relation (Sarandy, Duzzioni, and Moussa, 2007)

$$\frac{\partial \mathcal{I}}{\partial t} = [\mathcal{L}, \mathcal{I}]. \tag{117}$$

$\mathcal{I}$ is in general non-Hermitian. Decoherence-free evolution can further be constructed when the commutator of the Lindbladian and the superoperator $[\mathcal{L},\mathcal{I}]$ is independent of the noise parameters (Sarandy, Duzzioni, and Moussa, 2007).

Reservoir engineering to shortcut the thermalization process was also discussed in the context of nonadiabatic Markov equations (Dann, Levy, and Kosloff, 2018; Dann, Tobalina, and Kosloff, 2018). Such an approach, well suited for fast driving within the Markovian approximation, properly accounts for the coupling between population and coherence and explains the emergence of coherence associated with dissipation. Systems coupled to a non-Markovian bath have also been investigated. Villazon, Polkovnikov, and Chandran (2019) detailed the driving of such system using a protocol that controls in time both the system parameters and the coupling strength to the bath. This protocol was further exploited in an Otto-like engine operating at high power.

C. Mitigating the effect of environment

Quite often the coupling with the environment and the environment itself cannot be designed. For instance, the environment may induce noise in some parameters

(Ruschhaupt *et al.*, 2012; Kiely, Muga, and Ruschhaupt, 2017). In such a scenario STA techniques may be designed to mitigate its effects. Sun *et al.* (2016) investigated different variants of CD driving for a finite-time Landau-Zener process in the presence of a bath. Other strategies exploit the freedom on the phases $\xi_n(t)$ for the evolution operator $U(t) = \sum_n e^{i\xi_n(t)}|n(t)\rangle\langle n(0)|$ to minimize the effect of the coupling with the environment (Santos and Sarandy, 2018) in CD driving. In the same spirit, STA based on invariants can be readily adapted along the lines set in Ruschhaupt *et al.* (2012); see Sec. II.H. Levy, Torrontegui, and Kosloff (2017) minimized the effect of noise by reducing at best the commutators between invariants and the Lindblad noise operators X_k, specifically by minimizing the quantities $\mathcal{A}_k \sim \int_0^{t_f} ds\|[X_k(s), I(s)]\|$ over the process duration. Designing an invariant I that commutes with the noise operators X_k ensures that populations do not decay in the invariant eigenbasis and that decay of coherences is reduced. It is not always possible to minimize all $\mathcal{A}_k$ simultaneously, so a weighted average is minimized instead. Similarly, starting from an inverse engineering protocol, the parameters can be shaped in time to enforce the robustness against stochastic fluctuations in the Hamiltonian for a wide class of noise types (Jing *et al.*, 2013).

D. Non-Hermitian Hamiltonians

There is a class of quantum systems for which the environment can be modeled using non-Hermitian Hamiltonians. Such Hamiltonians usually describe subsystems of a larger system (Muga *et al.*, 2004). Complex energies imply that "adiabaticity theorems" apply only to weak non-Hermiticity regimes or to the least dissipative state (Nenciu and Rasche, 1992). Moreover, since right and left eigenvectors are normalized in a biorthogonal sense, the normalization factors are ambiguous and care must be exercised to extend the concept of "population" to define an adiabaticity criterion (Ibáñez and Muga, 2014).

Concerning the standard STA techniques, the counterdiabatic driving was generalized to weak non-Hermitian Hamiltonians (Ibáñez, Martínez-Garaot *et al.*, 2011; Ibáñez *et al.*, 2012; Chen, Xia *et al.*, 2016; J. Song *et al.*, 2016; G.-Q. Li *et al.*, 2017; H. Li *et al.*, 2017; Chen, Wu *et al.*, 2018). Ibáñez, Martínez-Garaot *et al.* (2011), in particular, applied the formalism to control a decaying two-level system. Later Torosov, Della Valle, and Longhi (2013) demonstrated that auxiliary gain and loss imaginary terms added in the diagonal of the Hamiltonian of Hermitian two-level models, which are feasible in waveguide optics, can be chosen to cancel nonadiabatic transitions and perform fast population transfers. The results were also generalized to three-level systems (Torosov, Della Valle, and Longhi, 2014; Q.-C. Wu *et al.*, 2016; G.-Q. Li *et al.*, 2017) and applied to a two-level system coupled to a dissipative spin chain (Diffo *et al.*, 2017). In Impens and Guéry-Odelin (2019), the extra driving field one has to superimpose to the original one to compensate for the distortion in the spin-1/2 direction on the Bloch sphere due to a dissipative non-Hermitian term, is explicitly worked out.

As for Lewis-Riesenfeld invariants for non-Hermitian Hamiltonians, they can be generalized in two different forms (Simón, Buendía, and Muga, 2018) corresponding to (Gao, Xu, and Qian, 1992; Khantoul, Bounames, and Maamache, 2017; Maamache *et al.*, 2017)

$$\frac{\partial I}{\partial t} + \frac{i}{\hbar}[H, I] = 0,$$
$$\frac{d}{dt}\langle\hat{\psi}(t)|I(t)|\psi(t)\rangle = 0, \tag{118}$$

where $\hat{\psi}(t)$ evolves with $H^\dagger(t)$ or to

$$\frac{\partial I'}{\partial t} + \frac{i}{\hbar}[H^\dagger(t)I'(t) - I'(t)H(t)] = 0,$$
$$\frac{d}{dt}\langle\psi(t)|I'(t)|\psi(t)\rangle = 0. \tag{119}$$

Combined with inverse engineering, the first option was considered, e.g., by Ibáñez, Martínez-Garaot *et al.* (2011) and Luo *et al.* (2015), and the potential of the second option is yet to be explored.

VI. OPTICAL DEVICES

There are some proposals to make use of time-dependent parameters to control light waves propagating in linear media via STA approaches (Lakehal, Maamache, and Choi, 2016), but the bulk of STA applications in optics substitutes time by a spatial coordinate. Thus shortcuts to adiabaticity in optics can lead to more compact waveguide devices, which favors device integration. After numerous theoretical works, the stage where actual STA-enhanced devices are constructed has just been reached.

STA applications in optics began exploiting the analogies (Longhi, 2009) between the electromagnetic wave propagation inside a waveguide in the paraxial approximation and the propagation of a quantum wave function inside a well. Consider a stationary scalar field $E(\mathbf{r})$ that satisfies the Helmholtz equation, a time-independent form of the wave equation,

$$\nabla^2 E(\mathbf{r}) + n^2(\mathbf{r})k^2 E(\mathbf{r}) = 0, \tag{120}$$

where $n(\mathbf{r})$ is the position-dependent refractive index inside the waveguide and $k = 2\pi/\lambda$, with λ the light wavelength in vacuum. Two common approximations are the small angle or paraxial approximation, which assumes the form

$$E(\mathbf{r}) = \mathcal{E}(\mathbf{r})e^{ik_z z}, \tag{121}$$

and a slowly varying envelope approximation (SVEA) in the scale of $2\pi/k_z$ to neglect $\partial^2\mathcal{E}/\partial z^2$. $k_z = kn_0$ plays the role of an "optical mass" and n_0 is the outer (bulk) refractive index. These approximations lead to a simplified form of Eq. (120) with the same form as the time-dependent Schrödinger equation, and the longitudinal space z coordinate playing the role of time,

$$i\frac{\partial\mathcal{E}}{\partial z} = \left[-\frac{1}{2kn_0}\nabla_\perp^2 + V(\mathbf{r})\right]\mathcal{E}, \tag{122}$$

$$V(\mathbf{r}) = \frac{k}{2n_0}[n_0^2 - n^2(\mathbf{r})]. \tag{123}$$

Coupled-mode theory.—Beam dynamics in coupled waveguides is usually addressed with "coupled-mode theory." Among the different formulations we focus here on the most used one in STA applications. Assume N-coupled waveguides, where the refractive index and geometry of the waveguides are allowed to vary along the propagation direction z. Under the scalar and paraxial approximations and the assumption of weak coupling, the variations of the guided-mode amplitudes of individual waveguides $\mathbf{A} = [a_1, a_2, \ldots, a_N]^T$ with propagation distance are described by the coupled-mode equations

$$i\frac{d\mathbf{A}}{dz} = H(z)\mathbf{A}. \tag{124}$$

Once again, replacing the spatial variation z with the temporal variation t, Eq. (124) is equivalent to the time-dependent Schrödinger equation ($\hbar \equiv 1$) describing the dynamics of an N-state system, with $H(z)$ playing the role of the Hamiltonian.

Lin *et al.* (2012) discovered the use of STA protocols to stabilize and reduce the size of coupled waveguide systems, applying the CD driving approach to the mode conversion in a multimode waveguide with three coupled modes. The results using coupled-mode theory were checked using the so-called wide-angle beam propagation numerical method, which solves the Helmholtz equation with SVEA, but no paraxial approximation.

Numerous works followed this line. Many of the methods presented in Sec. II were used to improve mode converters (Tseng and Chen, 2012; Tseng, 2013; Yeih, Cao, and Tseng, 2014) and also to design and optimize other devices such as mode-division multiplexing systems (Martínez-Garaot, Tseng, and Muga, 2014), see Fig. 15, directional couplers (Tseng, 2014; Tseng *et al.*, 2014), or polarization rotators (X. Chen *et al.*, 2014).

Stefanatos (2014) studied how to implement an STA in an optical semi-infinite system. A semi-infinite photonic lattice was designed to drive the input light to a controlled location at the output using the invariant-based inverse engineering approach, interpreting the photonic lattice as a quantum harmonic oscillator with time-dependent mass. One year later, Pan and Tseng (2015) applied the theory in Tseng *et al.* (2014) to design silicon-based platforms with high refractive index contrast, Paul and Sarma (2015) used the CD approach to improve the design of a directional coupler, and Ho and Tseng (2015) optimized the adiabaticity of coupled-waveguide devices using invariant-based inverse engineering.

Della Valle, Perozziello, and Longhi (2016) developed an STA for ultracompact waveguide junctions inspired by the streamlined version of the fast-forward approach (Torrontegui, Martínez-Garaot *et al.*, 2012). In this way they went beyond the coupled-mode equation formalism by extending the optical STA to full-wave problems for the Helmholtz equation, i.e., to an infinite-dimensional system.

Chen, Wen, and Tseng (2016) used the invariants to design stable directional couplers against errors in input wavelength and coupling coefficient simultaneously. Later Martínez-Garaot, Muga, and Tseng (2017) adapted the FAQUAD approach to the optical devices to design mode-sorting asymmetric Y junctions. This approach is quite useful in this context because the information it requires is accessible, and the simplicity of changing only one control parameter is ideal for device fabrication. Besides, Chung, Lee, and Tseng (2017) designed a short and broadband silicon asymmetric Y-junction two-mode (de)multiplexer using the theory by Martínez-Garaot, Muga, and Tseng (2017) and Wu, Ji, and Zhang (2017c) developed the generation of 3D entanglement using dressed states, and Huang, Ang, and Kyoseva (2017) applied the counterdiabatic approach to design shorter and robust two- and three-waveguide couplers. Finally, Chen, Wen *et al.* (2018) used the Lie-transform theory by Martínez-Garaot *et al.* (2014) to design compact beam splitters.

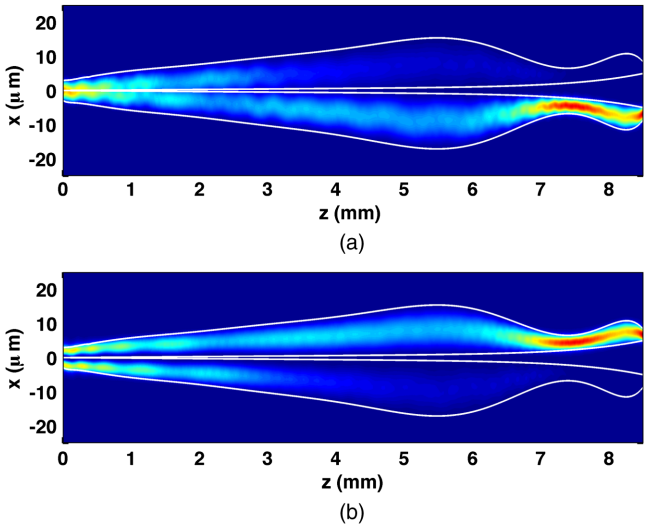

FIG. 15. Mode-sorting operation of the invariant-based Y junction. Input (a) fundamental mode and (b) second mode. From Martínez-Garaot, Tseng, and Muga, 2014.

In some recent works dealing with silicon waveguides with high index contrast, the scalar and paraxial approach is not accurate, so commercial software is used to solve the dynamics. Specifically, in Martínez-Garaot, Muga, and Tseng (2017) the shortcut was done using the scalar Helmholtz equation without the paraxial approximation and in Chung, Lee, and Tseng (2017) and Chung and Tseng (2018) the FAQUAD approach was applied without approximations, since it can incorporate the vectorial fields into the calculations without resorting to the coupled-mode equations. Moreover, Della Valle (2018) used shortcuts beyond the paraxial limit to achieve efficient rejection of higher order modes in a broad wavelength range for any two-dimensional multimode optical waveguide. Non-Hermitian systems with gain and loss were also considered (Torosov, Della Valle, and Longhi, 2013, 2014; Longhi, 2017).

The first experimental implementation of STA in optical devices was worked out by Guo and Chu (2017) demonstrating broadband silicon mode (de)multiplexers with optimized tapers using the method by Ho and Tseng (2015), and recently, the group of S.-Y. Tseng (Hung *et al.*, 2019) produced devices using the FAQUAD approach.

VII. EXTENSION TO CLASSICAL AND STATISTICAL PHYSICS

In this section, we reviewed the different STA methods which have been extended to classical mechanics and statistical physics, along with the presentation of a few proof-of-principle experiments that have been carried out to demonstrate their effectiveness.

A. Counterdiabatic methods in classical mechanics

As already discussed in Sec. II.B, the counterdiabatic term that we add to a time-dependent Hamiltonian in quantum mechanics inhibits any excitation in the system. A natural question is how we can transpose these ideas to a classical system, and to what extent they are related to their quantum counterpart.

We first address this question in the context of one-body classical mechanics. The essence of the method can be readily explained with a 1D integrable system described by a Hamiltonian $H_0(p,x,\lambda)$, where λ can be a multicomponent vector (for simplicity, we use a single component). Using a canonical transformation, there exist angle-action coordinates (θ,I) such that $H_0(p,x,\lambda)=\tilde{H}_0(I,\lambda)$, i.e., the Hamiltonian expressed in terms of the action-angle variables is independent of the angle θ as a result of its integrability. Assuming that the parameter is now time dependent, the new Hamiltonian resulting from the canonical transformation in action-angle variables takes the form (Goldstein, Poole, and Safko, 2002)

$$H(I,\theta,t)=\tilde{H}_0(I,\lambda)+\partial_t F=\tilde{H}_0(I,\lambda)+\dot{\lambda}\partial_\lambda F, \tag{125}$$

where F is a time-dependent generator whose "type" depends on its variables (Goldstein, Poole, and Safko, 2002; Deng *et al.*, 2013; Deffner, Jarzynski, and del Campo, 2014; Kolodrubetz *et al.*, 2017). For instance, $F=F_1(x,\theta,t)$ for type I. From Eq. (125), it is clear that the counterdiabatic Hamiltonian that one may superimpose to keep I constant with fast changes in λ is $H_{CD}=-\partial_t F$ (Deng *et al.*, 2013). In the adiabatic limit ($\dot{\lambda}\to 0$), the Hamiltonian H boils down to H_0. The counterdiabatic Hamiltonian H_{CD} added to the original Hamiltonian ensures that the volume of the phase space enclosed by a given energy shell remains constant despite the variation in time of the parameters (Jarzynski, 2013).

We now present some illustrative examples. Consider a 1D harmonic oscillator whose angular frequency $\omega(t)$ is time dependent:

$$H_0(p,x,t)=\frac{p^2}{2m}+\frac{1}{2}m\omega^2(t)x^2. \tag{126}$$

For such a Hamiltonian, the adiabatic criterion is

$$\frac{d\omega}{dt}\ll\omega^2. \tag{127}$$

Using the type-I generating function, the action-angle canonical transformation yields $p=\partial_x F_1$, $I=-\partial_\theta F_1$, and $H(I,\theta,t)=\tilde{H}_0(I,\lambda)+\dot{\omega}\partial_\omega F_1$ (Goldstein, Poole, and Safko, 2002). To get an expression of H_0 independent of θ, a natural choice is to search x and p in the form $p=f(I)\cos(\theta)$ and $x=[f(I)\sin\theta]/m\omega$ where the function $f(I)$ needs to be determined. We readily find $f(I)=(2Im\omega)^{1/2}$, $F_1(x,\theta,t)=(m\omega x^2\cot\theta)/2=px/2$, and $H_0(I,t)=I\omega$ and deduce $H_{CD}(p,x,t)=-\dot{\omega}F_1/\omega=-\dot{\omega}px/(2\omega)$. This result coincides perfectly with the classical limit of the quantum results (see Sec. II.C.2) (Muga *et al.*, 2010). The calculation performed here on a harmonic potential can be readily generalized to even-power-law potentials and to a particle in a one-dimensional box (Jarzynski, 2013).

We now consider the following example of the transport of a particle by moving a harmonic trap[14]:

$$H_0(p,x,t)=\frac{p^2}{2m}+\frac{1}{2}m\omega^2[x-x_0(t)]^2. \tag{128}$$

We can again work out the canonical transformation to recast the problem in terms of action-angle variables by replacing x by $x-x_0(t)$ in the previous calculation. The transformed Hamiltonian now reads $H=\tilde{H}_0(I,\lambda)+\dot{x}_0\partial_{x_0}F_1=\tilde{H}_0(I,\lambda)-p\dot{x}_0$. The counterdiabatic Hamiltonian is therefore $H_{CD}(p,x,t)=p\dot{x}_0$ (Sels and Polkovnikov, 2017), as in the quantum result (Torrontegui *et al.*, 2011). The quantum unitary transformation (Ibáñez *et al.*, 2012) to find an alternative local interaction corresponds classically to an additional canonical or gauge transformation. This procedure is referred to as the local counterdiabatic driving (Ibáñez *et al.*, 2012; Deffner, Jarzynski, and del Campo, 2014; Sels and Polkovnikov, 2017).

For a 1D Hamiltonian, a gauge transformation involves only a scalar potential $\chi(x,t)$. The momentum p is transformed as $\tilde{p}=p+\partial_x\chi$ for the Hamiltonian $\tilde{H}=H+\partial_t\chi$. For our first example, the gauge function $\chi(x,t)=\dot{\omega}mx^2/(4\omega)$ yields a gauged transformed Hamiltonian $\tilde{H}$ which is that of a harmonic oscillator of effective time-dependent angular frequency $\omega_{\rm eff}=[\omega^2+\ddot{\omega}/(2\omega)-3\dot{\omega}^2/(4\omega^2)]^{1/2}$, which coincides with its quantum counterpart; see Eq. (61) (Ibáñez *et al.*, 2012). For the second example, the gauge function $\chi(x,t)=-m\dot{x}_0x$ yields $\tilde{H}(p,x,t)=p^2/(2m)+(1/2)m\omega^2x^2-m\ddot{x}_0x$. The extra force $F=m\ddot{x}_0$ superimposed to the static Hamiltonian plays the role of an effective gravitational field whose amplitude is proportional to the acceleration $\ddot{x}_0$ and compensates for the inertial force in the frame attached to the potential.

Beyond the two specific examples previously detailed, the formalism can be generalized to scale-invariant systems, i.e., Hamiltonians of the form (Deffner, Jarzynski, and del Campo, 2014)

$$H_0(p,x,t)=\frac{p^2}{2m}+\frac{1}{\gamma^2(t)}U\left(\frac{x-x_0(t)}{\gamma(t)}\right), \tag{129}$$

where $\gamma(t)$ and $x_0(t)$ are real functions depending on time. Shortcuts are not restricted to scale-invariant systems as

[14]The same formalism still holds for an arbitrary transport potential.

explicitly shown by Patra and Jarzynski (2017a) on a simple example. The counterdiabatic Hamiltonian is also not unique. For instance, we have worked out its form linear in p for transport, but other solutions, e.g., cubic in p, are also possible; they are related to the dispersionless Korteweg–de Vries hierarchy [see Sec. II.C.4 and Okuyama and Takahashi (2016, 2017)].

Alternatively, one can construct a local dynamical invariant, or equivalently an extra potential to be added to the original Hamiltonian, to preserve the classical action for a fast time variation of the Hamiltonian parameters. Such an approach is reminiscent of the fast-forward method and can be solved implicitly as detailed by Jarzynski *et al.* (2017).

Finally, the counterdiabatic approach was also applied to classical spin dynamics (Hatomura and Mori, 2018). The construction makes use of the CD term for each single spin and is much easier to implement than in the corresponding quantum system. Moreover it does not need knowledge of the instantaneous stationary states. Starting from a stationary state of the initial Hamiltonian, it results in a stationary state of the final Hamiltonian if there is no criticality. The method can be used to solve combinatorial optimization problems.

B. Mechanical engineering

We discuss hereafter the interest of STA techniques to control a crane, then design robust solutions, and conclude with the link between STA and flatness based control in mathematics (Fliess *et al.*, 1995).

1. Cranes

The objective of mechanical cranes is to move loads fast avoiding final pendulations and large sway angles en route that could compromise safety. Since a slow, adiabatic operation avoids excitations but it takes an impractical long time, cranes are a natural domain for STA (González-Resines *et al.*, 2017). Crane control is an important engineering field; see Sun *et al.* (2012) and Kuo and Kang (2014) and references therein. Methods and ideas abound and many can be translated or adapted to other STA-driven processes in very different systems. For example, the work on closed-loop methods (in which measurements are performed en route to determine control operations) is an inspiring source to develop feedback-based STA in the microscopic realm. In reverse, existing STA methods may have quite an impact on crane operation routines. Overhead cranes usually operate under a small-oscillation regime so that simple operations such as horizontal transport and hoistingor lowering of the load are modeled by the same basic (mass independent) equations that apply to the transport or compression or expansion of an ion in a time-dependent harmonic trap. González-Resines *et al.* (2017) provided invariant-based STA protocols for the motion of the trolley in a transport operation or for hoisting that guarantee final adiabatic energies for the load. Furthermore, these energies are shown to be minimal when averaging over a microcanonical ensemble of initial conditions, consistently with the minimal work principle (Allahverdyan and Nieuwenhuizen, 2005, 2007). Indeed the possibility to design robust operations with respect to different perturbations or errors (such as dispersion in the initial conditions or in cable lengths) and STA and OCT combinations to limit, for example, en-route pendulations, offer a great potential. The different techniques to enhance robustness, such as the Fourier method [(Guéry-Odelin and Muga, 2014), see the next section], may be used to design trolley trajectories which are robust with respect to different errors, e.g., in the cable length. The bridge to perform analogous inverse engineering in quantum microscopic and classical macroscopic systems is much facilitated by the fact that the Lewis-Leach family of potentials implies the same classical (Lewis and Leach, 1982) and quantum formulations (Dhara and Lawande, 1984) for the invariants and auxiliary equations.

A crane model that treats the trolley position as a dynamical variable, instead of as a control function, subjected to inertia, the engine pulling force $\mathcal{F}_a$, dissipation, and the backaction of the load, is a neat, explicit test bed to study energy consumptions and the implications of shortcuts to adiabaticity from the point of view of the necessary external controls (Torrontegui *et al.*, 2017). In particular, the power produced by the engine force is due to the change of mechanical energy $\mathcal{H}_0$ of the whole system (load and trolley) plus the power needed to compensate the effect of friction

$$\mathcal{P} = \mathcal{F}_a\dot{x} = \frac{d\mathcal{H}_0}{dt} + \gamma\dot{x}^2,$$

where x is the trolley's position and γ the friction coefficient. In the harmonic approximation this becomes

$$\mathcal{P} = (M\ddot{x} - mq\omega^2 + \gamma\dot{x})\dot{x}, \tag{130}$$

where M is the trolley's mass and q the load horizontal displacement with respect to the trolley; see Fig. 13. The second term is exactly the power P defined as the derivative of the mechanical energy of the load. $\mathcal{P} = P$ under only rather extreme and even undesirable conditions.

Note that the shortcuts are by definition fast processes, so that the friction can hardly be avoided by the trick of slowing down the dynamics applied for ideal reversible operations. Only the typically unrealistic $\gamma = 0$ scenario would cancel the dissipation term. As for the M-dependent term, the limit $M = 0$ is again rather unrealistic, and in fact does not simplify matters, because the action of the engine would have to depend strongly on the initial conditions of the load; contrast this to ideal state-independent STA operations that require instead a large M/m ratio. Another interesting aspect of the model is the analysis of possible negative values of $\mathcal{P}$ corresponding to braking. Different scenarios (implying energy consumption or rather partial regenerative braking) are depicted by Torrontegui *et al.* (2017) and treated phenomenologically to examine the total energy consumption.

We focused on cranes but clearly other mechanical machines and robots with moving parts can benefit from shortcuts to adiabaticity (Stefanatos, 2018), as well as other areas of engineering. For example, Faure *et al.* (2018) introduced inverse engineering to drive a resistor-capacitor (RC) circuit.

2. Robustness issues

In Sec. II.A, we showed how the equation of motion of a particle in a moving harmonic potential of angular frequency ω_0 can be reversed. We proposed to extend this technique using a Fourier method (Guéry-Odelin and Muga, 2014). From the Newton equation, one can directly relate the excess energy after the transport $\Delta E(t_f) = m|\mathcal{F}(\omega_0;\{x_0(t)\})|^2$ to the motion of the trap $x_0(t)$ with

$$\mathcal{F}(\omega;\{x_0(t)\}) = \int_0^{t_f} \ddot{x}_0(t') e^{-i\omega t'} dt'. \tag{131}$$

An optimal trajectory $\{\tilde{x}_0(t)\}$ for the transport shall therefore fulfill the relation $\mathcal{F}(\omega_0;\{\tilde{x}_0(t)\}) = 0$. A systematic way to generate such trajectories is to define the acceleration $\ddot{x}_0(t)$ through an auxiliary time-dependent function $g(t)$ as $\ddot{x}_0(t) = \ddot{g}(t) + \omega_0^2 g(t)$, where $g(t)$ obeys the boundary conditions $g(0) = g(t_f) = \dot{g}(0) = \dot{g}(t_f) = 0$ and the relations

$$\int_0^{t_f} g(t)dt = 0 \quad \text{and} \quad \int_0^{t_f} dt' \int_0^{t'} g(t'')dt'' = \frac{d}{\omega_0^2}. \tag{132}$$

These conditions ensure that $x_0(0) = 0$, $\dot{x}_0(0) = 0$, $x_0(t_f) = d$, and $\dot{x}_0(t_f) = 0$. We then find

$$\mathcal{F}(\omega;\{x_0(t)\}) = (\omega_0^2 - \omega^2) \int_0^{t_f} g(t') e^{-i\omega t'} dt', \tag{133}$$

which vanishes for $\omega = \omega_0$, as expected for an optimal transport. Interestingly, using a fourth-order differential equation to relate $\ddot{x}_0$ and $g(t)$, and with appropriate boundary conditions for $g(t)$, one can factorize a polynomial in ω^2 in front of the Fourier transform of $g(t)$ of the form $(\omega_1^2 - \omega^2)(\omega_2^2 - \omega^2)$ (Guéry-Odelin and Muga, 2014). With such a solution, the same trajectory of the trap would be optimal for two different angular frequencies ω_1 and ω_2. This would apply for instance for two different atoms transported by the same moving optical tweezers (Couvert *et al.*, 2008). Alternatively, the protocol repeated for higher order polynomial with the same root ω_0 provides a generic method to enforce robustness against the exact value of the angular frequency experienced by the atoms (Guéry-Odelin and Muga, 2014). For an application in ion transport, see An *et al.* (2016).

Flatness based control theory.—From a more mathematical point of view, the previous solution can also be recovered using flatness based control theory commonly used for steering a system from one state to another (Rouchon, 2005). This formalism applies to differential systems of the form

$$dx/dt = f(x,u), \tag{134}$$

where the vector u contains the control variables. The control problem is readily solved when there exists a so-called flat-output map h, $y(t) = h(x,u,\dot{u},\ldots,u^{(\alpha)})$, such that $x = h_1(y,\dot{y},\ldots,y^{(\beta)})$ and $u = h_2(y,\dot{y},\ldots,y^{(\beta+1)})$, where α and β are some finite numbers, and h_1 and h_2 some smooth functions. For a given system described by Eq. (134) there is no algorithm to determine if a flat-output map h exists. However, many examples of engineering interest turn out to be flat including transport (Rouchon, 2005) and cranes (Fliess *et al.*, 1995).

C. STA for isolated dilute gases

So far we have essentially considered one-body problems. One may wonder to what extent the results can be generalized to an assembly of interacting atoms. We first consider a dilute gas trapped by a 3D isotropic harmonic potential of angular frequency ω_0. The notion of adiabaticity shall be revisited in this new context. Indeed, the gas has a relaxation time τ that is related to the collision rate $\gamma_c = n\sigma\bar{v}$, where n is the mean atomic density, σ the total cross section, and $\bar{v} \propto (k_B T/m)^{1/2}$ the mean thermal velocity for a temperature T. The relation between τ and γ_c depends on the collision regime: for $\gamma_c \ll \omega_0$, i.e., when there are few collisions per oscillation period $\tau \propto \gamma_c^{-1}$, while $\gamma_c \gg \omega_0$ in the hydrodynamic limit $\tau \propto \gamma_c/\omega_0^2$. The thermodynamical criterion for adiabaticity associated with a slow change of the angular frequency $\omega(t)$ now reads

$$\frac{d\omega}{dt} \ll \frac{\omega}{\tau}. \tag{135}$$

Once this criterion is fulfilled, the quantity $T(t)/\omega(t)$ remains constant. The physical interpretation of this conserved quantity is clear, it ensures that the populations $\pi_n \propto \exp(-\hbar n\omega/k_B T)$ of the eigenstates are conserved during a slow change of confining strength. Otherwise stated, the transformation corresponds to a work and is not accompanied by heat (modifications of the populations).

1. Boltzmann equation

The search for a shortcut on such transformations requires a rigorous mathematical modeling of the out-of-equilibrium dynamics. Under the approximation of diluteness, the evolution of the phase-space distribution $f(\mathbf{r},\mathbf{v},t)$ of the gas is well described by the Boltzmann equation where collisions are accounted for through the two-body collisional integral. In Guéry-Odelin *et al.* (2014), an exact solution of this equation for a time-dependent angular frequency $\omega(t)$ was worked out,

$$f(\mathbf{r},\mathbf{v},t) = \frac{(\alpha\beta - \gamma^2/4)^{3/2}}{\pi^3} e^{-\alpha r^2 - \beta v^2 - \gamma \mathbf{r}\cdot\mathbf{v}}, \tag{136}$$

where $\alpha(t)$, $\beta(t)$, and $\gamma(t)$ are functions that depend only on time. They are related through a linear set of differential equations which can be recast as a single third-order differential equation on the quantity β which plays the role of the inverse of an effective temperature,

$$\dddot{\beta} + 4\omega^2\dot{\beta} + 4\omega\dot{\omega}\beta = 0. \tag{137}$$

For a slow transformation, the third-order derivative can be neglected and the quantity $T(t)/\omega(t) \propto [\beta(t)\omega(t)]^{-1}$ is conserved. Fast transformations can be designed by inverse engineering, i.e., by fixing the boundary conditions on β and its derivatives, interpolating the β function accordingly,

and inferring $\omega(t)$ from the equation obeyed by β. For very fast decompression, we find as in quantum mechanics intervals of time over which the sign of the curvature of the potential is reversed. So far we have kept the trap isotropic. The extension of STA protocols to anisotropic 2D Bose gas and 3D unitary Fermi gases including in the presence of topological defects such as soliton or vortices was discussed by Papoular and Stringari (2015).

2. Extension to Navier-Stokes equation

The solution previously outlined hints at a related solution for hydrodynamics. Indeed, as originally demonstrated by Chapman and Enskog (Chapman, Cowling, and Burnet, 1970), the hydrodynamic equations can be derived from the Boltzmann equation. These equations relate the velocity field $\mathbf{v}(\mathbf{r},t)$, the temperature field $T(\mathbf{r},t)$, and the density $n(\mathbf{r},t)$,

$$\begin{aligned}
&\frac{\partial n}{\partial t}+\boldsymbol{\nabla}\cdot(n\mathbf{v})=0,\\
&mn\left(\frac{\partial}{\partial t}+\mathbf{v}\cdot\boldsymbol{\nabla}\right)\mathbf{u}=-n\boldsymbol{\nabla}U-\boldsymbol{\nabla}\left(P-\frac{\eta}{3}(\boldsymbol{\nabla}\cdot\mathbf{v})\right)+\frac{\eta}{\rho}\nabla^2\mathbf{v},\\
&\left(\frac{\partial}{\partial t}+\mathbf{v}\cdot\boldsymbol{\nabla}\right)T=-\frac{T}{c_V}(\boldsymbol{\nabla}\cdot\mathbf{v})+\frac{\kappa\nabla^2 T}{mnc_V},
\end{aligned}\tag{138}$$

where η is the viscosity, c_V the specific heat, and κ the thermal conductivity. The exact solution for a 3D isotropic harmonic trap with time-dependent angular frequency $\omega(t)$ is found through the search of an exact scaling solution of the form $n(\mathbf{r},t)=b^{-3}n_0(\mathbf{r}/b)$, $\mathbf{v}(\mathbf{r},t)=\dot{b}\mathbf{r}/b$, and $T(\mathbf{r},t)=\beta^{-1}(t)$. Remarkably, we found that the inverse of the effective temperature parameter β and $\omega(t)$ are connected once again by Eq. (137). The same STA strategy can therefore be applied in this context.

D. Shortcuts for systems in contact with a thermostat

So far we have considered only isolated systems. In this section, we answered the question of how a classical system in contact with a thermal bath can benefit from an accelerated equilibration protocol. Indeed, the control in the presence of a thermostat is of general interest with applications ranging from nano-oscillators, nanothermal engines, to the driving of mesoscopic chemical or biological processes.

The one-body equation to be considered is therefore a stochastic differential equation, the Langevin equation, whose noise is related to the temperature of the bath. In its most general form, it is given by

$$m\ddot{x}=-\partial_x U(x,t)-m\gamma\dot{x}+\xi(t),\tag{139}$$

where we consider the noise $\xi(t)$ as a white noise delta correlated in time $\langle\xi(t)\xi(t')\rangle=2m\gamma k_B T\delta(t-t')$. The inverse engineering method cannot be readily applied directly to a stochastic equation. Instead, the equation for the probability density $\rho(x,t)$ function associated with such a Brownian motion is used.

1. The overdamped regime

First we considered the overdamped regime for which inertial effects become negligible. This amounts to vanishing the mass in Eq. (139). The probability density then obeys the Fokker-Planck equation

$$\partial_t\rho(x,t)=\gamma^{-1}\partial_x[\rho(x,t)U(x,t)]+D\partial_{xx}^2\rho,\tag{140}$$

with the diffusion constant $D=k_BT/m\gamma$. Two standard STA methods can be applied to accelerate the equilibration: the transposition of the counterdiabatic ideas and the inverse engineering.

For the first method, we considered an equilibrium solution of Eq. (140), $\rho_0(x,\{\lambda\})$ that corresponds to the potential energy $U_0(x,\{\lambda\})$, where $\{\lambda\}$ refers to the control parameters of the potential. U_1 is the extra potential that we have to add to the original potential U_0 to compensate for the time variation of the parameters $\{\lambda\}$. This potential is the solution of the equation

$$\partial_t\rho_0(x,\{\lambda(t)\})=\gamma^{-1}\partial_x[\rho_0(x,\{\lambda(t)\})U_1(x,t)].\tag{141}$$

For instance, with a potential $U_0(x,t)=m\omega^2(t)[x-x_0(t)]^2/2$, we find

$$U_1(x,t)=-m\gamma\dot{x}_0[x-x_0(t)]+\frac{m\gamma\dot{\omega}[x-x_0(t)]^2}{2\omega}.\tag{142}$$

The potential $U_1(x,t)$ is nothing but the classical counterdiabatic Hamiltonian determined in Sec. VII.A (Li, Quan, and Tu, 2017).

The second strategy is to apply inverse engineering to the Fokker-Planck equation. For the compression or decompression of a harmonic oscillator from an angular frequency ω_i to ω_f, we use an exact scaling solution of the overdamped Fokker-Planck equation (Martínez *et al.*, 2016),

$$\rho(x,t)=\sqrt{\frac{\alpha(t)}{\pi}}\exp[-\alpha(t)x^2]\tag{143}$$

with

$$\frac{\dot{\alpha}}{\alpha}=\frac{2\omega^2(t)}{\gamma}-\frac{4k_BT\alpha}{\gamma}.\tag{144}$$

For our purpose, we imposed boundary conditions on the α parameter [$\alpha(0)=m\omega_i^2/2k_BT$, $\alpha(t_f)=m\omega_f^2/2k_BT$, $\dot{\alpha}(0)=0$, and $\dot{\alpha}(t_f)=0$], interpolated the $\alpha(t)$ functions, and inferred from Eq. (144) how one shall shape $\omega(t)$. This solution was successfully implemented experimentally for a compression using a 1 μm size microsphere trapped by an optical tweezer and immersed in a thermalized fluid chamber (Martínez *et al.*, 2016). The strength of the confinement was simply increased by designing in time the intensity of the trap beam. In this manner, the system has reached equilibrium 100 times faster than the natural equilibration rate. Alternatively, the minimum time to perform transitions between thermal equilibrium states was also studied using optimal control theory (see Sec. II.G) under different constraints on the domain of variation of the time-dependent angular frequency $\omega(t)$ (Stefanatos, 2017b; Plata *et al.*, 2019).

As for the system described by the Boltzmann equation or for the quantum counterpart, the protocol requires for very fast decompression the transient use of a repulsive potential. In practice, this is arduous if not impossible depending on the system. However, and contrary to the quantum case, an extra parameter can be tuned in statistical physics, namely, the temperature. Indeed the temperature can be related to noise as explicitly written in the Langevin equation (Martínez *et al.*, 2013). By a proper shaping of the noise, it is therefore possible to dramatically accelerate the decompression keeping the trap attractive as recently demonstrated experimentally (Chupeau, Besga *et al.*, 2018).

2. Connection with free energy and irreversible work

A natural question arises: what is the work that can be extracted from a given transformation? In the context of an overdamped dynamics, this question was theoretically addressed by Sekimoto and Sasa (1997). The mean work W done by the systems reads (Tu, 2014; Acconcia, Bonança, and Deffner, 2015; Martínez *et al.*, 2016; Li, Quan, and Tu, 2017)

$$W = \Delta F + W_{\mathrm{irr}}, \tag{145}$$

where ΔF refers to the increment of the Helmholtz free energy associated with the transformation and $W_{\mathrm{irr}} > 0$ to the irreversible work. In the limit of slow variation of the control parameter the work done boils down to the variation of the Helmholtz free energy which becomes independent of the path used for the transformation. If t_f refers to the interval over which the transformation is performed, one can show that the product $W_{\mathrm{irr}} t_f$ is bounded in the limit $t_f \to \infty$. For a compression or decompression, we found $\Delta F = k_B T \log(\omega_f/\omega_i)$ and $W_{\mathrm{irr}} = \eta k_B T (\omega_f^2/\omega_i^2)\tau_{\mathrm{relax}}/t_f$, where the numerical factor η depends upon the chosen protocol and $\tau_{\mathrm{relax}} = \gamma/m\omega_f^2$.

3. Extensions

The extension of the previous approach to the underdamped regime was worked out by Cunuder *et al.* (2016), Li, Quan, and Tu (2017), and Chupeau, Ciliberto *et al.* (2018). The inverse engineering approach can be readily generalized to manipulate the phase-space distribution $\rho(x, v, t)$ (Chupeau, Ciliberto *et al.*, 2018). This technique was used experimentally to accelerate the equilibration of a micromechanical oscillator (Cunuder *et al.*, 2016). However, the transposition of the counterdiabatic method provides an auxiliary potential linear in p that is not relevant from an experimental point of view (Li, Quan, and Tu, 2017).

VIII. OUTLOOK AND OPEN QUESTIONS

Since the birth of the term in 2010 until today, shortcuts to adiabaticity have experienced phenomenal growth.[15] We attribute this expansion to a double appeal, both practical and fundamental:

The practical side is rooted in the fact that adiabatic invariance is ubiquitous as a phenomenon and as a route for state preparation, in quantum physics and beyond. Shortcuts overcome adiabatic protocols, which imply long times and the concomitant accumulation of perturbations from the environment or the control system. Moreover a rich network of different pure or hybrid STA approaches provides a flexible toolbox that can be applied and adapted to many systems and operations. Only in the quantum arena proposals exist for STA-mediated cooling, interferometers, photon production, enantiomer separation, quantum gates, or information transfer. Methodological progress in one area can be translated to others allowing for synergies. Quantum physics has been indeed the main field to develop STA methodology and applications so far. As the control of microscopic systems improves, we get closer to realizing new quantum technologies. Yet, decoherence remains a stumbling block to go beyond proof-of-principle results. Shortcuts contribute to fight decoherence via shorter process times and robust protocols. An ideal quantum device is expected to operate fast and accurately despite a noisy environment or perturbations and with minimal consumption of resources. These are all goals that fit into the agenda and capabilities of STA methods.

The fundamental side rests on the fact that basic concepts and physical quantities and phenomena such as robustness, timing, energy and work, information, entropy, needed resources, controllability, environment effects, or classical or quantum borders and connections all play a role in shortcut design, so shortcuts motivate and contribute to the quest for their interrelations. Early work on the time-dependent harmonic oscillator made clear that the process time and time-averaged energies involved in the STA-driven process implied nontrivial inequalities and speed limits that helped to quantify cooling speeds. The scrutiny of energy-time relations has grown in different directions, e.g., to analyze energy costs and their scaling with process times. The fast nature of STA processes makes some conventional estimates based on slow reversible processes invalid. As well, fundamental questions on the meaning and appropriate definitions of work, heat, or efficiencies arise. The counterdiabatic Hamiltonian bridges the gap between actual and ideal transitionless dynamics and so it enters in a number of fundamental inequalities to set speed limits, see Sec. IV, but also as an aid to reach maximal precision limits as discussed in Sec. III.H. Recent work demonstrates energy and time relations may be quite rich for open systems bringing to the fore further elements such as entropy production, robustness, and/or information erasure (Takahashi, 2017a; Boyd *et al.*, 2018; Funo, Shiraishi, and Saito, 2019).

In this review we have seen a number of problem- or field-specific challenges. Here we underline a few open questions we consider to be important along broader conceptual or methodological lines.

• We have discussed examples for which the full spectral information of the original Hamiltonian is not necessary to perform the shortcuts. As well, approximate schemes are being developed. Improving approximations and

[15] A Web-of-Science search including the main keywords gives 7 citations in 2010, 359 in 2014, and 1543 in 2018, with an h index of ~40.

spectral-information independence are of upmost importance for complex quantum systems such as many-body systems, multiple levels, or for adiabatic computing. The question of the minimum required information for a given transformation that needs to be accelerated has not been investigated systematically so far.

• We have discussed the key role played by dynamical invariants and their link with other STA techniques. Open questions are (a) to find further families of Hamiltonian-invariant pairs beyond the Lewis-Leach family, e.g., via Lax pairs; (b) in n-dimensional systems, to find and implement effective schemes when the dynamical normal modes need a generalized transformation (involving coordinates and momenta); and (c) to explore the use for STA design of different generalizations of "invariant" operators for non-Hermitian systems.

• Steering a dynamical quantum system from an initial to a final state in the presence of an environment poses a challenge for quantum control on controllability, i.e., to which extent the target state is reachable; and control design, possibly including reservoir engineering. A framework to draw the frontiers of controllability is highly desirable for quantum control in open systems (Glaser *et al.*, 2015; Koch, 2016), but note that shortcuts may be applied even if the system is not fully controllable (Petiziol *et al.*, 2018).

• We have provided examples of hybrid control approaches, for instance, hybridation of shortcuts and optimal control theory that allows for optimal protocol selection. From a control perspective, shortcuts to adiabaticity have contributed to open-loop (with no-feedback) design. One could also envision the hybridation of such feed-forward techniques with feedback oriented techniques. Indeed, STA could help to approach the target very fast and the final convergence could be ensured by a feedback procedure. Such a strategy would benefit from the advantages of both techniques: short time processing and strong robustness.

• We need to clarify the energetic and resource cost of STA approaches, and the associated trade-off relations. This is of general interest both at the fundamental level and for specific experiments, for example, to determine the actual performance of STA-enhanced microscopic or mesoscopic engines and refrigerators.

• STA protocols can *a priori* be adapted to a large class of other dynamical or differential equations, e.g., in engineering, plasma physics, optics, soft condensed matter, or biology.

LIST OF SYMBOLS AND ABBREVIATIONS

1D, 2D, etc.	one dimensional, two dimensional, etc.
BEC	Bose-Einstein condensate
CD	counterdiabatic
CNOT	controlled not
CS	control system
dc	direct current
DFS	decoherence-free subspace
DRAG	derivative removal of adiabatic gate
FAQUAD	fast quasiadiabatic dynamics
FF	fast forward
GHZ	Greenberger-Horne-Zeilinger
IE	inverse engineering
IP	interaction picture
NV	nitrogen vacancy
OCT	optimal control theory
PDE	partial differential equation
PS	primary system
QED	quantum electrodynamics
QZD	quantum Zeno dynamics
STA	shortcut to adiabaticity
STIRAP	stimulated Raman adiabatic passage
SVEA	slowly varying envelope approximation
WAHWAH	weak anharmonicity with average Hamiltonian

ACKNOWLEDGMENTS

We thank P. Claeys, S. Deffner, C. Jarzynski, R. Kosloff, M. Sarandy, E. Sherman, D. Sugny, K. Takahashi, E. Trizac, and S.-Y. Tseng for clarifying comments or a critical reading of the manuscript or sections of it. Many colleagues and collaborators, too numerous to mention individually, have contributed through the last 10 years to our work on shortcuts. We are deeply indebted to all of them. This work was supported by the Basque Country Government (Grant No. IT986-16); PGC2018-101355-B-100 (MCIU/AEI/FEDER, UE); PGC2018-094792-B-100 (MCIU/AEI/FEDER, EU); CAM/FEDER Project No. S2018/TCS-4342 (QUITEMAD-CM); and by Programme Investissements d'Avenir under the Grant ANR-11-IDEX-0002-02, reference ANR-10-LABX-0037-NEXT, as well as the Grant ANR-18-CE30-0013.

APPENDIX A: EXAMPLE OF LIE TRANSFORM

As an example to illustrate the use of "physical" unitary transformations to generate alternative shortcuts we considered a two-level system in which we applied a Lie transform to get rid of a σ_y term in the Hamiltonian found with the CD approach. The reference Hamiltonian H_0 is given in Eq. (15) and H_{CD} in Eq. (16). The generators of the dynamical algebra are the Pauli matrices,

$$G_1=\begin{pmatrix}0 & 1\\ 1 & 0\end{pmatrix},\qquad G_2=\begin{pmatrix}0 & -i\\ i & 0\end{pmatrix},\qquad G_3=\begin{pmatrix}1 & 0\\ 0 & -1\end{pmatrix}, \tag{A1}$$

which satisfy the commutation relations $[G_a,G_b]=2i\epsilon_{abc}G_c$. The total Hamiltonian $H(t)=H_0(t)+H_{CD}(t)$ in terms of the algebra generators can be written as

$$H(t)=\frac{\hbar}{2}[\Omega_R(t)G_1-\Delta(t)G_3]+\frac{\hbar}{2}\Omega_a(t)G_2. \tag{A2}$$

Suppose that the generator G_2 is difficult or inconvenient to implement; see, for example, Bason *et al.* (2012). Setting $G=G_3$ in Eq. (29), and substituting into Eq. (30), the series of repeated commutators may be summed up. H' becomes

$$H'(t)=\frac{\hbar}{2}\{[\Omega_R(t)\cos(2g(t))+\Omega_a(t)\sin(2g(t))]G_1 - [\Omega_R(t)\sin(2g(t))-\Omega_a(t)\cos(2g(t))]G_2 - [\Delta(t)+2\dot{g}(t)]G_3\}. \tag{A3}$$

To cancel the G_2 term, we choose

$$g(t)=\frac{1}{2}\arctan\left[\frac{\Omega_a(t)}{\Omega_R(t)}\right]. \tag{A4}$$

Substituting Eq. (A4) into Eq. (A3) we have finally

$$H'(t)=\frac{\hbar}{2}\left\{\left[\sqrt{1+\frac{\Omega_a^2(t)}{\Omega_R^2(t)}}\Omega_R(t)\right]G_1 - \left[\Delta+\frac{\Omega_R(t)\dot{\Omega}_a(t)-\dot{\Omega}_R(t)\Omega_a(t)}{\Omega_R^2(t)+\Omega_a^2(t)}\right]G_3\right\}, \tag{A5}$$

which has the same structure (generators) as the reference Hamiltonian (15) but different time-dependent coefficients. A similar result can be found without starting from the reference shortcut (16), but following the bottom-up approach of Torrontegui, Martínez-Garaot, and Muga (2014); see Sec. II.C.1.

APPENDIX B: COUNTERDIABATIC HAMILTONIAN FOR A TWO-LEVEL HAMILTONIAN WITH COMPLEX COUPLING

We found here H_{CD} for a two-level Hamiltonian H_0 with complex-valued coupling Ω,

$$H_0(t)=\frac{\hbar}{2}\begin{pmatrix}-\Delta(t) & |\Omega(t)|e^{i\alpha(t)}\\ |\Omega(t)|e^{-i\alpha(t)} & \Delta(t)\end{pmatrix}, \tag{B1}$$

where $|\Omega(t)|$ is the modulus and $\alpha(t)$ the argument of the coupling. The instantaneous eigenvectors of this Hamiltonian are

$$|\lambda_-(t)\rangle=-\sin[\theta(t)/2]e^{i\alpha(t)/2}|1\rangle+\cos[\theta(t)/2]e^{-i\alpha(t)/2}|2\rangle,$$
$$|\lambda_+(t)\rangle=\cos[\theta(t)/2]e^{i\alpha(t)/2}|1\rangle+\sin[\theta(t)/2]e^{-i\alpha(t)/2}|2\rangle, \tag{B2}$$

with the mixing angle $\theta(t)\equiv\arccos[-\Delta(t)/\tilde{\Omega}(t)]$ and eigenvalues $E_\mp(t)=\mp\hbar\tilde{\Omega}/2$, where $\tilde{\Omega}=\sqrt{\Delta^2(t)+|\Omega(t)|^2}$. The counterdiabatic Hamiltonian is given by $H_{CD}=H_{CD}^{(1)}+H_{CD}^{(2)}$, where $H_{CD}^{(1)}=i\hbar\sum_n|\dot{n}(t)\rangle\langle n(t)|$ and $H_{CD}^{(2)}=-i\hbar\sum_n\langle n(t)|\dot{n}(t)\rangle|n(t)\rangle\langle n(t)|$. For the Hamiltonian $H_0(t)$ in Eq. (B1), we get

$$H_{CD}^{(1)}(t)=\frac{\hbar}{2}\begin{pmatrix}-\dot{\alpha}(t) & -ie^{i\alpha(t)}\dot{\theta}(t)\\ ie^{-i\alpha(t)}\dot{\theta}(t) & \dot{\alpha}(t)\end{pmatrix} \tag{B3}$$

and

$$H_{CD}^{(2)}(t)=\frac{\hbar}{2}\cos\theta(t)\dot{\alpha}(t) \times\begin{pmatrix}\cos\theta(t) & e^{i\alpha(t)}\sin\theta(t)\\ e^{-i\alpha(t)}\sin\theta(t) & -\cos\theta(t)\end{pmatrix}. \tag{B4}$$

If $\alpha(t)=0$, we have that $H_{CD}^{(2)}=0$, and the expression of $H_{CD}^{(1)}(t)$ simplifies to the one given, e.g., in Eq. (16) or Chen, Lizuain *et al.* (2010).

REFERENCES

Abah, O., and E. Lutz, 2016, Europhys. Lett. **113**, 60002.
Abah, O., and E. Lutz, 2017, Europhys. Lett. **118**, 40005.
Abah, O., and E. Lutz, 2018, Phys. Rev. E **98**, 032121.
Abah, O., and M. Paternostro, 2018, arXiv:1808.00580.
Acconcia, T. V., M. V. S. Bonança, and S. Deffner, 2015, Phys. Rev. E **92**, 042148.
Agundez, R. R., C. D. Hill, L. C. L. Hollenberg, S. Rogge, and M. Blaauboer, 2017, Phys. Rev. A **95**, 012317.
Albash, T., S. Boixo, D. A. Lidar, and P. Zanardi, 2012, New J. Phys. **14**, 123016.
Albash, T., S. Boixo, D. A. Lidar, and P. Zanardi, 2015, New J. Phys. **17**, 129501.
Albash, T., and D. A. Lidar, 2018, Rev. Mod. Phys. **90**, 015002.
Allahverdyan, A. E., and T. M. Nieuwenhuizen, 2005, Phys. Rev. E **71**, 046107.
Allahverdyan, A. E., and T. M. Nieuwenhuizen, 2007, Phys. Rev. E **75**, 051124.
Alonso, J., F. M. Leupold, Z. U. Solèr, M. Fadel, M. Marinelli, B. C. Keitch, V. Negnevitsky, and J. P. Home, 2016, Nat. Commun. **7**, 11243.
Amezcua, M., A. Golter, and H. Wang, 2017, in *2017 Conference on Lasers and Electro-Optics (CLEO)* (Optical Society of America, Washington, DC), pp. 1–2.
Amin, M. H. S., 2008, Phys. Rev. Lett. **100**, 130503.
Amri, S., R. Corgier, D. Sugny, E. Rasel, N. Gaaloul, and E. Charron, 2018, arXiv:1812.10999.
An, S., D. Lv, A. del Campo, and K. Kim, 2016, Nat. Commun. **7**, 12999.
Anandan, J., and Y. Aharonov, 1990, Phys. Rev. Lett. **65**, 1697.
Babajanova, G., J. Matrasulov, and K. Nakamura, 2018, Phys. Rev. E **97**, 042104.
Bachmann, S., W. De Roeck, and M. Fraas, 2017, Phys. Rev. Lett. **119**, 060201.
Baksic, A., R. Belyansky, H. Ribeiro, and A. A. Clerk, 2017, Phys. Rev. A **96**, 021801.
Baksic, A., H. Ribeiro, and A. A. Clerk, 2016, Phys. Rev. Lett. **116**, 230503.
Ban, Y., and X. Chen, 2014, Sci. Rep. **4**, 6258.
Ban, Y., X. Chen, S. Kohler, and G. Platero, 2019, arXiv:1904.05694.
Ban, Y., X. Chen, J. G. Muga, and E. Y. Sherman, 2015, Phys. Rev. A **91**, 023604.
Ban, Y., X. Chen, E. Y. Sherman, and J. G. Muga, 2012a, Phys. Rev. Lett. **109**, 249901.
Ban, Y., X. Chen, E. Y. Sherman, and J. G. Muga, 2012b, Phys. Rev. Lett. **109**, 206602.
Bason, M. G., M. Viteau, N. Malossi, P. Huillery, E. Arimondo, D. Ciampini, R. Fazio, V. Giovannetti, R. Mannella, and O. Morsch, 2012, Nat. Phys. **8**, 147.
Beau, M., J. Jaramillo, and A. del Campo, 2016, Entropy **18**, 168.

Benseny, A., A. Kiely, Y. Zhang, T. Busch, and A. Ruschhaupt, 2017, EPJ Quantum Techno. **4**, 3.

Bernardo, B. d. L., 2019, arXiv:1907.01916.

Berry, M. V., 1987, Proc. R. Soc. A **414**, 31.

Berry, M. V., 2009, J. Phys. A **42**, 365303.

Boldt, F., P. Salamon, and K. H. Hoffmann, 2016, J. Phys. Chem. A **120**, 3218.

Bowler, R., J. Gaebler, Y. Lin, T. R. Tan, D. Hanneke, J. D. Jost, J. P. Home, D. Leibfried, and D. J. Wineland, 2012, Phys. Rev. Lett. **109**, 080502.

Boyd, A. B., A. Patra, C. Jarzynski, and J. P. Crutchfield, 2018, arXiv:1812.11241.

Boyers, E., M. Pandey, D. K. Campbell, A. Polkovnikov, D. Sels, and A. O. Sushkov, 2018, arXiv:1811.09762.

Bravetti, A., and D. Tapias, 2017, Phys. Rev. E **96**, 052107.

Bücker, R., T. Berrada, S. Van Frank, J.-F. Schaff, T. Schumm, J. Schmiedmayer, G. Jäger, J. Grond, and U. Hohenester, 2013, J. Phys. B **46**, 104012.

Bücker, R., J. Grond, S. Manz, T. Berrada, T. Betz, C. Koller, U. Hohenester, T. Schumm, A. Perrin, and J. Schmiedmayer, 2011, Nat. Phys. **7**, 608.

Bukov, M., D. Sels, and A. Polkovnikov, 2019, Phys. Rev. X **9**, 011034.

Čadež, T., J. Jefferson, and A. Ramšak, 2013, New J. Phys. **15**, 013029.

Čadež, T., J. H. Jefferson, and A. Ramšak 2014, Phys. Rev. Lett. **112**, 150402.

Çakmak, B., and Ö. E. Müstecaplıoğlu, 2018, arXiv:1812.00969.

Calzetta, E., 2018, Phys. Rev. A **98**, 032107.

Campbell, S., G. De Chiara, M. Paternostro, G. M. Palma, and R. Fazio, 2015, Phys. Rev. Lett. **114**, 177206.

Campbell, S., and S. Deffner, 2017, Phys. Rev. Lett. **118**, 100601.

Campisi, M., P. Hänggi, and P. Talkner, 2011, Rev. Mod. Phys. **83**, 771.

Castin, Y., and R. Dum, 1996, Phys. Rev. Lett. **77**, 5315.

Chapman, S., T. G. Cowling, and D. Burnet, 1970, *The Mathematical Theory of Non-Uniform Gases: An Account of the Kinetic Theory of Viscosity, Thermal Conduction, and Diffusion in Gases* (Cambridge University Press, Cambridge, England).

Chen, J., and L. F. Wei, 2015, Phys. Rev. A **91**, 023405.

Chen, X., R.-L. Jiang, J. Li, Y. Ban, and E. Y. Sherman, 2018, Phys. Rev. A **97**, 013631.

Chen, X., I. Lizuain, A. Ruschhaupt, D. Guéry-Odelin, and J. G. Muga, 2010, Phys. Rev. Lett. **105**, 123003.

Chen, X., and J. G. Muga, 2010, Phys. Rev. A **82**, 053403.

Chen, X., and J. G. Muga, 2012, Phys. Rev. A **86**, 033405.

Chen, X., A. Ruschhaupt, S. Schmidt, A. del Campo, D. Guéry-Odelin, and J. G. Muga, 2010, Phys. Rev. Lett. **104**, 063002.

Chen, X., E. Torrontegui, and J. G. Muga, 2011, Phys. Rev. A **83**, 062116.

Chen, X., E. Torrontegui, D. Stefanatos, J.-S. Li, and J. G. Muga, 2011, Phys. Rev. A **84**, 043415.

Chen, X., H.-W. Wang, Y. Ban, and Shuo-Yen, 2014, Opt. Express **22**, 24169.

Chen, X., R.-D. Wen, J.-L. Shi, and S.-Y. Tseng, 2018, J. Opt. **20**, 045804.

Chen, X., R.-D. Wen, and S.-Y. Tseng, 2016, Opt. Express **24**, 18322.

Chen, Y.-H., B.-H. Huang, J. Song, and Y. Xia, 2016, Opt. Commun. **380**, 140.

Chen, Y.-H., Z.-C. Shi, J. Song, and Y. Xia, 2018, Phys. Rev. A **97**, 023841.

Chen, Y.-H., Z.-C. Shi, J. Song, Y. Xia, and S.-B. Zheng, 2017, Phys. Rev. A **95**, 062319.

Chen, Y.-H., Q.-C. Wu, B.-H. Huang, J. Song, Y. Xia, and S.-B. Zheng, 2018, Ann. Phys. (Berlin) **530**, 1700247.

Chen, Y.-H., Y. Xia, Q.-Q. Chen, and J. Song, 2014a, Phys. Rev. A **89**, 033856.

Chen, Y.-H., Y. Xia, Q.-Q. Chen, and J. Song, 2014b, Laser Phys. Lett. **11**, 115201.

Chen, Y.-H., Y. Xia, Q.-Q. Chen, and J. Song, 2015, Phys. Rev. A **91**, 012325.

Chen, Y.-H., Y. Xia, J. Song, and Q.-Q. Chen, 2015, Sci. Rep. **5**, 15616.

Chen, Y.-H., Y. Xia, Q.-C. Wu, B.-H. Huang, and J. Song, 2016, Phys. Rev. A **93**, 052109.

Chen, Z., Y.-H. Chen, Y. Xia, J. Song, and B.-H. Huang, 2016, Sci. Rep. **6**, 22202.

Choi, S., R. Onofrio, and B. Sundaram, 2011, Phys. Rev. A **84**, 051601.

Choi, S., R. Onofrio, and B. Sundaram, 2012, Phys. Rev. A **86**, 043436.

Chotorlishvili, L., M. Azimi, S. Stagraczyński, Z. Toklikishvili, M. Schüler, and J. Berakdar, 2016, Phys. Rev. E **94**, 032116.

Chung, H.-C., K.-S. Lee, and S.-Y. Tseng, 2017, Opt. Express **25**, 13626.

Chung, H.-C., and S.-Y. Tseng, 2018, Opt. Express **26**, 9655.

Chupeau, M., B. Besga, D. Guéry-Odelin, E. Trizac, A. Petrosyan, and S. Ciliberto, 2018, Phys. Rev. E **98**, 010104.

Chupeau, M., S. Ciliberto, D. Guéry-Odelin, and E. Trizac, 2018, arXiv:1802.10512.

Claeys, P. W., M. Pandey, D. Sels, and A. Polkovnikov, 2019, arXiv:1904.03209.

Cohn, J., A. Safavi-Naini, R. J. Lewis-Swan, J. G. Bohnet, M. Gärttner, K. A. Gilmore, J. E. Jordan, A. M. Rey, J. J. Bollinger, and J. K. Freericks, 2018, New J. Phys. **20**, 055013.

Corgier, R., S. Amri, W. Herr, H. Ahlers, J. Rudolph, D. Guéry-Odelin, E. M. Rasel, E. Charron, and N. Gaaloul, 2018, New J. Phys. **20**, 055002.

Coto, R., V. Jacques, G. Hétet, and J. R. Maze, 2017, Phys. Rev. B **96**, 085420.

Coulamy, I. B., A. C. Santos, I. Hen, and M. S. Sarandy, 2016, Front. ICT **3**, 19.

Couvert, A., T. Kawalec, G. Reinaudi, and D. Guéry-Odelin, 2008, Europhys. Lett. **83**, 13001.

Cui, Y.-Y., X. Chen, and J. G. Muga, 2016, J. Phys. Chem. A **120**, 2962.

Cunuder, A. L., I. A. Martínez, A. Petrosyan, D. Guéry-Odelin, E. Trizac, and S. Ciliberto, 2016, Appl. Phys. Lett. **109**, 113502.

Daems, D., A. Ruschhaupt, D. Sugny, and S. Gurin, 2013, Phys. Rev. Lett. **111**, 050404.

Damski, B., **2014**, J. Stat. Mech. 12, P12019.

Damski, B., 2015, Sci. Rep. **5**, 15779.

Dann, R., A. Levy, and R. Kosloff, 2018, Phys. Rev. A **98**, 052129.

Dann, R., A. Tobalina, and R. Kosloff, 2018, arXiv:1812.08821.

Deffner, S., 2016, New J. Phys. **18**, 012001.

Deffner, S., and S. Campbell, 2017, J. Phys. A **50**, 453001.

Deffner, S., C. Jarzynski, and A. del Campo, 2014, Phys. Rev. X **4**, 021013.

Deffner, S., and E. Lutz, 2013a, J. Phys. A **46**, 335302.

Deffner, S., and E. Lutz, 2013b, Phys. Rev. Lett. **111**, 010402.

del Campo, A., 2011, Phys. Rev. A **84**, 031606.

del Campo, A., 2013, Phys. Rev. Lett. **111**, 100502.

del Campo, A., and M. G. Boshier, 2012, Sci. Rep. **2**, 648.

del Campo, A., J. Goold, and M. Paternostro, 2014, Sci. Rep. **4**, 6208.

del Campo, A., and K. Kim, 2019, arXiv:1902.06283.

del Campo, A., M. M. Rams, and W. H. Zurek, 2012, Phys. Rev. Lett. **109**, 115703.

del Campo, A., and K. Sengupta, 2015, Eur. Phys. J. Spec. Top. **224**, 189.

Della Valle, G., 2018, Phys. Rev. A **98**, 053861.

Della Valle, G., G. Perozziello, and S. Longhi, 2016, J. Opt. **18**, 09LT03.

Demirplak, M., and S. A. Rice, 2003, J. Phys. Chem. A **107**, 9937.

Demirplak, M., and S. A. Rice, 2005, J. Phys. Chem. B **109**, 6838.

Demirplak, M., and S. A. Rice, 2008, J. Chem. Phys. **129**, 154111.

Deng, J., Q.-h. Wang, Z. Liu, P. Hänggi, and J. Gong, 2013, Phys. Rev. E **88**, 062122.

Deng, S., A. Chenu, P. Diao, F. Li, S. Yu, I. Coulamy, A. del Campo, and H. Wu, 2018, Sci. Adv. **4**, eaar5909.

Deng, S., P. Diao, Q. Yu, A. del Campo, and H. Wu, 2018, Phys. Rev. A **97**, 013628.

Dhara, A. K., and S. V. Lawande, 1984, J. Phys. A **17**, 2423.

Diffo, J., M. Ateuafack, G. Fouokeng, L. Fai, and M. Tchoffo, 2017, Superlattices Microstruct. **111**, 310.

Dorner, U., P. Fedichev, D. Jaksch, M. Lewenstein, and P. Zoller, 2003, Phys. Rev. Lett. **91**, 073601.

Dowdall, T., A. Benseny, T. Busch, and A. Ruschhaupt, 2017, Phys. Rev. A **96**, 043601.

Du, Y.-X., Z.-T. Liang, Y.-C. Li, X.-X. Yue, Q.-X. Lv, W. Huang, X. Chen, H. Yan, and S.-L. Zhu, 2016, Nat. Commun. **7**, 12479.

Du, Y.-X., B.-J. Liu, Q.-X. Lv, X.-D. Zhang, H. Yan, and S.-L. Zhu, 2017, Phys. Rev. A **96**, 012333.

Duncan, C. W., and A. del Campo, 2018, New J. Phys. **20**, 085003.

Dupont-Nivet, M., C. I. Westbrook, and S. Schwartz, 2016, New J. Phys. **18**, 113012.

Emmanouilidou, A., X.-G. Zhao, P. Ao, and Q. Niu, 2000, Phys. Rev. Lett. **85**, 1626.

Ermakov, V. P., 1880, Universita Izvestia Kiev, Series III **9**, 1.

Facchi, P., and S. Pascazio, 2002, Phys. Rev. Lett. **89**, 080401.

Faure, S., S. Ciliberto, E. Trizac, and D. Guéry-Odelin, 2018, arXiv:1808.01321.

Fliess, M., J. Lévine, P. Martin, and P. Rouchon, 1995, International Journal of Control **61**, 1327.

Fogarty, T., L. Ruks, J. Li, and T. Busch, 2019, SciPost Phys. **6**, 21.

Funo, K., N. Lambert, B. Karimi, J. Pekola, Y. Masuyama, and F. Nori, 2019, arXiv:1905.03480.

Funo, K., N. Shiraishi, and K. Saito, 2019, New J. Phys. **21**, 013006.

Funo, K., J.-N. Zhang, C. Chatou, K. Kim, M. Ueda, and A. del Campo, 2017, Phys. Rev. Lett. **118**, 100602.

Fürst, H. A., M. H. Goerz, U. G. Poschinger, M. Murphy, S. Montangero, T. Calarco, F. Schmidt-Kaler, K. Singer, and C. P. Koch, 2014, New J. Phys. **16**, 075007.

Gao, X.-C., J.-B. Xu, and T.-Z. Qian, 1992, Phys. Rev. A **46**, 3626.

Garrido, L., 1964, J. Math. Phys. (N.Y.) **5**, 355.

Giannelli, L., and E. Arimondo, 2014, Phys. Rev. A **89**, 033419.

Glaser, S. J., *et al.*, 2015, Eur. Phys. J. D **69**, 279.

Goldstein, H., C. Poole, and J. Safko, 2002, *Classical Mechanics* (Pearson, Hoboken).

González-Resines, S., D. Guéry-Odelin, A. Tobalina, I. Lizuain, E. Torrontegui, and J. G. Muga, 2017, Phys. Rev. Applied **8**, 054008.

Gritsev, V., P. Barmettler, and E. Demler, 2010, New J. Phys. **12**, 113005.

Guérin, S., V. Hakobyan, and H. R. Jauslin, 2011, Phys. Rev. A **84**, 013423.

Guérin, S., S. Thomas, and H. R. Jauslin, 2002, Phys. Rev. A **65**, 023409.

Guéry-Odelin, D., and J. G. Muga, 2014, Phys. Rev. A **90**, 063425.

Guéry-Odelin, D., J. G. Muga, M. J. Ruiz-Montero, and E. Trizac, 2014, Phys. Rev. Lett. **112**, 180602.

Güngördü, U., Y. Wan, M. A. Fasihi, and M. Nakahara, 2012, Phys. Rev. A **86**, 062312.

Guo, D., and T. Chu, 2017, Opt. Express **25**, 9160.

Hartmann, A., and W. Lechner, 2018, arXiv:1807.02053.

Hatomura, T., 2017, J. Phys. Soc. Jpn. **86**, 094002.

Hatomura, T., 2018, New J. Phys. **20**, 015010.

Hatomura, T., and T. Mori, 2018, arXiv:1806.00229.

Hatomura, T., and K. Pawłowski, 2019, arXiv:1901.03519.

He, S., S.-L. Su, D.-Y. Wang, W.-M. Sun, C.-H. Bai, A.-D. Zhu, H.-F. Wang, and S. Zhang, 2016, Sci. Rep. **6**, 30929.

Hegerfeldt, G. C., 2013, Phys. Rev. Lett. **111**, 260501.

Herrera, M., M. S. Sarandy, E. I. Duzzioni, and R. M. Serra, 2014, Phys. Rev. A **89**, 022323.

Ho, C.-P., and S.-Y. Tseng, 2015, Opt. Lett. **40**, 4831.

Hoffmann, K. H., P. Salamon, Y. Rezek, and R. Kosloff, 2011, Europhys. Lett. **96**, 60015.

Hollenberg, L. C. L., 2012, Nat. Phys. **8**, 113.

Home, J. P., and A. M. Steane, 2005, arXiv:quant-ph/0411102.

Horowitz, J. M., and K. Jacobs, 2015, Phys. Rev. Lett. **115**, 130501.

Hu, C.-K., J.-M. Cui, A. C. Santos, Y.-F. Huang, M. S. Sarandy, C.-F. Li, and G.-C. Guo, 2018, Opt. Lett. **43**, 3136.

Huang, B.-H., Y.-H. Chen, Q.-C. Wu, J. Song, and Y. Xia, 2016, Laser Phys. Lett. **13**, 105202.

Huang, W., L. Ang, and E. Kyoseva, 2017, arXiv:1711.05507.

Huang, X.-B., Y.-H. Chen, and Z. Wang, 2016a, Sci. Rep. **6**, 25707.

Huang, X.-B., Y.-H. Chen, and Z. Wang, 2016b, Eur. Phys. J. D **70**, 171.

Huang, X.-B., Z.-R. Zhong, and Y.-H. Chen, 2015, Quantum Inf. Process. **14**, 4475.

Hung, Y.-J., Z.-Y. Li, H.-C. Chung, F.-C. Liang, M.-Y. Jung, T.-H. Yen, and S.-Y. Tseng, 2019, Opt. Lett. **44**, 815.

Ibáñez, S., X. Chen, and J. G. Muga, 2013, Phys. Rev. A **87**, 043402.

Ibáñez, S., X. Chen, E. Torrontegui, J. G. Muga, and A. Ruschhaupt, 2012, Phys. Rev. Lett. **109**, 100403.

Ibáñez, S., Y.-C. Li, X. Chen, and J. G. Muga, 2015, Phys. Rev. A **92**, 062136.

Ibáñez, S., S. Martínez-Garaot, X. Chen, E. Torrontegui, and J. G. Muga, 2011, Phys. Rev. A **84**, 023415.

Ibáñez, S., S. Martínez-Garaot, X. Chen, E. Torrontegui, and J. G. Muga, 2012, Phys. Rev. A **86**, 019901.

Ibáñez, S., and J. G. Muga, 2014, Phys. Rev. A **89**, 033403.

Ibáñez, S., A. Peralta Conde, D. Guéry-Odelin, and J. G. Muga, 2011, Phys. Rev. A **84**, 013428.

Impens, F., and D. Guéry-Odelin, 2017, Phys. Rev. A **96**, 043609.

Impens, F., and D. Guéry-Odelin, 2019, Sci. Rep. **9**, 4048.

Issoufa, Y. H., and A. Messikh, 2014, Phys. Rev. A **90**, 055402.

Jaramillo, J., M. Beau, and A. del Campo, 2016, New J. Phys. **18**, 075019.

Jarzynski, C., 2013, Phys. Rev. A **88**, 040101.

Jarzynski, C., S. Deffner, A. Patra, and Y. Subaşı, 2017, Phys. Rev. E **95**, 032122.

Jing, J., L.-A. Wu, M. S. Sarandy, and J. G. Muga, 2013, Phys. Rev. A **88**, 053422.

Juliá-Díaz, B., E. Torrontegui, J. Martorell, J. G. Muga, and A. Polls, 2012, Phys. Rev. A **86**, 063623.

Kagan, Y., E. L. Surkov, and G. V. Shlyapnikov, 1996, Phys. Rev. A **54**, R1753.

Kamsap, M. R., J. Pedregosa-Gutierrez, C. Champenois, D. Guyomarc'h, M. Houssin, and M. Knoop, 2015, Phys. Rev. A **92**, 043416.

Kang, Y.-H., Y.-H. Chen, Z.-C. Shi, B.-H. Huang, J. Song, and Y. Xia, 2017, Phys. Rev. A **96**, 022304.
Kang, Y.-H., Y.-H. Chen, Z.-C. Shi, B.-H. Huang, J. Song, and Y. Xia, 2018, Phys. Rev. A **97**, 033407.
Kang, Y.-H., Y.-H. Chen, Z.-C. Shi, J. Song, and Y. Xia, 2016a, Phys. Rev. A **94**, 052311.
Kang, Y.-H., Y.-H. Chen, Q.-C. Wu, B.-H. Huang, J. Song, and Y. Xia, 2016b, Sci. Rep. **6**, 36737.
Kang, Y.-H., Y.-H. Chen, Q.-C. Wu, B.-H. Huang, Y. Xia, and J. Song, 2016c, Sci. Rep. **6**, 30151.
Kang, Y.-H., B.-H. Huang, P.-M. Lu, and Y. Xia, 2017, Laser Phys. Lett. **14**, 025201.
Kang, Y.-H., Z.-C. Shi, B.-H. Huang, J. Song, and Y. Xia, 2017, Ann. Phys. (Berlin) **529**, 1700154.
Karzig, T., F. Pientka, G. Refael, and F. von Oppen, 2015, Phys. Rev. B **91**, 201102.
Kastberg, A., W. D. Phillips, S. L. Rolston, R. J. C. Spreeuw, and P. S. Jessen, 1995, Phys. Rev. Lett. **74**, 1542.
Kato, T., 1950, J. Phys. Soc. Jpn. **5**, 435.
Kaufmann, H., T. Ruster, C. T. Schmiegelow, F. Schmidt-Kaler, and U. G. Poschinger, 2014, New J. Phys. **16**, 073012.
Kaufmann, P., T. F. Gloger, D. Kaufmann, M. Johanning, and C. Wunderlich, 2018, Phys. Rev. Lett. **120**, 010501.
Khantoul, B., A. Bounames, and M. Maamache, 2017, Eur. Phys. J. Plus **132**, 258.
Khomitsky, D. V., L. V. Gulyaev, and E. Y. Sherman, 2012, Phys. Rev. B **85**, 125312.
Khujakulov, A., and K. Nakamura, 2016, Phys. Rev. A **93**, 022101.
Kieferová, M., and N. Wiebe, 2014, New J. Phys. **16**, 123034.
Kielpinski, D., C. Monroe, and D. J. Wineland, 2002, Nature (London) **417**, 709.
Kiely, A., A. Benseny, T. Busch, and A. Ruschhaupt, 2016, J. Phys. B **49**, 215003.
Kiely, A., J. P. L. McGuinness, J. G. Muga, and A. Ruschhaupt, 2015, J. Phys. B **48**, 075503.
Kiely, A., J. G. Muga, and A. Ruschhaupt, 2017, Phys. Rev. A **95**, 012115.
Kiely, A., J. G. Muga, and A. Ruschhaupt, 2018, Phys. Rev. A **98**, 053616.
Kiely, A., and A. Ruschhaupt, 2014, J. Phys. B **47**, 115501.
Kiely, A., and A. Ruschhaupt, 2019, unpublished.
Kirk, R. E., 2004, *Optimal Control Theory An Introduction* (Dover Publications, New York).
Kleißler, F., A. Lazariev, and S. Arroyo-Camejo, 2018, npj Quantum Inf. **4**, 49.
Koch, C. P., 2016, J. Phys. Condens. Matter **28**, 213001.
Kölbl, J., A. Barfuss, M. S. Kasperczyk, L. Thiel, A. A. Clerk, H. Ribeiro, and P. Maletinsky, 2019, Phys. Rev. Lett. **122**, 090502.
Kolodrubetz, M., D. Sels, P. Mehta, and A. Polkovnikov, 2017, Phys. Rep. **697**, 1.
Kosloff, R., 2013, Entropy **15**, 2100.
Kosloff, R., and Y. Rezek, 2017, Entropy **19**, 136.
Kuo, T.-Y. T., and S.-C. J. Kang, 2014, Automation in Construction **42**, 25.
Kyaw, T. H., and L.-C. Kwek, 2018, New J. Phys. **20**, 045007.
Lakehal, H., M. Maamache, and J. R. Choi, 2016, Sci. Rep. **6**, 19860.
Landauer, R., 1961, IBM J. Res. Dev. **5**, 183.
Lax, P. D., 1968, Commun. Pure Appl. Math. **21**, 467.
Levy, A., A. Kiely, J. G. Muga, R. Kosloff, and E. Torrontegui, 2018, New J. Phys. **20**, 025006.
Levy, A., E. Torrontegui, and R. Kosloff, 2017, Phys. Rev. A **96**, 033417.
Lewis, H. R., and P. G. L. Leach, 1982, J. Math. Phys. (N.Y.) **23**, 2371.
Lewis, Jr., H. R., and W. Riesenfeld, 1969, J. Math. Phys. (N.Y.) **10**, 1458.
Li, G., H. T. Quan, and Z. C. Tu, 2017, Phys. Rev. E **96**, 012144.
Li, G.-Q., G.-D. Chen, P. Peng, and W. Qi, 2017, Eur. Phys. J. D **71**, 14.
Li, H., H. Z. Shen, S. L. Wu, and X. X. Yi, 2017, Opt. Express **25**, 30135.
Li, J., T. Fogarty, S. Campbell, X. Chen, and T. Busch, 2018, New J. Phys. **20**, 015005.
Li, J., K. Sun, and X. Chen, 2016, Sci. Rep. **6**, 38258.
Li, J., Q. Zhang, and X. Chen, 2017, Phys. Lett. A **381**, 3272.
Li, Y., L.-A. Wu, and Z. D. Wang, 2011, Phys. Rev. A **83**, 043804.
Li, Y.-C., and X. Chen, 2016, Phys. Rev. A **94**, 063411.
Li, Y.-C., X. Chen, J. G. Muga, and E. Y. Sherman, 2018, New J. Phys. **20**, 113029.
Li, Y.-C., D. Martínez-Cercós, S. Martínez-Garaot, X. Chen, and J. G. Muga, 2018, Phys. Rev. A **97**, 013830.
Liang, Y., X. Ji, H.-F. Wang, and S. Zhang, 2015, Laser Phys. Lett. **12**, 115201.
Liang, Y., C. Song, X. Ji, and S. Zhang, 2015, Opt. Express **23**, 23798.
Liang, Y., S.-L. Su, Q.-C. Wu, X. Ji, and S. Zhang, 2015, Opt. Express **23**, 5064.
Liang, Y., Q.-C. Wu, S.-L. Su, X. Ji, and S. Zhang, 2015, Phys. Rev. A **91**, 032304.
Liang, Z.-T., X. Yue, Q. Lv, Y.-X. Du, W. Huang, H. Yan, and S.-L. Zhu, 2016, Phys. Rev. A **93**, 040305.
Lin, J.-B., Y. Liang, C. Song, X. Ji, and S. Zhang, 2016, J. Opt. Soc. Am. B **33**, 519.
Lin, T.-Y., F.-C. Hsiao, Y.-W. Jhang, C. Hu, and S.-Y. Tseng, 2012, Opt. Express **20**, 24085.
Liu, B.-J., Z.-H. Huang, Z.-Y. Xue, and X.-D. Zhang, 2017, Phys. Rev. A **95**, 062308.
Liu, B.-J., X.-K. Song, Z.-Y. Xue, X. Wang, and M.-H. Yung, 2018, arXiv:1806.07904.
Liu, Y.-H., and S.-Y. Tseng, 2017, J. Phys. B **50**, 205501.
Lizuain, I., M. Palmero, and J. G. Muga, 2017, Phys. Rev. A **95**, 022130.
Lizuain, I., A. Tobalina, A. Rodriguez-Prieto, and J. G. Muga, 2019, arXiv:1904.08987v2.
Lohe, M. A., 2009, J. Phys. A **42**, 035307.
Longhi, S., 2009, Laser Photonics Rev. **3**, 243.
Longhi, S., 2017, Phys. Rev. A **95**, 062122.
Lu, M., Y. Xia, L.-T. Shen, and J. Song, 2014, Laser Phys. **24**, 105201.
Lu, M., Y. Xia, L.-T. Shen, J. Song, and N. B. An, 2014, Phys. Rev. A **89**, 012326.
Lu, X.-J., X. Chen, J. Alonso, and J. G. Muga, 2014, Phys. Rev. A **89**, 023627.
Lu, X.-J., X. Chen, A. Ruschhaupt, D. Alonso, S. Guérin, and J. G. Muga, 2013, Phys. Rev. A **88**, 033406.
Lu, X.-J., M. Li, Z. Y. Zhao, C.-L. Zhang, H.-P. Han, Z.-B. Feng, and Y.-Q. Zhou, 2017, Phys. Rev. A **96**, 023843.
Lu, X.-J., J. G. Muga, X. Chen, U. G. Poschinger, F. Schmidt-Kaler, and A. Ruschhaupt, 2014, Phys. Rev. A **89**, 063414.
Lu, X.-J., M. Palmero, A. Ruschhaupt, X. Chen, and J. G. Muga, 2015, Phys. Scr. **90**, 074038.
Lu, X.-J., A. Ruschhaupt, and J. G. Muga, 2018, Phys. Rev. A **97**, 053402.
Luo, D.-W., P. V. Pyshkin, C.-H. Lam, T. Yu, H.-Q. Lin, J. Q. You, and L.-A. Wu, 2015, Phys. Rev. A **92**, 062127.

Lv, Q.-X., H.-Z. Liu, J.-H. Liang, K.-Y. Liao, and Y.-X. Du, 2019, arXiv:1903.03397.

Ma, W., X. J. Cao, and S. L. Wu, 2017, Opt. Express **25**, 23850.

Maamache, M., O. Kaltoum Djeghiour, N. Mana, and W. Koussa, 2017, Eur. Phys. J. Plus **132**, 383.

Mandelstam, L., and I. Tamm, 1945, J. Phys. USSR **9**, 249.

Marr, C., A. Beige, and G. Rempe, 2003, Phys. Rev. A **68**, 033817.

Martínez, I. A., A. Petrosyan, D. Guéry-Odelin, E. Trizac, and S. Ciliberto, 2016, Nat. Phys. **12**, 843.

Martínez, I. A., E. Roldán, J. M. R. Parrondo, and D. Petrov, 2013, Phys. Rev. E **87**, 032159.

Martínez-Garaot, S., J. G. Muga, and S.-Y. Tseng, 2017, Opt. Express **25**, 159.

Martínez-Garaot, S., M. Palmero, D. Guéry-Odelin, and J. G. Muga, 2015, Phys. Rev. A **92**, 053406.

Martínez-Garaot, S., M. Palmero, J. G. Muga, and D. Guéry-Odelin, 2016, Phys. Rev. A **94**, 063418.

Martínez-Garaot, S., A. Rodriguez-Prieto, and J. G. Muga, 2018, Phys. Rev. A **98**, 043622.

Martínez-Garaot, S., A. Ruschhaupt, J. Gillet, T. Busch, and J. G. Muga, 2015, Phys. Rev. A **92**, 043406.

Martínez-Garaot, S., E. Torrontegui, X. Chen, M. Modugno, D. Guéry-Odelin, S.-Y. Tseng, and J. G. Muga, 2013, Phys. Rev. Lett. **111**, 213001.

Martínez-Garaot, S., E. Torrontegui, X. Chen, and J. G. Muga, 2014, Phys. Rev. A **89**, 053408.

Martínez-Garaot, S., S.-Y. Tseng, and J. G. Muga, 2014, Opt. Lett. **39**, 2306.

Martinis, J. M., and M. R. Geller, 2014, Phys. Rev. A **90**, 022307.

Masuda, S., and K. Nakamura, 2008, Phys. Rev. A **78**, 062108.

Masuda, S., and K. Nakamura, 2010, Proc. R. Soc. A **466**, 1135.

Masuda, S., and K. Nakamura, 2011, Phys. Rev. A **84**, 043434.

Masuda, S., K. Nakamura, and A. del Campo, 2014, Phys. Rev. Lett. **113**, 063003.

Masuda, S., K. Nakamura, and M. Nakahara, 2018, New J. Phys. **20**, 025008.

Masuda, S., and S. A. Rice, 2014, Phys. Rev. A **89**, 033621.

Masuda, S., and S. A. Rice, 2015a, J. Phys. Chem. A **119**, 3479.

Masuda, S., and S. A. Rice, 2015b, J. Chem. Phys. **142**, 244303.

Masuda, S., and S. A. Rice, 2015c, J. Phys. Chem. B **119**, 11079.

Masuda, S., and S. A. Rice, 2016, Adv. Chem. Phys. **159**, 51.

Menchon-Enrich, R., A. Benseny, V. Ahufinger, A. D. Greentree, T. Busch, and J. Mompart, 2016, Rep. Prog. Phys. **79**, 074401.

Messiah, A., 1962, *Quantum Mechanics*, Vol. II (North-Holland, Amsterdam).

Mishima, H., and Y. Izumida, 2017, Phys. Rev. E **96**, 012133.

Morita, S., 2007, J. Phys. Soc. Jpn. **76**, 104001.

Mortensen, H. L., J. J. Sørensen, K. Mølmer, and J. F. Sherson, 2018, New J. Phys. **20**, 025009.

Motzoi, F., J. M. Gambetta, P. Rebentrost, and F. K. Wilhelm, 2009, Phys. Rev. Lett. **103**, 110501.

Muga, J., J. Palao, B. Navarro, and I. Egusquiza, 2004, Phys. Rep. **395**, 357.

Muga, J. G., X. Chen, S. Ibáñez, I. Lizuain, and A. Ruschhaupt, 2010, J. Phys. B **43**, 085509.

Muga, J. G., X. Chen, A. Ruschhaupt, and D. Guéry-Odelin, 2009, J. Phys. B **42**, 241001.

Muga, J. G., J. Echanobe, A. del Campo, and I. Lizuain, 2008, J. Phys. B **41**, 175501.

Muga, J. G., M. A. Simón, and A. Tobalina, 2016, New J. Phys. **18**, 021005.

Mukherjee, V., S. Montangero, and R. Fazio, 2016, Phys. Rev. A **93**, 062108.

Nakamura, K., A. Khujakulov, S. Avazbaev, and S. Masuda, 2017, Phys. Rev. A **95**, 062108.

Navez, P., S. Pandey, H. Mas, K. Poulios, T. Fernholz, and W. von Klitzing, 2016, New J. Phys. **18**, 075014.

Ndong, M., G. Djotyan, A. Ruschhaupt, and S. Gurin, 2015, J. Phys. B **48**, 174007.

Nenciu, G., and G. Rasche, 1992, J. Phys. A **25**, 5741.

Ness, G., C. Shkedrov, Y. Florshaim, and Y. Sagi, 2018, New J. Phys. **20**, 095002.

Nishimura, K., and K. Takahashi, 2018, SciPost Phys. **5**, 29.

Nizamani, A. H., and W. K. Hensinger, 2012, Appl. Phys. B **106**, 327.

Oh, S., and S. Kais, 2014, J. Chem. Phys. **141**, 224108.

Okuyama, M., and K. Takahashi, 2016, Phys. Rev. Lett. **117**, 070401.

Okuyama, M., and K. Takahashi, 2017, J. Phys. Soc. Jpn. **86**, 043002.

Onofrio, R., 2016, Phys. Usp. **59**, 1129.

Opatrný, T., and K. Mølmer, 2014, New J. Phys. **16**, 015025.

Opatrný, T., H. Saberi, E. Brion, and K. Mølmer, 2016, Phys. Rev. A **93**, 023815.

Oreshkov, O., and J. Calsamiglia, 2010, Phys. Rev. Lett. **105**, 050503.

Ozcakmakli, Z., and C. Yuce, 2012, Phys. Scr. **86**, 055001.

Palmero, M., R. Bowler, J. P. Gaebler, D. Leibfried, and J. G. Muga, 2014, Phys. Rev. A **90**, 053408.

Palmero, M., S. Martínez-Garaot, J. Alonso, J. P. Home, and J. G. Muga, 2015, Phys. Rev. A **91**, 053411.

Palmero, M., S. Martínez-Garaot, D. Leibfried, D. J. Wineland, and J. G. Muga, 2017, Phys. Rev. A **95**, 022328.

Palmero, M., S. Martínez-Garaot, U. G. Poschinger, A. Ruschhaupt, and J. G. Muga, 2015, New J. Phys. **17**, 093031.

Palmero, M., E. Torrontegui, D. Guéry-Odelin, and J. G. Muga, 2013, Phys. Rev. A **88**, 053423.

Palmero, M., S. Wang, D. Guéry-Odelin, J.-S. Li, and J. G. Muga, 2016, New J. Phys. **18**, 043014.

Pan, T.-H., and S.-Y. Tseng, 2015, Opt. Express **23**, 10405.

Pang, S., and A. N. Jordan, 2017, Nat. Commun. **8**, 14695.

Papoular, D. J., and S. Stringari, 2015, Phys. Rev. Lett. **115**, 025302.

Patra, A., and C. Jarzynski, 2017a, J. Phys. Chem. B **121**, 3403.

Patra, A., and C. Jarzynski, 2017b, New J. Phys. **19**, 125009.

Paul, K., and A. K. Sarma, 2015, Phys. Rev. A **91**, 053406.

Pedregosa-Gutierrez, J., C. Champenois, M. R. Kamsap, and M. Knoop, 2015, Int. J. Mass Spectrom. **381–382**, 33.

Pekola, J. P., V. Brosco, M. Möttönen, P. Solinas, and A. Shnirman, 2010, Phys. Rev. Lett. **105**, 030401.

Peng, R., Y. Zheng, S.-W. Liu, X.-P. Li, J.-L. Wu, and X. Ji, 2017, Quantum Inf. Process. **16**, 172.

Petiziol, F., B. Dive, S. Carretta, R. Mannella, F. Mintert, and S. Wimberger, 2019, arXiv:1901.07344.

Petiziol, F., B. Dive, F. Mintert, and S. Wimberger, 2018, Phys. Rev. A **98**, 043436.

Pinch, E. R., 1993, *Optimal Control and the Calculus of Variations* (Oxford University Press, New York).

Plata, C. A., D. Guéry-Odelin, E. Trizac, and A. Prados, 2019, Phys. Rev. E **99**, 012140.

Puri, S., S. Boutin, and A. Blais, 2017, npj Quantum Inf. **3**, 18.

Qi, S., and J. Jing, 2019, arXiv:1905.09524.

Quan, H. T., and W. H. Zurek, 2010, New J. Phys. **12**, 093025.

Ran, D., Z.-C. Shi, J. Song, and Y. Xia, 2017, Phys. Rev. A **96**, 033803.

Reichle, R., D. Leibfried, R. B. Blakestad, J. Britton, J. D. Jost, E. Knill, C. Langer, R. Ozeri, S. Seidelin, and D. J. Wineland, 2006, Fortschritte der Physik: Progress of Physics **54**, 666.

Ren, F.-H., Z.-M. Wang, and Y.-J. Gu, 2017, Phys. Lett. A **381**, 70.
Rezakhani, A. T., A. K. Pimachev, and D. A. Lidar, 2010, Phys. Rev. A **82**, 052305.
Rezek, Y., P. Salamon, K. H. Hoffmann, and R. Kosloff, 2009, Europhys. Lett. **85**, 30008.
Richerme, P., C. Senko, J. Smith, A. Lee, S. Korenblit, and C. Monroe, 2013, Phys. Rev. A **88**, 012334.
Ritland, K., and A. Rahmani, 2018, New J. Phys. **20**, 065005.
Rohringer, W., D. Fischer, F. Steiner, I. E. Mazets, J. Schmiedmayer, and M. Trupke, 2015, Sci. Rep. **5**, 9820.
Roland, J., and N. J. Cerf, 2002, Phys. Rev. A **65**, 042308.
Rouchon, P., 2005, ZAMM—Journal of Applied Mathematics and Mechanics/Zeitschrift für Angewandte Mathematik und Mechanik **85**, 411.
Ruschhaupt, A., X. Chen, D. Alonso, and J. G. Muga, 2012, New J. Phys. **14**, 093040.
Ruschhaupt, A., and J. Muga, 2014, J. Mod. Opt. **61**, 828.
Ruster, T., C. Warschburger, H. Kaufmann, C. T. Schmiegelow, A. Walther, M. Hettrich, A. Pfister, V. Kaushal, F. Schmidt-Kaler, and U. G. Poschinger, 2014, Phys. Rev. A **90**, 033410.
Saberi, H., T. Opatrný, K. Mølmer, and A. del Campo, 2014, Phys. Rev. A **90**, 060301.
Salamon, P., K. H. Hoffmann, Y. Rezek, and R. Kosloff, 2009, Phys. Chem. Chem. Phys. **11**, 1027.
Santos, A. C., 2018, J. Phys. B **51**, 015501.
Santos, A. C., A. Nicotina, A. M. de Souza, R. S. Sarthour, I. S. Oliveira, and M. S. Sarandy, 2019, arXiv:1906.08065.
Santos, A. C., and M. S. Sarandy, 2015, Sci. Rep. **5**, 15775.
Santos, A. C., and M. S. Sarandy, 2018, J. Phys. A **51**, 025301.
Santos, A. C., R. D. Silva, and M. S. Sarandy, 2016, Phys. Rev. A **93**, 012311.
Sarandy, M., E. Duzzioni, and R. Serra, 2011, Phys. Lett. A **375**, 3343.
Sarandy, M. S., E. I. Duzzioni, and M. H. Y. Moussa, 2007, Phys. Rev. A **76**, 052112.
Sarandy, M. S., and D. A. Lidar, 2005, Phys. Rev. A **71**, 012331.
Schaff, J.-F., P. Capuzzi, G. Labeyrie, and P. Vignolo, 2011, New J. Phys. **13**, 113017.
Schaff, J.-F., X.-L. Song, P. Capuzzi, P. Vignolo, and G. Labeyrie, 2011, Europhys. Lett. **93**, 23001.
Schaff, J.-F., X.-L. Song, P. Vignolo, and G. Labeyrie, 2010, Phys. Rev. A **82**, 033430.
Schaller, G., S. Mostame, and R. Schützhold, 2006, Phys. Rev. A **73**, 062307.
Schloss, J., A. Benseny, J. Gillet, J. Swain, and T. Busch, 2016, New J. Phys. **18**, 035012.
Schmiedl, T., E. Dieterich, P.-S. Dieterich, and U. Seifert, **2009**, J. Stat. Mech. 07, P07013.
Schutjens, R., F. A. Dagga, D. J. Egger, and F. K. Wilhelm, 2013, Phys. Rev. A **88**, 052330.
Sekimoto, K., and S.-i. Sasa, 1997, J. Phys. Soc. Jpn. **66**, 3326.
Sels, D., and A. Polkovnikov, 2017, Proc. Natl. Acad. Sci. U.S.A. **114**, E3909.
Setiawan, I., B. E. Gunara, S. Avazbaev, and K. Nakamura, 2019, Phys. Rev. A **99**, 062116.
Setiawan, I., B. E. Gunara, S. Masuda, and K. Nakamura, 2017, Phys. Rev. A **96**, 052106.
Shan, W.-J., Y. Xia, Y.-H. Chen, and J. Song, 2016, Quantum Inf. Process. **15**, 2359.
Shen, C.-P., and S. Su, 2018, arXiv:1807.02808.
Shi, X., and L. F. Wei, 2015, Laser Phys. Lett. **12**, 015204.
Simón, M. Á., Á. Buendía, and J. G. Muga, 2018, Mathematics **6**, 111.
Smith, A., Y. Lu, S. An, X. Zhang, J.-N. Zhang, Z. Gong, H. T. Quan, C. Jarzynski, and K. Kim, 2018, New J. Phys. **20**, 013008.
Song, C., S.-L. Su, C.-H. Bai, X. Ji, and S. Zhang, 2016, Quantum Inf. Process. **15**, 4159.
Song, J., Z.-J. Zhang, Y. Xia, X.-D. Sun, and Y.-Y. Jiang, 2016, Opt. Express **24**, 21674.
Song, K.-H., and M.-F. Chen, 2016, Quantum Inf. Process. **15**, 3169.
Song, L.-C., Y. Xia, and J. Song, 2014, J. Mod. Opt. **61**, 1290.
Song, X.-K., Q. Ai, J. Qiu, and F.-G. Deng, 2016, Phys. Rev. A **93**, 052324.
Song, X.-K., F.-G. Deng, L. Lamata, and J. G. Muga, 2017, Phys. Rev. A **95**, 022332.
Song, X.-K., H. Zhang, Q. Ai, J. Qiu, and F.-G. Deng, 2016d, New J. Phys. **18**, 023001.
Stefanatos, D., 2013, Automatica **49**, 3079.
Stefanatos, D., 2014, Phys. Rev. A **90**, 023811.
Stefanatos, D., 2017a, Phys. Rev. E **96**, 042103.
Stefanatos, D., 2017b, IEEE Trans. Autom. Control **62**, 4290.
Stefanatos, D., 2018, J. Appl. Math. Bioinformatics **8**, 17.
Stefanatos, D., and J.-S. Li, 2014, IEEE Trans. Autom. Control **59**, 733.
Stefanatos, D., and E. Paspalakis, 2018a, arXiv:1805.07129.
Stefanatos, D., and E. Paspalakis, 2018b, New J. Phys. **20**, 055009.
Stefanatos, D., and E. Paspalakis, 2019a, Phys. Rev. A **100**, 012111.
Stefanatos, D., and E. Paspalakis, 2019b, arXiv:1907.00166.
Stefanatos, D., J. Ruths, and J.-S. Li, 2010, Phys. Rev. A **82**, 063422.
Sun, C., A. Saxena, and N. A. Sinitsyn, 2017, J. Phys. B **50**, 175501.
Sun, N., X. Zhang, Y. Fang, and Y. Yuan, 2012, IET Control Theory & Applications **6**, 1410.
Sun, Z., L. Zhou, G. Xiao, D. Poletti, and J. Gong, 2016, Phys. Rev. A **93**, 012121.
Takahashi, K., 2013a, J. Phys. A **46**, 315304.
Takahashi, K., 2013b, Phys. Rev. E **87**, 062117.
Takahashi, K., 2014, Phys. Rev. A **89**, 042113.
Takahashi, K., 2015, Phys. Rev. A **91**, 042115.
Takahashi, K., 2017a, New J. Phys. **19**, 115007.
Takahashi, K., 2017b, Phys. Rev. A **95**, 012309.
Takahashi, K., 2019, J. Phys. Soc. Jpn. **88**, 061002.
Takahashi, K., and M. Ohzeki, 2016, Phys. Rev. E **93**, 012129.
Theis, L. S., F. Motzoi, S. Machnes, and F. K. Wilhelm, 2018, Europhys. Lett. **123**, 60001.
Theis, L. S., F. Motzoi, and F. K. Wilhelm, 2016, Phys. Rev. A **93**, 012324.
Thunström, P., J. Åberg, and E. Sjöqvist, 2005, Phys. Rev. A **72**, 022328.
Tian, L., 2018, arXiv:1802.02285.
Tobalina, A., J. Alonso, and J. G. Muga, 2018, New J. Phys. **20**, 065002.
Tobalina, A., I. Lizuain, and J. G. Muga, 2019, arXiv:1906.07473.
Tobalina, A., M. Palmero, S. Martínez-Garaot, and J. G. Muga, 2017, Sci. Rep. **7**, 5753.
Torosov, B. T., G. Della Valle, and S. Longhi, 2013, Phys. Rev. A **87**, 052502.
Torosov, B. T., G. Della Valle, and S. Longhi, 2014, Phys. Rev. A **89**, 063412.
Torrontegui, E., X. Chen, M. Modugno, A. Ruschhaupt, D. Guéry-Odelin, and J. G. Muga, 2012, Phys. Rev. A **85**, 033605.
Torrontegui, E., X. Chen, M. Modugno, S. Schmidt, A. Ruschhaupt, and J. G. Muga, 2012, New J. Phys. **14**, 013031.
Torrontegui, E., S. Dawkins, M. Göb, and K. Singer, 2018, New J. Phys. **20**, 105001.
Torrontegui, E., and J. J. García-Ripoll, 2019, Europhys. Lett. **125**, 30004.

Torrontegui, E., S. Ibáñez, X. Chen, A. Ruschhaupt, D. Guéry-Odelin, and J. G. Muga, 2011, Phys. Rev. A **83**, 013415.
Torrontegui, E., S. Ibáñez, S. Martínez-Garaot, M. Modugno, A. del Campo, D. Guéry-Odelin, A. Ruschhaupt, X. Chen, and J. G. Muga, 2013, Adv. At. Mol. Opt. Phys. **62**, 117.
Torrontegui, E., and R. Kosloff, 2013, Phys. Rev. E **88**, 032103.
Torrontegui, E., I. Lizuain, S. González-Resines, A. Tobalina, A. Ruschhaupt, R. Kosloff, and J. G. Muga, 2017, Phys. Rev. A **96**, 022133.
Torrontegui, E., S. Martínez-Garaot, M. Modugno, X. Chen, and J. G. Muga, 2013, Phys. Rev. A **87**, 033630.
Torrontegui, E., S. Martínez-Garaot, and J. G. Muga, 2014, Phys. Rev. A **89**, 043408.
Torrontegui, E., S. Martínez-Garaot, A. Ruschhaupt, and J. G. Muga, 2012, Phys. Rev. A **86**, 013601.
Tseng, S.-Y., 2013, Opt. Express **21**, 21224.
Tseng, S.-Y., 2014, Opt. Lett. **39**, 6600.
Tseng, S.-Y., and X. Chen, 2012, Opt. Lett. **37**, 5118.
Tseng, S.-Y., R.-D. Wen, Y.-F. Chiu, and X. Chen, 2014, Opt. Express **22**, 18849.
Tu, Z. C., 2014, Phys. Rev. E **89**, 052148.
Unanyan, R. G., L. P. Yatsenko, K. Bergmann, and B. W. Shore, 1997, Opt. Commun. **139**, 48.
Vacanti, G., R. Fazio, S. Montangero, G. M. Palma, M. Paternostro, and V. Vedral, 2014, New J. Phys. **16**, 053017.
Van-Damme, L., D. Schraft, G. T. Genov, D. Sugny, T. Halfmann, and S. Guérin, 2017, Phys. Rev. A **96**, 022309.
Venuti, L. C., T. Albash, D. A. Lidar, and P. Zanardi, 2016, Phys. Rev. A **93**, 032118.
Vepsäläinen, A., S. Danilin, and G. Paraoanu, 2018, Quant. Sci. Technol. **3**, 024006.
Vepsäläinen, A., S. Danilin, and G. S. Paraoanu, 2019, Sci. Adv. **5**, eaau5999.
Villazon, T., A. Polkovnikov, and A. Chandran, 2019, arXiv:1902.05964.
Vitanov, N. V., and M. Drewsen, 2019, Phys. Rev. Lett. **122**, 173202.
Vitanov, N. V., A. A. Rangelov, B. W. Shore, and K. Bergmann, 2017, Rev. Mod. Phys. **89**, 015006.
Vitanov, N. V., and B. W. Shore, 2015, J. Phys. B **48**, 174008.
Walther, A., F. Ziesel, T. Ruster, S. T. Dawkins, K. Ott, M. Hettrich, K. Singer, F. Schmidt-Kaler, and U. Poschinger, 2012, Phys. Rev. Lett. **109**, 080501.
Wang, T., *et al.*, 2018, New J. Phys. **20**, 065003.
Wang, Z., Y. Xia, Y.-H. Chen, and J. Song, 2016, Eur. Phys. J. D **70**, 162.
Wang, Z.-M., C. A. Bishop, J. Jing, Y.-J. Gu, C. Garcia, and L.-A. Wu, 2016, Phys. Rev. A **93**, 062338.
Wendin, G., 2017, Rep. Prog. Phys. **80**, 106001.
Wiebe, N., and N. S. Babcock, 2012, New J. Phys. **14**, 013024.
Wineland, D. J., C. Monroe, W. M. Itano, D. Leibfried, B. E. King, and D. M. Meekhof, 1998, J. Res. Natl. Inst. Stand. Technol. **103**, 259.
Wu, J.-L., X. Ji, and S. Zhang, 2016, Sci. Rep. **6**, 33669.
Wu, J.-L., X. Ji, and S. Zhang, 2017a, Quantum Inf. Process. **16**, 294.
Wu, J.-L., X. Ji, and S. Zhang, 2017b, Sci. Rep. **7**, 46255.
Wu, J.-L., X. Ji, and S. Zhang, 2017c, Opt. Express **25**, 21084.
Wu, J.-L., C. Song, X. Ji, and S. Zhang, 2016, J. Opt. Soc. Am. B **33**, 2026.
Wu, J.-L., S.-L. Su, X. Ji, and S. Zhang, 2017, Ann. Phys. (Amsterdam) **386**, 34.
Wu, Q.-C., Y.-H. Chen, B.-H. Huang, J. Song, Y. Xia, and S.-B. Zheng, 2016, Opt. Express **24**, 22847.
Wu, S. L., X. L. Huang, H. Li, and X. X. Yi, 2017, Phys. Rev. A **96**, 042104.
Wu, S. L., X. Y. Zhang, and X. X. Yi, 2015, Phys. Rev. A **92**, 062122.
Xiao, G., and J. Gong, 2014, Phys. Rev. E **90**, 052132.
Xing-Xin, C., Z. Jun, N. Xi-Jing, and Z. Wen-Xian, 2013, Chin. Phys. B **22**, 090310.
Xu, J., L. Yu, J.-L. Wu, and X. Ji, 2017, Chin. Phys. B **26**, 090301.
Yan, T., *et al.*, 2019, Phys. Rev. Lett. **122**, 080501.
Yan, Y., Y. Li, A. Kinos, A. Walther, C. Shi, L. Rippe, J. Moser, S. Kröll, and X. Chen, 2019, Opt. Express **27**, 8267.
Yang, Y.-F., Y.-H. Chen, Q.-C. Wu, Y.-H. Kang, B.-H. Huang, and Y. Xia, 2017, Quantum Inf. Process. **16**, 15.
Yang, Y.-F., Y.-H. Chen, Q.-C. Wu, Z.-C. Shi, J. Song, and Y. Xia, 2018, Can. J. Phys. **96**, 81.
Ye, L.-X., X. Lin, X. Chen, J. He, R.-C. Yang, and H.-Y. Liu, 2016, Quantum Inf. Process. **15**, 2785.
Yeih, C.-S., H.-X. Cao, and S.-Y. Tseng, 2014, IEEE Photonics Technol. Lett. **26**, 123.
Yi, X. X., D. M. Tong, L. C. Kwek, and C. H. Oh, 2007, J. Phys. B **40**, 281.
Yoshimura, B., and J. K. Freericks, 2015, Front. Phys. **3**, 85.
Yu, L., J. Xu, J.-L. Wu, and X. Ji, 2017, Chin. Phys. B **26**, 060306.
Yu, X.-T., Q. Zhang, Y. Ban, and X. Chen, 2018, Phys. Rev. A **97**, 062317.
Yuce, C., 2012, Phys. Lett. A **376**, 1717.
Yuste, A., B. Juliá-Díaz, E. Torrontegui, J. Martorell, J. G. Muga, and A. Polls, 2013, Phys. Rev. A **88**, 043647.
Zhang, H., X.-K. Song, Q. Ai, H. Wang, G.-J. Yang, and F.-G. Deng, 2018, arXiv:1809.00102.
Zhang, J., T. H. Kyaw, D. M. Tong, E. Sjöqvist, and L.-C. Kwek, 2015, Sci. Rep. **5**, 18414.
Zhang, J., F.-G. Li, Y. Xie, C.-W. Wu, B.-Q. Ou, W. Wu, and P.-X. Chen, 2018, Phys. Rev. A **98**, 052323.
Zhang, J., *et al.*, 2013, Phys. Rev. Lett. **110**, 240501.
Zhang, J.-Q., Y. Li, and M. Feng, 2013, J. Phys. Condens. Matter **25**, 142201.
Zhang, Q., X. Chen, and D. Guéry-Odelin, 2015, Phys. Rev. A **92**, 043410.
Zhang, Q., X. Chen, and D. Guéry-Odelin, 2017, Sci. Rep. **7**, 15814.
Zhang, Q., J. G. Muga, D. Guéry-Odelin, and X. Chen, 2016, J. Phys. B **49**, 125503.
Zhang, X., Y.-H. Chen, Q.-C. Wu, Z.-C. Shi, J. Song, and Y. Xia, 2017, Laser Phys. **27**, 015202.
Zhang, Z., T. Wang, L. Xiang, J. Yao, J. Wu, and Y. Yin, 2017, Phys. Rev. A **95**, 042345.
Zhang, Z., *et al.*, 2018, New J. Phys. **20**, 085001.
Zhao, Y. J., B. Liu, Y. Q. Ji, S. Q. Tang, and X. Q. Shao, 2017, Sci. Rep. **7**, 16489.
Zheng, Y., S. Campbell, G. De Chiara, and D. Poletti, 2016, Phys. Rev. A **94**, 042132.
Zhong, Z.-R., 2016, Sci. Rep. **6**, 8.
Zhou, B. B., A. Baksic, H. Ribeiro, C. G. Yale, F. J. Heremans, P. C. Jerger, A. Auer, G. Burkard, A. A. Clerk, and D. D. Awschalom, 2017, Nat. Phys. **13**, 330.
Zhou, X., S. Jin, and J. Schmiedmayer, 2018, New J. Phys. **20**, 055005.
Zhou, X., B.-J. Liu, L. Shao, X.-D. Zhang, and Z.-Y. Xue, 2017, Laser Phys. Lett. **14**, 095202.